

Novel Approaches of Molecular Targeting in Philadelphia Chromosome Positive Leukemia

Dissertation

to obtain the Degree of Doctor of Philosophy
at the Faculty of Natural Sciences

Submitted to the Faculty of Biochemistry, Chemistry and Pharmacy
of the Goethe University
in Frankfurt am Main

By

Afsar Ali Mian
from Swat, Pakistan

Frankfurt am Main, 2009

(D30)

Submitted to the Faculty of Biochemistry, Chemistry and Pharmacy of
the Goethe University in Frankfurt am Main

Dean: Prof. Dr. Dieter Steinhilber

Examiners:

1. Examiner: Prof. Dr. Rolf Marschalek
2. Examiner: PD. Dr. Martin Ruthardt

Date:

*Dedicated to my late father in law
Khurshid Khan (DPO Dir Lower)
who sacrificed his life for
the Nation*

1	INTRODUCTION.....	14
1.1	Normal hematopoiesis	14
1.2	Leukemia.....	14
1.2.1	Acute leukemia.....	15
1.2.1.1	Acute lymphoid leukemia (ALL)	16
1.2.1.2	Acute myeloid leukemia (AML).....	17
1.2.2	Chronic leukemia	18
1.2.2.1	Chronic lymphocytic leukemia (CLL).....	18
1.2.2.2	Chronic myelogenous leukemia (CML)	18
1.3	Cytogenetic abnormalities involved in leukemia	20
1.3.1	The Philadelphia-Chromosome associated translocation products	20
1.3.2	Chromosome 22q+: p185 ^{BCR/ABL} and p210 ^{BCR/ABL}	20
1.4	The Philadelphia chromosome	22
1.4.1	Breakpoint cluster region (BCR).....	22
1.4.2	Abelson murine leukemia virus homology gene (ABL).....	23
1.4.3	Breakpoint regions and fusion protein tyrosine kinase	24
1.4.4	BCR-ABL signaling.....	24
1.4.4.1	Stat signaling	25
1.4.4.2	Ras/MAPK.....	26
1.4.4.3	PI-3K/Akt	26
1.5	Molecular therapy of Ph+ leukemia.....	28
1.5.1	Abl-kinase-inhibitor Imatinib Mesylate	29
1.5.2	Resistance towards kinase inhibitors /Resistant BCR/ABL Mutations	30
1.5.3	Mechanisms of Imatinib resistance	31
1.5.3.1	Imatinib-dependent mechanism.....	31
1.5.3.2	Non-Imatinib-dependent mechanism.....	31
1.5.4	Strategies to overcome resistance towards kinase inhibitors.....	32
1.5.5	Targeting the tetramerization domain of BCR/ABL	33
1.5.6	Targeting the Coiled coil (CC) enhances the effect of Imatinib and inhibits mutant BCR/ABL ..	34
1.5.7	Allosteric inhibition of BCR/ABL	34
1.6	Dissertation Hypothesis and Aims	36
2	MATERIALS	39
2.1	Instruments and apparatus.....	39

2.2	Chemicals	41
2.3	Special reagents and materials	43
2.3.1	Cell culture medium and reagents	43
2.3.2	Chemokines and cytokines.....	43
2.3.3	Enzymes	44
2.3.4	Polymerase Chain Reaction (PCR)	44
2.3.5	Antibodies	44
2.3.5.1	Primary antibodies used for western blotting	44
2.3.5.2	Secondary antibodies.....	45
2.3.5.3	FACS antibodies.....	45
2.3.6	Buffers.....	45
2.3.7	Plasmids and vectors	49
2.3.8	Bacterial <i>E. Coli</i> Strain and genotype	50
2.3.9	Medium for bacterium.....	50
2.3.10	Cell lines	50
2.3.10.1	Ph+ cells	50
2.3.10.2	Other Cell lines.....	51
2.3.11	Medium for Cell culture.....	51
2.3.12	Materials for animal experiments.....	52
2.3.12.1	Mice.....	52
2.4	Miscellaneous	53
3	METHODS	54
3.1	Preparation of plasmid DNA	54
3.1.1	Transformation of <i>E.coli</i>	54
3.1.2	Bacterium growth in liquid media.....	54
3.1.2.1	Growing an overnight culture	54
3.1.2.2	Growing larger cultures	54
3.1.3	Miniprep: a small scale preparation of plasmid DNA.....	54
3.1.4	Maxi prep: a large scale preparation of plasmid DNA.....	55
3.1.5	Determining of DNA yield and quality.....	55
3.1.6	Enzymatic Modification of Nucleotide Acids.....	55
3.1.6.1	Restriction digestion of Plasmid DNA	55
3.1.6.2	Dephosphorylation of Linear Plasmid-DNA by Alkaline Phosphatase CIP (Calf Intestinal Phosphatase)	55
3.1.6.3	Fill-in of 5'-Overhangs to form blunt ends by Klenow-Reaction.....	55
3.1.6.4	Ligation of DNA Fragments	56
3.1.6.5	Quick change site-directed mutagenesis.....	56
3.1.6.6	Recombination („gateway LR clonase enzyme kit“from Invitrogen).....	56

3.1.6.7	Cloning of Gateway Destination vector.....	57
3.1.7	Electrophoretic separation of DNA.....	57
3.1.8	Cloning of the used Plasmids	57
3.1.8.1	Cloning of Eukaryotic expression plasmids	57
3.1.8.2	Cloning of prokaryotic expression plasmids.....	59
3.2	Immunoblot.....	60
3.2.1	Lysis of cells (Sambrook <i>et al.</i> , 1989).....	60
3.2.2	Determining of protein concentration	60
3.2.3	SDS-polyacrylamide gel electrophoresis (SDS-PAGE).....	60
3.2.4	Transfer of proteins onto a nitrocellulose membrane (Western blot).....	61
3.2.5	Immunodetection of specific proteins	61
3.3	Characterization of high molecular weight complexes (HPLC).....	62
3.4	Production of GST-Fusion protein in bacteria	62
3.4.1	Protein mini preparation.....	62
3.4.2	Protein maxi preparation	62
3.5	GST “Pull-down” assays.....	63
3.6	Cell biology techniques.....	63
3.6.1	Cell cultures	63
3.6.1.1	Used Cell lines.....	64
3.6.1.2	Cell counting and determination of cell viability.....	64
3.6.1.3	Freezing and thawing.....	64
3.6.2	Genetic modification of mammalian cell	65
3.6.2.1	Transfection of mammalian cells.....	65
3.6.2.2	Retroviral infection.....	65
3.6.3	Cell growth and proliferation assay.....	66
3.6.4	Proliferation-competition assays (PCA).....	66
3.6.5	Apoptosis measurement by 7-aminoactinomycin D (7-AAD).....	66
3.6.6	Transformation assays.....	67
3.6.6.1	Focus formation assay	67
3.6.6.2	Soft agar anchorage-independent growth assay.....	67
3.7	Production of recombinant TAT- fusion proteins	67
3.8	Determination of TAT-fusion protein uptake	67
3.9	„Pull-down-assays“for TAT-fusion protein	68
3.10	Animal experiments	68
3.10.1	<i>In vivo</i> peptide transduction	68

3.10.1.1	Raring of mice.....	68
3.10.1.2	Delivery of peptides to the mice	68
3.10.1.3	Analysis of the mice.....	68
3.11	Statistical Analyses.....	68
4	RESULTS	69
4.1	Targeting of the N-terminal coiled-coil (CC) oligomerization interface by a Helix-2 peptide inhibits BCR/ABL.....	69
4.1.1	The Helix-2 but not Helix-1 of coiled-coil (CC) interacts with 185 ^{BCR/ABL}	69
4.1.2	Co-expression of Helix-2 disrupts p185 ^{BCR/ABL} tetramers.....	69
4.1.3	Helix-2 reduces the autophosphorylation of p185 ^{BCR/ABL}	70
4.1.4	Helix-2 inhibits growth of p185BCR/ABL positive cells and increases its sensitivity towards Imatinib	71
4.1.5	Helix-2 specifically inhibits Ph+ human cell lines.....	72
4.2	Targeting the oligomerization of BCR/ABL by membrane permeable competitive.....	74
4.2.1	HIV-TAT-fusion peptides were efficiently delivered to fibroblasts	74
4.2.2	HIV-TAT mediates the efficient cellular uptake of Helix-2 fusion proteins.....	74
4.2.3	MPH-2 interacts with BCR/ABL	76
4.2.4	MPH-2 efficiently reduces the autophosphorylation of BCR/ABL.....	77
4.2.5	MPH-2 selectively inhibits Ph+ leukemic cell lines.....	77
4.2.6	TAT-fusion protein are efficiently delivered <i>in vivo</i>	78
4.3	Mechanism of the resistance of “gatekeeper” mutation T315I and strategies to overcome this sresistance	80
4.3.1	Helix-2 interacts with mutant p185 ^{BCR/ABL} and disrupts the HMW-complexes of	80
4.3.2	Helix-2 inhibits the factor independence and overcomes Imatinib resistance of	82
4.3.3	Helix-2 reduces the transforming activity of unmutated and mutant p185 ^{BCR/ABL}	84
4.3.4	ABL kinase inhibitor (AKI)-resistance mutations restore both transformation	86
4.3.5	The “gatekeeper” mutation T315I restores the capacity to mediate factor.....	88
4.3.6	Deletion of BCR AA 64-412 (BCC/ABL) sensitizes T315I towards inhibitory	88
4.3.7	In case of ΔS/T (BCR 1-196ABL) construct: T315I enhances factor independence while transformation of fibroblast is not changed.....	91
4.3.8	Resistance of p185 ^{BCR/ABL-T315I} against inhibition of the oligomerization depends on the phosphorylation at Y177	92
4.3.9	Autophosphorylation at Y177 is not affected by the oligomerization inhibition, but phosphorylation at Y177 of endogenous BCR parallels the effects of T315I.....	93
4.3.10	The effects of T315I are associated with an intact ABL-kinase activity	96
4.3.11	Deletion of regulatory SH3 domain (ΔSH3-ABL) restores factor-independent growth of T315I	96
4.3.12	Oligomerization domain & GRB-2 binding site double deletions (ΔCCp185-	97

4.3.13	The presence of T315I is associated with increased ABL-kinase activity also in.....	99
4.4	Oligomerization inhibition combined with allosteric inhibition abrogates the.....	100
4.4.1	Targeting the oligomerization of BCR/ABL increases the efficacy of GNF-2 against unmutated p185 ^{BCR/ABL} and p185 ^{BCR/ABL} harboring the T315I mutation.....	100
4.4.2	Targeting the oligomerization of BCR/ABL in combination with GNF-2 induces apoptosis in unmutated p185 ^{BCR/ABL} and p185 ^{BCR/ABL} harboring the T315I mutation.....	103
4.4.3	Helix-2 in combination with GNF-2 reduce transformation potential of Fibroblast.....	104
4.4.4	GNF-2 completely abolishes growth of p185 ^{BCR/ABL} and oligomerization-deficient.....	105
4.4.5	Effects of the combination of GNF-2 and Helix-2 on the autophosphorylation of BCR/ABL and its downstream signaling.....	105
5	DISCUSSION.....	108
6	SUMMARY.....	121
7	ZUSAMMENFASSUNG.....	124
8	REFERENCES.....	127
9	EHRENWÖRTLICHE ERKLÄRUNG.....	143
10	CURRICULUM VITAE.....	144

Figure 1- Normal hematopoiesis:	15
Figure 2- The Translocation of t(9;22)(q34;q11) in CML.	21
Figure 3 - Structure of the BCR protein	22
Figure 4 - Structure of the Abl protein	23
Figure 5 - Locations of the breakpoints in the Abl and Bcr genes and structure of the chimeric mRNAs derived from the various breaks	25
Figure 6 - Schematic representation of the main BCR-ABL -activated pathways.	27
Figure 7 - Proposed mechanisms of action of Imatinib-resistant mutations based upon the crystal structure of the Abl kinase domain complexed with Imatinib. Ribbon representation of the Abl kinase domain complexed with Imatinib (Nagar et al., 2002)	32
Figure 8: Structure of GNF-2	35
Figure 9 – Different constructs used in the study.....	59
Figure 10- Interaction of Coiled-Coil Subdomains with p185 BCR/ABL.....	70
Figure 11- Disruption of p185BCR/ABL High Molecular Weight Complexes and Reduction of p185 BCR/ABL autophosphorylation by Helix-2.	71
Figure 12- Growth Inhibition of p185BCR/ABL Expressing Ba/F3 Cells and Philadelphia Chromosome positive human cell lines	73
Figure 13 - Recombinant membrane permeable peptides.....	75
Figure 14 - Uptake of HIV-TAT fusion peptides by leukemic cell lines and primary stem cells.....	76
Figure 15 - Interaction between MPH-2 and BCR/ABL.....	77
Figure 16 - MPH-2 inhibits the autophosphorylation of BCR/ABL.....	78
Figure 17 - Growth inhibition of Ph ⁺ leukemic cell lines upon exposure to MPH-2.	79
Figure 18 - In vivo transduction of MPH-2.....	80
Figure 19 - Helix-2 Interacts with Mutant p185 BCR/ABL, Disrupts HMW-Complexes and Inhibits Autophosphorylation of WT and Mutant p185 BCR/ABL.....	81
Figure 20 - Effect of Helix-2 on BCR/ABL mutants resistant to Imatinib.	83
Figure 21 - Fibroblast Transformation Assays.....	85
Figure 22 - The influence of the resistance mutations on the transformation potential of oligomerization-deficient p185BCR/ABL	87
Figure 23 - The influence of the resistance mutations on the transformation potential of oligomerization-deficient p210BCR/ABL	89

Figure 24 - Role of serine/threonine and Grb-2 binding domains in the resistance of T315I mutants against the oligomerization inhibition by Helix-2.....	90
Figure 25 - Role of serine/threonine domain in the resistance of T315I mutants against the oligomerization inhibition by Helix-2.....	92
Figure 26 - Role of Y177 in the resistance of T315I mutants against the oligomerization inhibition by Helix-2.	94
Figure 27 - Y177-phosphorylation in the autophosphorylation of p185BCR/ABL and its mutants and the transphosphorylation of endogenous BCR in relationship to the presence of T315I upon the inhibition of oligomerization.....	95
Figure 28 - Role of the ABL-kinase in the activity of T315I in p185BCR/ABL and its mutants.	97
Figure 29 - Role of the SH3 domain in the activity of T315I in p185BCR/ABL.	98
Figure 30 - The influence of the resistance mutations on the transformation potential of oligomerization-deficient & GRB-2 binding site (Y177F) double mutant BCR/ABL.	99
Figure 31 - Influence of T315I on the kinase activity p185 ^{BCR/ABL} and its mutants – autophosphorylation.	100
Figure 32 - Effects of the oligomerization inhibitor Helix-2 on the response of p185BCR/ABL and p185BCR/ABL-T315I towards allosteric inhibition by GNF-2.....	102
Figure 33 - Induction of apoptosis in Ba/F3 expressing p185BCR/ABL and p185BCR/ABL-T315I by oligomerization inhibitor Helix-2 in combination with allosteric inhibitor GNF-2	103
Figure 34 - Impairment of transformation potential of Fibroblast expressing unmutated p185BCR/ABL and p185BCR/ABL-T315I by GNF-2 in combination with Helix-2... ..	104
Figure 35 - Role of oligomerization in the sensitivity of unmutated p185BCR/ABL and p185-T315I towards allosteric inhibition by GNF-2.....	105
Figure 36 - The combination of Helix-2 and GNF-2 inhibits the autophosphorylation of p185-T315I and dependent signaling pathways.	106

Table 1 : FAB classification of acute lymphoid leukemia(Begemann <i>et al.</i> , 1998a)	16
Table 2: Immunological subtypes of acute lymphoid leukemia (Begemann <i>et al.</i> , 1998a).....	16
Table 3: FAB classification of acute myeloid leukemia(Bennett <i>et al.</i> , 1985)	18

Acknowledgements

First of all I am grateful to God Almighty for giving me the wisdom, strength and means of completing this research project. You have made my life more bountiful and meaningful. May your name be exalted, honored, and glorified.

Foremost, I would like to express my sincere gratitude to my supervisor PD Dr. Martin Ruthardt for the continuous support of my Ph.D study and research, for his patience, motivation, enthusiasm and immense knowledge. His guidance helped me in all the time of research and writing of this thesis. I could not have imagined having a better supervisor and mentor for my Ph.D study.

I am thankful to my external supervisor Prof. Dr. Rolf Marschalek, for supervising me during my PhD studies. I really appreciate his valuable suggestions and scientific discussions.

It will be my great pleasure to express my appreciation to Prof. Dr. Hubert Serve, Director Department of Hematology/Oncology, for providing the opportunity to work in the field of Hematology.

My sincere thanks are to Dr. Tim Beissert for his unanimous support, great patience, lively discussion and great sense of generosity in sharing scientific ideas and laboratory logistics during my experimental work. I would further like to thank Dr. Claudia Oancea, Dr. Elena Puccetti, Dr. Xiaomin Zheng, Dr. Gunnar Steinert, and Dr. Anita Seshire for the help they extended during my research. The former two are also acknowledged for their fruitful suggestions and most valuable comments which helped me in expediting my research. I am thankful to Pavan for helping me compiling this dissertation.

I am grateful to my current and past colleagues in the lab like, Zihan Zhao, Marion Schüll, Alena Hundertmark, Velina Kaburova, Jessica Roos, Hannelore Held, Tania Michaelis and Anjali Dubei, who helped me in many ways in the lab. I am indeed obliged to my friends Lala Iqbal, Wali Sher, Dr. Muhammad Naseem, Anwar Khan, Malak, and Zafar for their moral support and efforts in making my stay comfortable here in Germany.

My deepest gratitude goes to my family for their unflagging love and support throughout my life. This dissertation is simply impossible without them. I am indebted to my father for his care and love. He is a great father, great teacher and big source of encouragement for me. He spared no effort to provide the best possible environment for me to grow up and get higher education. His love for knowledge and interest in medical science is a great source of motivation for me.

Last but not the least; I am grateful to my wife for extending a great sense of exaltation and immense encouragement during my PhD study. Her patience, understanding and unconditional support is indispensable for my future professional forthcoming.

Afsar A. Mian

1 Introduction

1.1 Normal hematopoiesis

The term hematopoiesis refers to the highly orchestrated process of blood cell production and homeostasis. In adults, hematopoiesis occurs in bone marrow. The cells from the hematopoietic system are continually generated from self-renewing progenitors in the bone marrow called hematopoietic stem cells (HSCs), which have been isolated in both humans and mice. HSCs can be divided into a long-term subset (LT-HSC), capable of indefinite self-renewal, and a short-term subset (ST-HSC) that self-renew for a defined interval. HSCs give rise to non-self-renewing oligolineage progenitors, which in turn give rise to progeny that are more restricted in their differentiation potential and finally to functionally mature cells. (Passegue *et al.*, 2003)

HSC generates the multiple hematopoietic lineages through a successive series of intermediate progenitors. These multipotent stem and/or progenitor cells then commit either to the myeloid or lymphoid lineage by differentiating to common myeloid progenitors (CMP) or common lymphoid progenitors (CLP) (Passegue *et al.*, 2003). These progenitor cells go through a number of proliferation and commitment steps to give rise to all the myeloid and lymphoid lineages of the blood. The CLP give rise to T cells, B cells, natural killer (NK) cells, and antigen presenting dendritic cells. The CMP give rise to granulocytes, monocytes, megakaryocytes, erythrocyte and dendritic cells. Ultimately, terminally differentiated cells are produced that cannot divide and undergo apoptosis after a period of time ranging from hours (for neutrophils) to decades (for some lymphocytes). Process of hematopoiesis is schematically shown in Figure 1 (Passegue *et al.*, 2003). The regulation of hematopoiesis involves a complex interplay between the intrinsic genetic processes of blood cells and their environment. This interplay determines whether HSCs, progenitors, and mature blood cells remain quiescent, proliferate, differentiate, self-renew, or undergo apoptosis.

1.2 Leukemia

Leukemia is used to describe a variety of cancers of the white blood cells that have their origin in blood-forming cells of the bone marrow. White blood cells evolve from the immature cells referred to as blasts, some of which are lymphoblasts and myeloblasts, depending on whether they eventually mature into lymphocytes or myeloid cells. Normally, blasts constitute less than 5% of healthy bone marrow. In leukemia, however, these blasts remain abnormally immature and multiply continuously, eventually constituting from 30% to 100% of the bone marrow. The malignant cells fill up the marrow and prevent production of

healthy red cells, platelets, and white cells. They often leave the marrow and migrate into the blood stream and lymphatic system and occasionally to the central nervous system. As the number of normal cells declines, symptoms develop which, if untreated, become lethal (Lemez, 1989). Leukemias are divided into two measure types: acute (which progresses quickly with many immature white cells) and chronic (which progresses more slowly and has more mature white cells (Seipelt *et al.*, 1998).

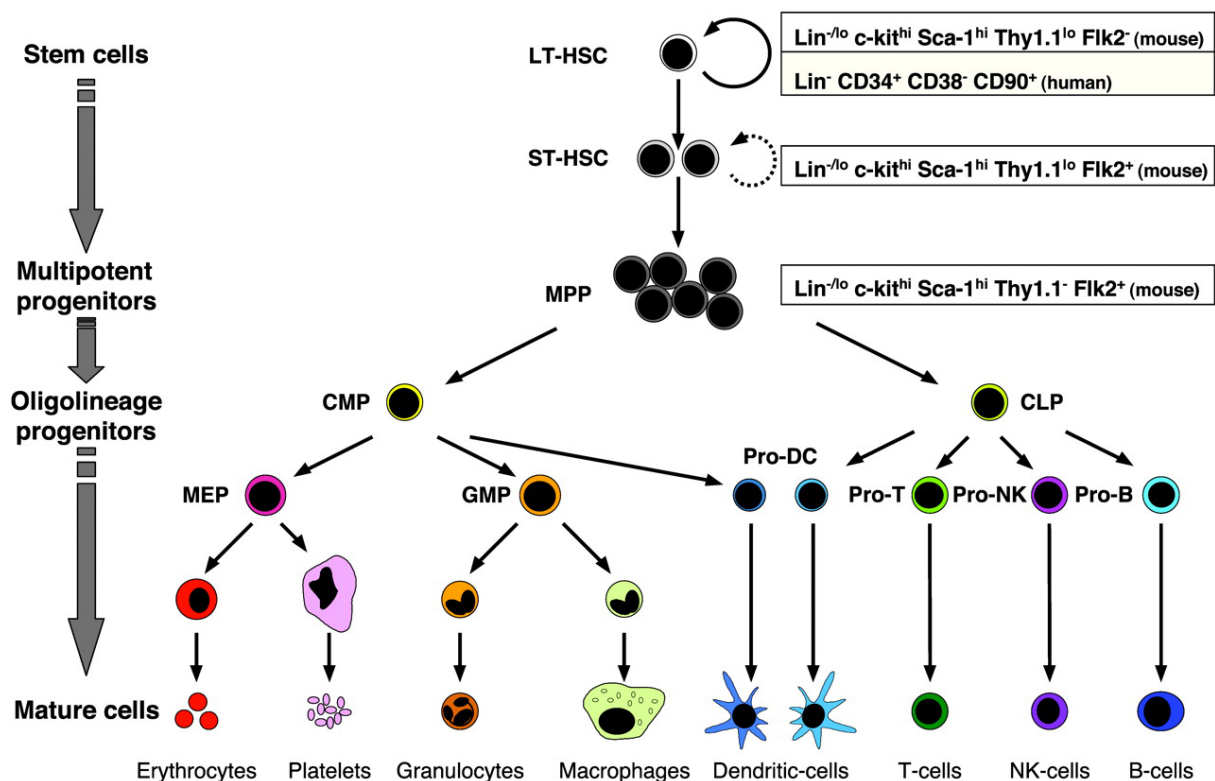


Figure 1- Normal hematopoiesis: ST-HSCs differentiate into multipotent progenitors (MPPs), which do not or briefly self-renew, and have the ability to differentiate into oligolineage-restricted progenitors that ultimately give rise to differentiated progeny through functionally irreversible maturation steps. The CLPs give rise to T lymphocytes, B lymphocytes and natural killer (NK) cells. The CMPs give rise to GMPs, which then differentiate into monocytes/macrophages and granulocytes, and to megakaryotic/erythroid progenitors (MEP), which produce megakaryocyte/platelets and erythrocytes. Both CMPs and CLPs can give rise to dendritic cells (Passegue *et al.*, 2003).

1.2.1 Acute leukemia

Acute leukemias are clonal hematopoietic stem cell disorders and characterized by the uncontrolled growth of the immature blast cells which usually constitute more than 30% of bone marrow cells. The immature cells also accumulate in the peripheral blood, infiltrate other tissues and cause bone marrow failure. The clinical picture of acute leukemia is marked by the effects of anemia, which is usually severe (fatigue, malaise), an absence of functioning granulocytes (proneness to infection and inflammation), and thrombocytopenia (hemorrhagic diathesis) (Hoelzer and Seipelt, 1998). When untreated, patients have a life span of several weeks or months, because their normal blood cells become outnumbered by the leukemic

ones. Acute leukemias require immediate and aggressive treatment (Hoelzer and Seipelt, 1998). It is important to distinguish between acute lymphoid (ALL) and acute myeloid leukemia (AML) because of the different therapeutic approaches which must be undertaken by these two malignancies. They can be distinguished based on a variety of morphological, cytoplasmatic, cytochemical and biochemical features.

1.2.1.1 Acute lymphoid leukemia (ALL)

The acute lymphoid leukemia results from the malignant transformation of immature lymphoid blast cells in the bone marrow, thymus or other lymphoid organs (Hoelzer and Seipelt, 1998). According to FAB classification acute lymphoid leukemia is divided into 3 subgroups as shown in Table 1. Acute lymphoid leukaemia can also be subdivided based on immunologic and cytogenetic abnormalities (Table 2). Major cytogenetic subgroups include the t(9;22) (Philadelphia chromosome-positive acute lymphoblastic leukemia) and the t(8;14) found in the L3 or Burkitt's lymphoma.

Acute lymphoid leukaemia	Features
L1	Small cells, high nuclear/cytoplasmic ratio
L2	Larger cells, lower high nuclear/cytoplasmic ratio
L3	Vacuolated, basophilic blast cells

Table 1 : FAB classification of acute lymphoid leukemia(Begemann *et al.*, 1998a)

Immunologic subtype	% of cases	FAB subtype	Cytogenetic abnormality
Pre-B ALL	75	L1, L2	t(9;22), t(4;11), t(1;19)
T cell ALL	20	L1, L2	14q11 or 7q34
T cell ALL	5	L3	t(8;14). t(8;12). t(2;8)

Table 2: Immunological subtypes of acute lymphoid leukemia (Begemann *et al.*, 1998a)

Treatment results in elderly patients with acute lymphoblastic leukemia (ALL) are poor. Chemotherapy induces complete remission (CR) in approximately 50% of patients, with remission duration ranging from 3 to 12 months and a probability of long-term survival below

10%.1–9 Comorbidity, poor tolerability of cytotoxic drugs, high induction mortality, and the high frequency of the Philadelphia (Ph) chromosome contribute to the dismal prognosis of elderly patients(Annino *et al.*, 2002), The Ph chromosome, resulting from a reciprocal translocation between chromosomes 9 and 22 [t(9;22)], confers an extremely poor prognosis even in younger patients,(Annino *et al.*, 2002) and dose-intensification has not significantly affected survival despite higher rates of CR (Annino *et al.*, 2002; Delannoy *et al.*, 1990; Gleissner *et al.*, 2002). Allogeneic stem cell transplantation (SCT) is potentially curative but is not generally applicable in elderly patients (Radich, 2001).

Children with acute lymphoblastic leukemia (ALL) are treated with combination chemotherapy with an expected cure rate of 80%. However a small proportion of children treated for ALL develop secondary acute myelogenous leukemia (AML). For B cell ALL (B-ALL) t(12;21)/TEL-AML1 and t(1;19)/E2A-PBX1 translocations define patients with relatively good treatment outcome, especially following dose intensified chemotherapy. Patients with t(9;22)/BCR/ABL or t(4;11)/MLL-AF4 translocations have a relatively poor prognosis(Ford *et al.*, 1993; Gokbuget *et al.*, 2000) .

1.2.1.2 Acute myeloid leukemia (AML)

Acute myeloid leukemia (AML) represents a group of clonal hematopoietic stem cell disorders in which both over proliferation and failure to differentiate in the stem cell compartment result in accumulation of non-functional cells termed blasts (Hoelzer and Seipelt, 1998). AML is the most common acute leukemia in adults. It is possible to distinguish between de novo, primary AML, and secondary AML, which arises as a consequence of myelodysplastic syndrome, exposure to mutagenic agents or chemo/radiotherapy due to treatment of another cancer. There are several other factors, which can provoke the onset of secondary leukemias and among which are exposure to benzene, different genetic abnormalities (trisomy 21) and Fancony's anemia (Ferti *et al.*, 1996).

In AML, blast cells are blocked in their normal differentiation at very early stage in their myelopoiesis. In bone marrow and peripheral blood, AML leads to accumulation of large number of proliferating precursors, which are not able to terminally differentiate and become functional blood cells. In this way space needed for normal hematopoietic processes is occupied by leukemic blasts which will finally be clinically manifested as leukemia.

In 1976, a group of hematologists from France, America and England has founded a morphologically and cytochemically based classification of myeloid and lymphoid leukemias (FAB classification). According to FAB classification, acute myeloid leukemias are divided

into 8 subtypes designated M0 through M7. The percentage of blasts, the presence of cytochemical myeloperoxidase, and the major cell types present defined by morphology and esterase cytochemistry, and the immunophenotype define the 8 FAB subtypes (Bennett et al., 1985) (Table 3)

Myeloid leukemia	Features
M0	Undifferentiated by morphology + cytochemistry, peroxidase -, CD13 +, CD33 +
M1	Little differentiation , > 90% blasts, peroxidase -/+
M2	Differentiated, 30-90% blasts, azurophilic granular, peroxidase +
M3	Promyelocytic: intensely granular, variant form is microgranular, auer rods, peroxidase +
M4	Myelomonocytic, peroxidase +++
M5	Monocytic, peroxidase +++
M6	Erythroid differentiation, > 50% of mononuclear cells are erythroid, peroxidase
M7	Megakaryoblastic, peroxidase -/+, CD41+ and/or CD61+

Table 3: FAB classification of acute myeloid leukemia(Bennett *et al.*, 1985)

1.2.2 Chronic leukemia

1.2.2.1 Chronic lymphocytic leukemia (CLL)

Chronic leukemia results in an accumulation of mature granulocytes or lymphocytes. Chronic leukemia progresses slowly but can develop into an acute form. Major types include chronic lymphocytic leukemia (CLL) and chronic myeloid leukemia (CML).

Ninety percent of CLL cases are seen in people who are 50 years or older and is almost never seen in children. In CLL, lymphocytes accumulate in peripheral blood, bone marrow, lymph nodes, spleen, and liver (Kolyvanos *et al.*, 2003).

1.2.2.2 Chronic myelogenous leukemia (CML)

Chronic myeloid leukemia is a clonal myeloproliferative disorder (MPD) that results from the neoplastic transformation of a hematopoietic stem cell (Begemann *et al.*, 1998a). The leukemic cells of >95% of CML patients have a reciprocal translocation between the long arms of chromosomes 9 and 22, t(9;22). The derived chromosome 22 is termed the Philadelphia (Ph) chromosome (Faderl *et al.*, 1999).

The initial chronic phase of this biphasic disease is characterized by a massive expansion of the granulocytic cell lineage, even though most, if not all, hematopoietic lineages can be produced from the CML stem cell. The median duration of the chronic phase is 3–4 years.

Acquisition of additional genetic and/or epigenetic abnormalities causes the progression of CML from chronic phase to blast phase. This phase is characterized by a block of cell differentiation that results in the presence of 30% or more myeloid or lymphoid blast cells in peripheral blood or bone marrow, or the presence of extramedullary infiltrates of blast cells (Hoelzer *et al.*, 1998).

Allogeneic stem-cell transplantation is the only known curative therapy for CML. However, most patients are not eligible for this therapy, because of advanced age which makes them unable to tolerate the serious side effects of the treatment or lack of a suitable stem-cell donor. The discovery that BCR/ABL is required for the pathogenesis of CML, and that the tyrosine-kinase activity of ABL is essential for BCR–ABL mediated transformation, made the ABL kinase an attractive target for therapeutic intervention. Imatinib mesylate (Glivec, previously known as STI571), a potent inhibitor of the tyrosine kinases ABL, ARG, platelet-derived growth factor receptor and KIT, has been shown to selectively induce apoptosis of BCR/ABL+ cells, and is remarkably successful in treating patients with CML (Deininger *et al.*, 2005). In newly diagnosed patients with CML in chronic phase, imatinib induces complete cryptogenic response in more than 80% patients. Patients with more advanced phases of CML also respond to imatinib, but this occurs much less frequently and treatment is less durable.

There are two major obstacles to imatinib-based therapies for patients with CML. One is the persistence of BCR/ABL-positive cells, this is known as ‘residual disease’, and is detected by a sensitive nested reverse-transcriptase PCR assay. Suppression of the disease therefore relies on continuous imatinib therapy. The other major problem is relapse of the disease due to the emergence of resistance to imatinib. Several mechanisms of resistance have been described, the most frequent of which are the appearance of point mutations in the BCR/ABL gene that impair the drug binding (Ren, 2005).

The fact that the resistance to imatinib is most commonly associated with point mutations in the kinase domain of BCR/ABL further demonstrates the importance of this activity in the pathogenesis of CML. On the other hand, the persistence of BCR/ABL-positive cells in patients on imatinib therapy indicates that inhibition of the ABL kinase activity alone might not be sufficient to eradicate the leukemia cells. Identification of additional essential components in the pathogenesis of CML remains crucial for developing improved therapies for CML.

1.3 Cytogenetic abnormalities involved in leukemia

The pathogenesis of leukemia is linked to oncogenic fusion proteins, generated as a consequence of primary chromosome translocations or inversions. About 80-85 % of AML and ALL patients and 98% of CML patients have chromosomal translocation (Begemann *et al.*, 1998b; Faderl *et al.*, 1999). In most cases this chromosome translocations refer to reciprocal translocations between different chromosomes.

1.3.1 The Philadelphia-Chromosome associated translocation products

Over 95% of CML cases involve a balanced translocation of a fragment of the long arm of chromosome 9 to the long arm of chromosome 22: t(9;22) (Faderl *et al.*, 1999). The shortened chromosome 22 was first described in 1960 by Peter Nowell and termed the Philadelphia chromosome. The Philadelphia chromosome also occurs in 10-20% of adult patients with acute lymphoblastic leukemia (ALL) (Faderl *et al.*, 1999).

The balanced reciprocal translocation t(9;22) creates a fusion between the BCR (breakpoint cluster region) gene on chromosome 22 and the ABL gene on chromosome 9 (Figure 5). The breakpoint in the abl gene locus is constantly found between exons 1 and 2 (a1 and a2). On chromosome 22, translocation t(9;22) involves three different breakpoints in the bcr locus : (minor) m-bcr, which maps in the first intron of bcr; (major) M-bcr, which spans between exons 12 to 16 (also referred to as b1 to b5) and (micro) μ -bcr which was found between exon e19 and e20 (Faderl *et al.*, 1999). The translocation t(9;22) results in translocation of BCR exon 1, exons 1–12/13, or exons 1–19 , respectively, to the ABL exons 2 to 11 (also called a2 to a11) on chromosome 9. These different oncogenes give rise to three distinct fusion proteins of molecular mass 190, 210, and 230 KD, which contain the same portion of the c-Abl tyrosine kinase in the COOH terminus but include different amounts of BCR sequence at the NH2 terminus.

1.3.2 Chromosome 22q+: p185^{BCR/ABL} and p210^{BCR/ABL}

The product of fusion between M-bcr and abl is a protein of 210KD, the p210^{BCR/ABL}, which is highly specific for CML. Different p210^{BCR/ABL} has been found depending on the exon involved, for example: b2a2- p210^{BCR/ABL} or b3a3- p210^{BCR/ABL}. p210^{BCR/ABL} constructs were tested from many groups, but without paying special attention to the breakpoint of translocation.

Due to the fact that in Ph+ ALL related p185^{BCR/ABL} the m-bcr breakpoint maps within an intron, the p185^{BCR/ABL} transcript is constant and appears in e1a2 form (Faderl *et al.*, 1999).

C-ABL kinase activity is in normal cells finely regulated in response to growth factors and other stimuli. By the fusion to BCR, ABL becomes constitutively activated. This leads to constitutive activation of the “down-stream” signal transduction pathways in particular to activation of RAS oncogene.

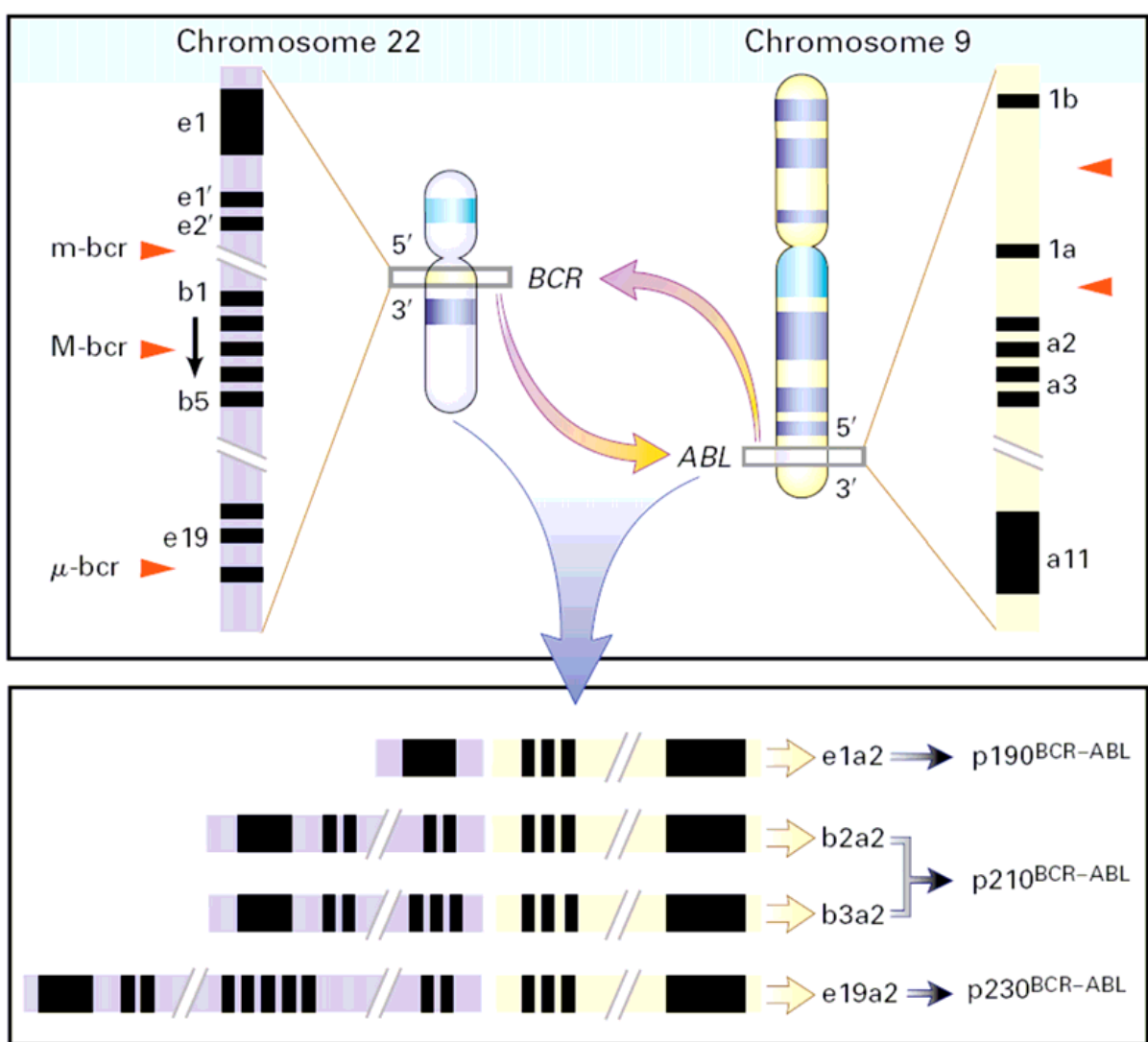


Figure 2- The Translocation of t(9;22)(q34;q11) in CML. The Philadelphia (Ph) chromosome is a shortened chromosome 22 that results from the translocation of 3' (toward the telomere) ABL segments on chromosome 9 to 5' BCR segments on chromosome 22. Breakpoints (arrowheads) on the ABL gene are located 5' (toward the centromere) of exon a2 in most cases. Various breakpoint locations have been identified along the BCR gene on chromosome 22. Depending on which breakpoints are involved, different-sized segments from BCR are fused with the 3' sequences of the ABL gene. This results in fusion messenger RNA molecules (e1a2, b2a2, b3a2, and e19a2) of different lengths that are transcribed into chimeric protein products (p190, p210, and p230) with variable molecular weights and presumably variable function. The abbreviation m-bcr denotes minor breakpoint cluster region, M-bcr major breakpoint cluster region, and μ -bcr a third breakpoint location in the BCR gene that is downstream from the M-bcr region between exons e19 and e20 (Faderl *et al.*, 1999).

The suppression of constitutively active ABL kinase by the specific kinase inhibitor STI571 (Novartis) induces apoptosis in BCR/ABL transformed cells (Gambacorti-Passerini *et al.*, 1997). JAK-STAT and PI-3 kinase are also among the signal transduction pathways induced

by BCR/ABL translocation products. Furthermore the capacity of BCR/ABL to bind f-actin is indispensable for its transformation potential (Faderl *et al.*, 1999).

Noteworthy there seem to exist no differences between p185^{BCR/ABL} and p210^{BCR/ABL} regarding their biological functions. Studies with BCR/ABL infected bone marrow cells in mice proved the correlation between expression BCR/ABL in precursor cells and induction of leukemia (Huettner *et al.*, 2000; Kelliher *et al.*, 1990).

1.4 The Philadelphia chromosome

1.4.1 Breakpoint cluster region (BCR)

The breakpoint cluster region protein, BCR, is a multidomain protein, of 160 kDa and is ubiquitously expressed (Laneville, 1995) (Figure 3). The first N-terminal exon encodes a serine-threonine kinase (Maru and Witte, 1991), with substrates being Bap-1 and BCR itself. A coiled-coil domain at the N-terminus allows dimer formation *in vivo* (McWhirter *et al.*, 1993). The centre of the molecule contains a dbl-like pleckstrin-homology (PH) domain with guanine nucleotide exchange factor (GEF) function for Rho, which may activate the transcription factor NF- κ B (Montaner, Perona *et al.* 1998). The C-terminus has a GTPase-activating domain for Rac (regulates actin polymerisation) (Diekmann *et al.*, 1991). BCR can be phosphorylated on Tyrosine-177. The Grb-2 adapter molecule involved in the activation of the Ras pathway, binds BCR on phosphorylated Tyrosine-177 (Ma *et al.*, 1997).

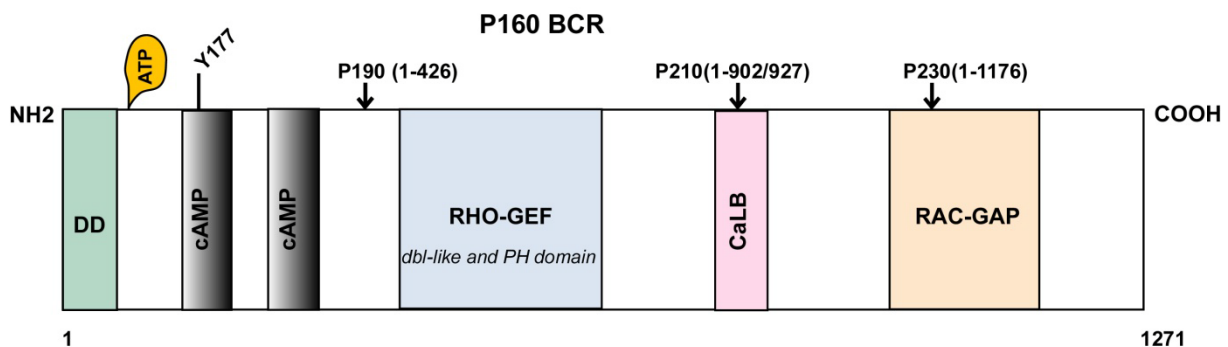


Figure 3 - Structure of the BCR protein (Deininger *et al.*, 2000). The dimerization domain (DD) and the 2 cyclic adenosine monophosphate kinase homologous domains are located at the N terminus. Y177 is the auto-phosphorylation site crucial for binding to Grb-2. The center of the molecule contains a region homologous to Rho guanidine nucleotide exchange factors (Rho-GEF) as well as dbl-like and pleckstrin homology (PH) domains. Toward the C-terminus a putative site for calcium-dependent lipid binding (CaLB) and a domain with activating function for Rac-GTPase (Rac-GAP) are found. Arrowheads indicate the position of the breakpoints in the BCR-ABL fusion protein.

ABL has been shown to reduce the activity of BCR by phosphorylation. The fact that BCR knockout mice are viable with no change in the incidence and biology of p190^{BCR/ABL} as compared to wild-type mice, makes it difficult to discern the role of BCR in Ph⁺ leukemia (Voncken *et al.*, 1998).

1.4.2 Abelson murine leukemia virus homology gene (ABL)

The Abl gene is the human homologue of the v-abl oncogene carried by the Abelson murine leukaemia virus (A-MuLV), and it encodes a non-receptor tyrosine kinase localized in the nucleus and cytoplasm (Deininger *et al.*, 2000; Ling *et al.*, 2003). Human ABL is a ubiquitously expressed 145 kDa protein with two isoforms, arising from alternative splicing of the first exon (Laneuville, 1995). It contains several structural domains (Figure 4). Three Src homology domains (SH1-SH3) are located towards the NH₂ terminus. The SH1 domain carries the tyrosine kinase function, whereas the SH2 and SH3 domains allow for interaction with other proteins (Cohen *et al.*, 1995). Proline-rich sequences in the center of the molecule interact with the SH3 domains of other proteins such as Crk (Feller *et al.*, 1994). Towards the 3' end, nuclear localization signals, DNA-binding and, actin-binding motifs are found (Deininger *et al.*, 2000).

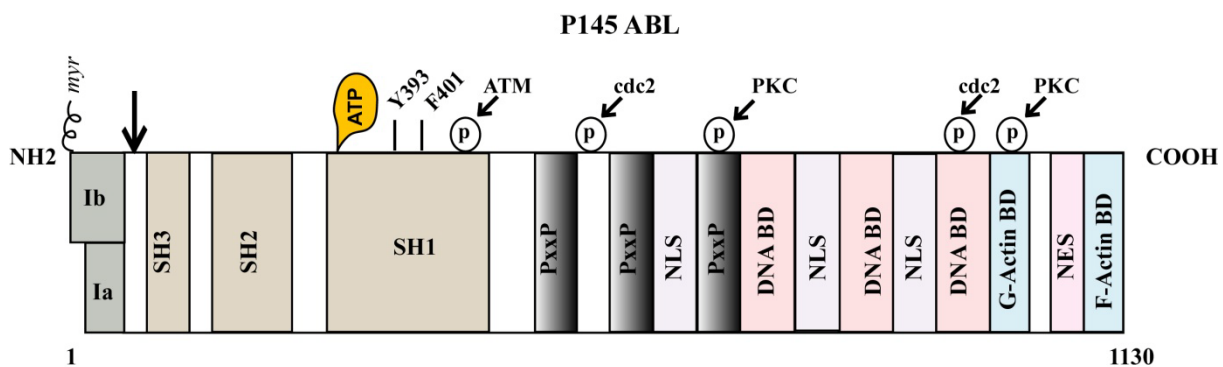


Figure 4 - Structure of the Abl protein (Deininger *et al.*, 2000)

Type Ia isoform is slightly shorter than type Ib, which contains a myristylation (myr) site for attachment to the plasma membrane. Note the 3 SRC-homology (SH) domains situated toward the NH₂ terminus. Y393 is the major site of autophosphorylation within the kinase domain, and Phenylalanine-401 (F401) is highly conserved in PTKs containing SH3 domains. The middle of each protein is dominated by proline-rich regions (PxxP) capable of binding to SH3 domains, and it harbors 1 of 3 nuclear localization signals (NLS). The carboxy terminus contains DNA as well as G- and F-actin-binding domains. Phosphorylation sites by Atm, cdc2, and PKC are shown. The arrowhead indicates the position of the breakpoint in the BCR-ABL fusion protein.

The normal ABL protein serves a complex role as a cellular module that integrates signals from various extracellular and intracellular sources, thereby influencing cell cycle and apoptosis (Deininger *et al.*, 2000).

1.4.3 Breakpoint regions and fusion protein tyrosine kinase

The breakpoints within the Abl gene on 9q34 occur at its 5' end, either upstream of the first alternative exon 1b, downstream of the second alternative exon 1a, or more frequently, between the two (Melo, 1996) (Figure 5). Bcr sequences are always fused to Abl exon a2. In contrast to Abl, breakpoints within Bcr localize to 1 of 3 so-called breakpoint cluster regions (bcr). In most CML patients and in one third of ALL patients, the breakpoint spans Bcr exons b1-b5, defined as major breakpoint cluster region (M-bcr). Fusion transcripts with either b2a2 or b3a2 junctions are formed, due to alternative splicing. A 210-kDa chimeric protein (p210 BCR/ABL) is derived from this mRNA. In the remaining patients with ALL and rarely in patients with CML (with prominent monocytosis), (Ravandi *et al.*, 1999), the breakpoint is between the alternative Bcr exons e2' and e2 termed the minor breakpoint cluster region (m-bcr). The resultant e1a2 mRNA is translated into a 190 kDa protein (p190^{BCR/ABL}). A third breakpoint cluster region (μ -BCR) has been identified downstream of exon 19, giving rise to p230^{BCR/ABL}, a 230 kDa fusion protein, associated with the rare Ph⁺ chronic neutrophilic leukaemia (Pane, Frigeri *et al.* 1996), (Figure 5). In contrast to p190 and p210, transformation to growth factor independence by p230 is incomplete, consistent with the benign clinical course of p230- positive chronic neutrophilic leukaemia (Pane *et al.*, 1996). Occasional cases with other junctions, such as b2a3, b3a3, e1a3, e6a2, or e2a2 have been reported in patients with ALL or CML.

Based on the observation that the ABL part in the chimeric protein is constant, while the BCR portion varies, it can be concluded that ABL is likely to carry the transforming principle, whereas different sizes of the BCR sequence may determine the phenotype of the disease (Deininger *et al.*, 2000).

1.4.4 BCR-ABL signaling

Features in the chimeric protein that are essential for cellular transformation include, the SH1, SH2 and actin binding domains in ABL (Figure 5), and; a coiled-coil motif contained in amino acids 1-63 (McWhirter *et al.*, 1993), the tyrosine at position 177, and the phosphoserine-threonine-rich sequence between amino 192-242 and 298-413 in BCR (Figure 2).

Under physiological conditions, Abl tyrosine kinase activity is tightly regulated. The SH3 domain plays a critical role in this inhibitory process, because its deletion or positional alteration activates the kinase (Mayer and Baltimore, 1994). Other inhibitory mechanisms include binding of SH3 inhibitory proteins, conformational changes of the SH3 domain and

mutations within the kinase domain (Dai *et al.*, 1998; Goga *et al.*, 1993; Mayer and Baltimore, 1994).

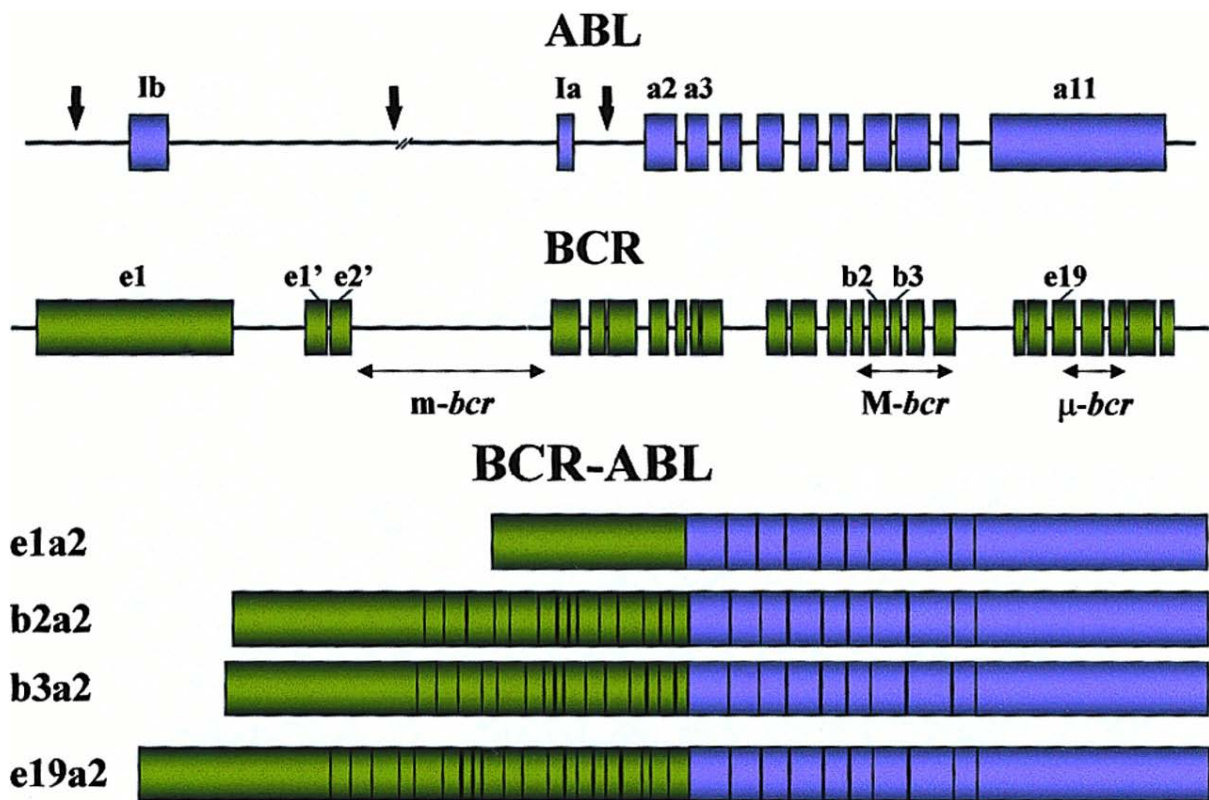


Figure 5 - Locations of the breakpoints in the Abl and Bcr genes and structure of the chimeric mRNAs derived from the various breaks (Deininger *et al.*, 2000).

Fusion of the BCR sequence 5' of the ABL SH3 domain abrogates the physiological suppression of the kinase. This is a consequence of homodimer formation by the N-terminal dimerization domain, in the BCR portion of the BCR/ABL protein. Autophosphorylation increases the phosphotyrosine on BCR/ABL itself which create binding sites for the SH2 domains of other proteins. Proliferation and survival pathways of BCR/ABL are shown in Figure 7. Effects of the BCR/ABL tyrosine kinase are regulated by tyrosine phosphatases. These include protein tyrosine phosphatase 1B (PTP1B) and receptor protein tyrosine phosphatase K (RPTP-K).

1.4.4.1 Stat signaling

STAT (signal transducers and activators of transcription) are a seven member family of cellular proteins, that function as both cytoplasmic signaling molecules and nuclear transcription factors (reviewed in (Darnell, 1997)). Stats are phosphorylated by receptor tyrosine kinases, or various cytoplasmic kinases such as Jaks or SFKs, in response to numerous cytokines and growth factor signals (Wilson *et al.*, 2002).

BCR/ABL may also directly activate Stat1 and Stat5, and there seems to be specificity for Stat6 activation by p190^{BCR-ABL}, as opposed to p210^{BCR/ABL} (Ilaria and Van Etten, 1996).

Stat5 is activated by BCR/ABL via the SFK, Hck (Klejman *et al.*, 2002). On interaction with the SH3 and SH2 domains of BCR/ABL, this kinase is activated and phosphorylates Stat5, leading to its translocation to the nucleus, where it functions as a transcription factor

(Klejman *et al.*, 2002). A Stat5 target gene involved in BCR/ABL leukemogenesis is the antiapoptotic Bcl-X_L gene, whose level is down-modulated in Imatinib treated BCR/ABL - expressing cells (Horita, Andreu *et al.* 2000). Two other Stat5 targets are the antiapoptotic proteins A1 (member of the Bcl-2 family) and pim-1 (it is a serine/threonine kinase and a proto-oncogene) (Calabretta and Perrotti, 2004).

Evidence of Stat5 in BCR/ABL leukemogenesis is supported by the following observations:

(1) BCR/ABL mutants defective in Stat5 activation were less efficient than the wild-type form in transformation of myeloid precursor cells, and (2) a constitutively active Stat5 mutant rescued the leukemogenic potential of Stat5 activation-deficient BCR/ABL mutants (Nieborowska-Skorska *et al.*, 1999).

1.4.4.2 Ras/MAPK

Autophosphorylation of Tyrosine-177 provides a docking site for the adaptor molecule Grb-2 (Pendergast *et al.*, 1993). Grb-2 then binds to Gab2, and the phosphorylation of SHC leads to enhanced activity of the guanosine diphosphate/guanosine triphosphate (GDP/GTP) exchange factor SOS, which promotes the accumulation of the active GTP bound form of Ras. Crkl which is a direct substrate of BCR/ABL can also activate Ras (Calabretta and Perrotti, 2004). Activation of Ras leads to the subsequent recruitment of the serine-threonine kinase Raf to the cell membrane. Raf initiates a signaling cascade through the serine-threonine kinases Mek1/Mek2 and Erk, which ultimately leads to activation of gene transcription (Deininger *et al.*, 2000).

Other pathways activated are the Jnk/Sapk, p38, Dok-1 (forms complexes with Crkl, Ras, Gab, and BCR/ABL). In any case, signals are transduced to the transcriptional machinery of the cell. The importance of Ras dependent signaling for the phenotype of BCR/ABL - expressing cells is supported by observations that, down-regulation of these pathways by antisense strategies, expression of dominant negative molecules, or chemical inhibitors, suppresses proliferation and sensitizes cells to apoptotic stimuli (Calabretta and Perrotti, 2004).

1.4.4.3 PI-3K/Akt

BCR/ABL interacts indirectly with the p85 regulatory subunit of PI-3K via various adapter proteins including Grb-2/Gab2 and c-cbl (Figure 6). PI-3K activates the serine-threonine kinase Akt, triggering an Akt-dependent cascade, which regulates the subcellular localization or activity of several targets such as BAD, MDM2, I κ B-kinase- α and members of the forkhead family of transcription factors (Vivanco and Sawyers, 2002).

Phosphorylation of BAD by Akt suppresses its pro-apoptotic activity, because when phosphorylated, BAD is sequestered in the cytoplasm, in a complex with 14-3-3 β . Phosphorylation of MDM2 enhances its nuclear-cytoplasmic export, inducing a more efficient degradation of p53 (transcription factor that regulates the cell cycle and functions as a tumor suppressor).

Phosphorylation of I κ B-kinase- α enhances its activity towards its substrate I κ B. On phosphorylation, I κ B is subjected to ubiquitination and proteasome-dependent degradation allowing the translocation of nuclear factor κ B (NF- κ B) into the nucleus, where it functions as a transcription factor (Silverman and Maniatis, 2001).

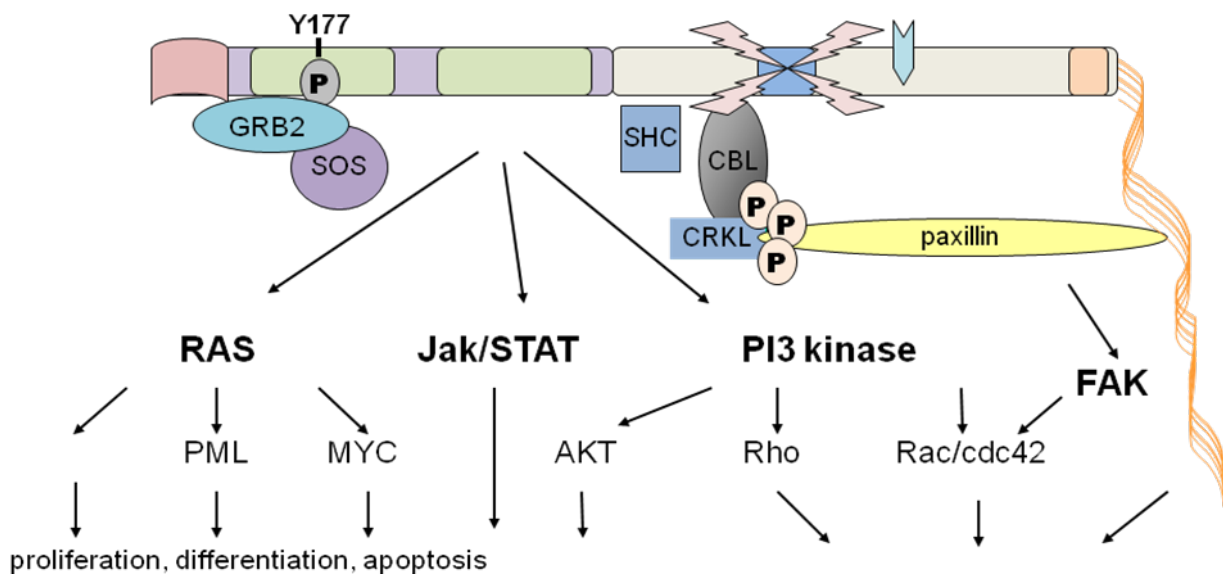


Figure 6 - Schematic representation of the main BCR-ABL-activated pathways. These pathways regulate proliferation and survival of BCR-ABL-transformed haematopoietic cells (Deininger *et al.*, 2000).

Phosphorylation of the transcription factor FKHRL1 prevents its translocation to the nucleus, and the transactivation of genes promoting apoptosis (for example TRAIL), or inhibiting cell cycle progression (for example p27) (Komatsu *et al.*, 2003).

Consistent with the effects of Akt, inhibition of the PI-3K/Akt pathway suppresses *in vitro* colony formation and *in vivo* leukemogenesis of BCR/ABL expressing cells (Skorski, Bellacosa *et al.* 1997). Marrow cells with inactivated PI-3K/Akt are resistant to BCR-ABL transformation (Calabretta and Perrotti, 2004).

Other biological properties of BCR/ABL include: (1) altered adhesion to bone marrow stromal cells and extracellular matrix (which negatively regulates proliferation) by expression of an adhesion inhibitory variant of α 1 integrin not found in normal progenitors, (2) Degradation of inhibitory proteins Abi-1 and Abi-2 in acute leukaemias (Lewis *et al.*, 1996).

1.5 Molecular therapy of Ph+ leukemia

Given the fact that BCR/ABL is the causative agent for Ph+ leukemia it was obvious that targeting the function of the fusion protein itself would provide an excellent therapeutic approach. It was shown that the transforming capacity of BCR/ABL is strictly dependent on its TK activity (Lugo *et al.*, 1990). Thus, a selective ABL-kinase inhibitor called Imatinib was developed, which competes with ATP for the binding to the TK domain and inhibits oncogenic ABL proteins like v-ABL, BCR/ABL and TEL/ABL (Deininger *et al.*, 1997; Druker *et al.*, 1996; Weisberg and Griffin, 2000). Imatinib proved to be clinically very effective: 95% of CML-chronic phase patients achieve a complete hematologic and cytogenetic remission upon Imatinib treatment (O'Dwyer *et al.*, 2003). 70% of CML blast crisis or Ph+ ALL patients achieve a transient complete remission, but relapse frequently within 4 – 6 months and become refractory towards further treatment with Imatinib. The most important resistance mechanisms towards Imatinib consist of the clonal selection of point BCR/ABL-mutants (Ottmann and Hoelzer, 2002). These mutations concern amino acid residues that are critical for the binding of Imatinib to the kinase domain (Cowan-Jacob *et al.*, 2004; Deininger *et al.*, 2005). Other mechanisms that confer Imatinib resistance are the upregulation of BCR/ABL expression, upregulation of “multiple drug resistance” proteins and a functional inactivation of Imatinib through binding to the acidic glycoprotein “acute phase protein alpha 1” (Gambacorti-Passerini *et al.*, 2000; Ottmann and Hoelzer, 2002).

Recently, much effort has been undertaken to solve the problem of Imatinib resistance. In vitro, but not in patients, many point mutations are inhibited by increased doses of Imatinib, as the achievable serum levels of Imatinib are below the concentrations necessary to overcome resistance (O'Hare *et al.*, 2005b; Weisberg *et al.*, 2006; Weisberg *et al.*, 2005). Therefore research focuses mainly on the development of second generation kinase inhibitors. Nilotinib (Novartis, Basle), like Imatinib, is a selective ABL-kinase inhibitor. Nilotinib inhibits many Imatinib-resistant point mutants because of its 20-fold higher affinity for the ABL kinase domain and achievable plasma levels for Nilotinib are sufficient for inhibition (O'Hare *et al.*, 2005a). The dual SRC-ABL kinase inhibitor Dasatinib (Bristol-Myer-Squibb, New York) takes advantage of a characteristic difference between SRC- and ABL-kinase domain conformations to inhibit Imatinib-resistant mutations: the inactive conformations of SRC and ABL are different, while the active conformations are closely related (Schindler, Bornmann *et al.* 2000). Dasatinib has a 325-fold higher affinity towards ABL than Imatinib (O'Hare *et al.*, 2005a). Imatinib and Nilotinib bind to the inactive ABL-kinase conformation which is the reason for their selectivity, while Dasatinib binds to active ABL and active SRC.

Therefore the binding of Dasatinib is dependent on another choice of aminoacid residues as Imatinib or Nilotinib (Schindler *et al.*, 2000). Dasatinib inhibits most mutations identified in Imatinib resistant patients (O'Hare, Walters *et al.* 2005). Unfortunately, the mutation T315I, which clinically accounts for about 20% of Imatinib-resistant cases, is neither inhibited by Nilotinib nor Dasatinib (O'Hare *et al.*, 2005b; von Bubnoff *et al.*, 2006).

1.5.1 Abl-kinase-inhibitor Imatinib Mesylate

Imatinib (Gleevec, Novartis, Basel, Switzerland) previously known as STI571 (signal transduction inhibitor 571) is an inhibitor of specific protein tyrosine kinases that is targeted to the constitutively active Philadelphia chromosome (of CML and Ph+ ALL), c-Kit (CD117) (overexpressed in gastrointestinal tumors), and the platelet derived growth factor (PDGF) receptor. Imatinib was approved by the Food and Drug Administration in May 2001 for the treatment of Ph+ leukemias, which does not respond to interferon therapy, and in February 2002 for the treatment of gastrointestinal stromal tumors (Litzow, 2006; Savage and Antman, 2002). Imatinib is a 2-phenyl-amino-pyrimidine and an orally available, therapeutic agent (Druker and Lydon, 2000).

In June 1998, a phase 1 trial designed to determine the safety and efficacy of Imatinib in chronic-phase CML was initiated (Druker *et al.*, 2001). Likewise, clinical trials of Imatinib were carried out in Ph+ ALL (Wassmann *et al.*, 2003). The initial phase I study included 83 CML patients in chronic phase (less than 15% blast), who had failed interferon-based therapy. With Imatinib having a terminal half-life of 14-16 hours, patients were treated with once-daily oral doses ranging from 25-1,000 mg. In this phase I study, no dose-limiting toxicity was encountered and toxicity at all dose levels was minimal (Mauro and Druker, 2001). Based on the effectiveness of Imatinib in chronic phase CML patients, the phase I studies were expanded to include CML patients in myeloid and lymphoid blast crisis, and patients with relapsed Ph+ ALL (Talpaz *et al.*, 1983). Patients were treated with Imatinib once daily, at doses of 300 to 1000 mg. 55% of patients with myeloid blast crisis responded to therapy (decrease in percentage of myeloid blast to less than 15%), and 70% of patients with CML in lymphoid blast crisis or Ph+ ALL responded with 55% having less than 5% of marrow blast. The success of the phase I study prompted phase II study. In a phase II study, an initial once-daily oral dose of 400 mg and then 600 mg of Imatinib was used for the studies. Hematologic and cytogenetic responses were less common in patients with accelerated- or blast-phase CML than in patients with chronic-phase CML, and adverse events were more common in advanced disease, but it was unclear whether this was due to the phase of the disease or to the higher dose of Imatinib that were used (Savage and Antman, 2002). In Ph+ ALL the initial

overall response rates were 60-70%, but were almost invariably followed by relapse with very rapid kinetics (Schiffer *et al.*, 2003).

1.5.2 Resistance towards kinase inhibitors /Resistant BCR/ABL Mutations

BCR/ABL is characterized by a deregulated and constitutively activated ABL tyrosine kinase (TK) activity which determines its transformation potential (Faderl *et al.*, 1999). Cellular transformation and leukemogenesis are strictly dependent on the TK activity of BCR/ABL (Deininger *et al.*, 1997; Druker *et al.*, 1996; Lugo *et al.*, 1990; Weisberg and Griffin, 2000). Molecular-targeted therapy with selective ABL-kinase inhibitors (AKI) such as Imatinib, Dasatinib or Nilotinib induces complete hematological and cytogenetic remissions in the majority of Ph⁺ leukemia patients (Ramirez and DiPersio, 2008). In advanced disease stages relapse frequently occurs and is accompanied by resistance to further treatment with the used compound. In the majority of the cases clones harboring point mutations in the ABL-portion of the fusion protein which interfere with the binding affinity for the inhibitors are selected upon exposure to AKI (Cowan-Jacob *et al.*, 2004; Deininger, 2005). The most frequent mutations are the “P-loop” mutations Y253F and E255K, the “activation loop” mutation H396P, the “catalytic domain” mutation M351T, and the “gatekeeper” mutation T315I (Shah *et al.*, 2002). The activity spectrum of actually available AKI covers 14/15 of these mutations. The T315I is the only mutation, which confers resistance against virtually all ATP competitors (Druker, 2008). There is increasing evidence that these mutations not only interfere with the binding affinity to the kinase inhibitors, but modify biological functions of BCR/ABL. The observation that additional factors influence transformation potential of the AKI-resistant BCR/ABL T315I mutant was supported by our recent findings on the inhibition of tetramerization of BCR/ABL and its AK-resistant mutants. Tetramerization of ABL through the N-terminal coiled-coil region (CC) of BCR is essential for the aberrant ABL-kinase activation.

Targeting the CC-domain forces BCR/ABL into a monomeric conformation, abolishes its transformation potential by interfering with its kinase activity and increases the sensitivity for Imatinib (Beissert *et al.*, 2008; Beissert *et al.*, 2003) showed that factor dependent hematopoietic progenitors expressing BCR/ABL harboring the Y253F and E255K but not the T315I responded to the inhibition of tetramerization. Together with previous findings these results led to the hypothesis that BCR/ABL harboring the T315I mutation exhibits additional functions contributing to its leukemogenic potential, which are not present in the unmutated BCR/ABL. In fact it has been shown that the BCR/ABL mutants Y253F and E255K exhibited increased and the M351T and H396P reduced transformation potential, whereas that of T315I

was assay dependent (Griswold *et al.*, 2006). Interestingly the transformation potential of these BCR/ABL mutants is not constantly correlated with the intrinsic ABL-kinase activity.

1.5.3 Mechanisms of Imatinib resistance

Although Imatinib produces high rates of complete clinical and cytogenetic responses in the chronic phase, resistance, and clinical relapse develops rapidly in Ph⁺ ALL and in the advanced phases of CML (Litzow, 2006; Nimmanapalli and Bhalla, 2002).

Two broad mechanisms of resistance have been characterized (Litzow, 2006). These include

1.5.3.1 Imatinib-dependent mechanism

- 1- Mutations in the Abl kinase portion of the BCR/ABL gene affecting drug interaction or kinase activity.
- 2- Increased expression of BCR/ABL kinase from genomic amplification.

1.5.3.2 Non-Imatinib-dependent mechanism

- 1- Clonal evolutions involving survival signaling genes: SFKs, and MAP kinases
- 2- Decreased intracellular drug levels which result from, plasma binding by α -1 acid glycoprotein or drug efflux from P-glycoprotein (MDR-1) over expression.

To predict the different mechanisms of Imatinib resistance, human cell lines that are BCR/ABL positive and murine hematopoietic cells that have been transformed with BCR/ABL, have been exposed to Imatinib with subsequent development of resistance (Griswold *et al.*, 2006). A mouse model has shown that although *in vivo* tumors were resistant to Imatinib, they retained *in vitro* sensitivity to Imatinib (Gambacorti-Passerini *et al.*, 2000).

The best studied mechanisms of resistance to Imatinib in patients are gene mutations in the Abl (tyrosine kinase) domain of the BCR/ABL gene. The first such mutation was described in 2001, in which was a substitution of isoleucine (T315I) for threonine on positions 315, in the Abl tyrosine kinase domain of the BCR/ABL gene (Gorre *et al.*, 2001). This substitution interfered with a critical hydrogen bond that forms between the Abl kinase and Imatinib, preventing Imatinib binding to BCR-ABL, and hence conferring resistance to Imatinib *in vitro*. This is a significant mechanism to Imatinib resistance, because the mutation T315I has been seen in many patients with Imatinib resistance.

Some of the mutations in the Abl domain of BCR-ABL that are associated with Imatinib resistance. Both Abl and Src shift between an inactive or a closed conformation and a catalytically active or open conformation (Litzow, 2006). It has also been shown that Imatinib binds BCR-ABL in an inactive state (Schindler *et al.*, 2000). Mutations conferring

Imatinib resistance fall into two groups; (1) those that change amino acids in direct contact with Imatinib, and (2) mutations that prevent BCR/ABL from achieving a conformational state that is inactive and required for Imatinib binding. The mutations in the second group will increase the ability to induce autophosphorylation, and a growth advantage to Ph⁺ cells even in the absence of Imatinib. Mutations within the P-loop are among the most common (Nardi *et al.*, 2004).

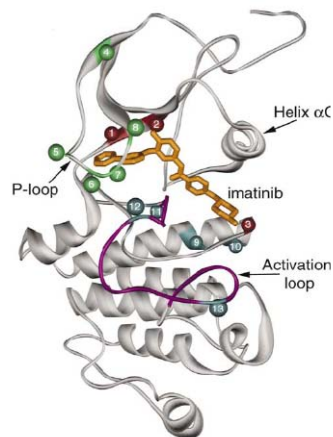


Figure 7 - Proposed mechanisms of action of Imatinib-resistant mutations based upon the crystal structure of the Abl kinase domain complexed with Imatinib. Ribbon representation of the Abl kinase domain complexed with Imatinib (Nagar *et al.*, 2002)

Imatinib is depicted in gold. Amino-acid residues implicated in resistance are enumerated. Spheres 1–3 (red) represent mutations that directly affect Imatinib binding. All remaining spheres are likely to affect the ability of the kinase to adopt the conformation required for binding Imatinib, including those in the P-loop (4–8; green) and those in the vicinity of the activation loop (9–13; cyan). The activation loop is colored purple. The positions of amino acids are as follows: 1, F317L; 2, T315I; 3, F359; 4, M244; 5, G250; 6, Q252; 7, Y253; 8, E255; 9, M351; 10, E355; 11, V379; 12, L387; 13, H396. F311 is not depicted. V379I has been detected in a patient who failed to achieve a cytogenetic response, but has thus far not been implicated in acquired resistance to Imatinib.

1.5.4 Strategies to overcome resistance towards kinase inhibitors

As outlined above, the possibilities to overcome resistance towards a particular kinase inhibitor by choosing a second or third inhibitor might finally fail. Therefore, a closer look to other critical functions of the BCR/ABL fusion protein itself or to the BCR/ABL activated signaling pathways is now undertaken. Strategies under investigation include: the tetramerization interface (Beissert *et al.*, 2008; Beissert *et al.*, 2003), targeting the substrate binding site, the allosteric site and downstream pathways (for review (Quintas-Cardama *et al.*, 2007).

Regarding the inhibition of T315I all these approaches show promising effects in preclinical trials. As BCR/ABL results in the simultaneous activation of various signaling pathways that contribute to the disease phenotype, the selective inhibition of singular downstream targets might be clinically disappointing, as it happened in the case of RAS inhibitors (Quintas-Cardama *et al.*, 2007; Walz and Sattler, 2006). Therefore targets within the BCR/ABL molecule (upstream targets) might be more promising.

1.5.5 Targeting the tetramerization domain of BCR/ABL

From the point of view of c-ABL, the structurally most dramatic consequence of the fusion to BCR is the enforced tetramerization mediated by the BCR coiled-coil (CC), which leads to the constitutive activation of the ABL-TK domain (McWhirter *et al.*, 1993; Tauchi *et al.*, 1997). The CC domain encompasses the N-terminal 72 amino acids (a.a.) of BCR. It consists of a short N-terminal Helix-alpha-1 (a.a. 5-15) followed by a flexible linker (a.a. 16-27) and subsequently by the larger Helix-alpha-2 (Helix-2) (a.a. 28-67). The interaction between BCR or BCR/ABL monomers is mediated basically by the direct interaction of Helix-2 (Zhao *et al.*, 2002). The importance of the CC is illustrated by the fact that its deletion reduces the BCR/ABL-TK-activity to such an extent that CC-deletion mutants (delta-CC-BCR/ABL) do no longer induce an MPD in mice. Delta-CC-BCR/ABL rather induces T-cell leukemia or lymphoma with a 5 to 6 fold longer mean latency than the MPD induced by BCR/ABL (Zhang *et al.*, 2001). Although Delta-CC-BCR/ABL transduced murine hematopoietic cell lines acquire factor-independence the growth rates are greatly reduced (Beissert *et al.*, 2003; Zhang *et al.*, 2001) and fibroblasts expressing Delta-CC-BCR/ABL are not transformed (Beissert *et al.*, 2003; Zhang *et al.*, 2001).

First indications that a competitive inhibition of the tetramerization is a promising approach were revealed in a study showing that the co expression of the first 160 a.a. of BCR (BCR1-160) reduces the transformation potential of BCR/ABL (Guo *et al.*, 1998). Furthermore it was shown that the hetero-oligomerization of BCR/ABL with over expressed BCR inhibits the TK-activity of the fusion protein (Lin *et al.*, 2001). Our group has shown that the first 63 a.a. (BCR1-63) are sufficient for the hetero-oligomeric inhibition of BCR/ABL (Beissert *et al.*, 2003). Within the CC, the amino acid (a.a.) residues 5–15 and 28–67 form helices (Helix alpha 1 and alpha 2) separated by a flexible loop. The dimer interface is formed by the direct interaction of Helices-2 of both monomers, while Helix-1 from one monomer swings back and packs against the “outside” of the Helix-2 dimer and interacts with Helix-2 of the other monomer (Zhao *et al.*, 2002). Helix-2 deletion leads to impaired oligomerization and reduced

kinase activity (Smith *et al.*, 2003), suggesting a fundamental role of Helix-2 for the biology of BCR/ABL.

1.5.6 Targeting the Coiled coil (CC) enhances the effect of Imatinib and inhibits mutant BCR/ABL

Upon CC deletion BCR/ABL is no longer forming tetramers (McWhirter *et al.*, 1993). Therefore the deletion of the CC could be regarded as an experimental monomerization of BCR/ABL. Delta-CC-BCR/ABL monomers show a severely reduced kinase activity (Zhang *et al.*, 2001). Imatinib binds to the inactive conformation of the ABL-TK domain (Schindler *et al.*, 2000). Accordingly, monomeric delta-CC-BCR/ABL is very sensitive towards Imatinib (Beissert *et al.*, 2003). Hetero-oligomers of BCR/ABL and BCR1-63 peptides in a 1:3 ratio can be interpreted as BCR/ABL monomers. Consistent with this hypothesis BCR1-63 significantly increases the sensitivity of BCR/ABL towards Imatinib (Beissert *et al.*, 2003).

The transformation potential of BCR/ABL is dependent on the ABL-kinase activity ((Lugo *et al.*, 1990), which in turn is activated by and dependent on tetramerization (McWhirter *et al.*, 1993; Zhang *et al.*, 2001). As it is known that Imatinib binds to the inactive conformation of the ABL-kinase domain (Schindler *et al.*, 2000), we hypothesized and proved that the experimental monomerization of BCR/ABL through the deletion of the CC-domain leads to a dramatic increase of the Imatinib-sensitivity of BCR/ABL (Beissert *et al.*, 2003).

It has been shown that the hetero-oligomerization of full length BCR or the first 160 a.a. of BCR (BCR1-160) with BCR/ABL inhibit the TK-activity and revert the BCR/ABL mediated transformation (Guo *et al.*, 1998; Lin *et al.*, 2001). We deduced from these data that the formation of hetero-oligomers of BCR/ABL with either BCR or the truncated construct is regarding the consequences for the ABL-part of the fusion protein similar to the experimental monomerization by CC deletion. Consequently it has been shown by our group that CC-derived peptides (i.e. BCR1-63) that hetero-oligomerize with BCR/ABL are sufficient to inhibit the TK-activity of BCR/ABL and subsequently the transformation potential. Furthermore, consistent with the data obtained with the monomeric CC-deletion mutant. CC-derived peptides increase the sensitivity of BCR/ABL towards Imatinib. It is clear that the CC-domain is a suitable target for the inhibition of BCR/ABL and that targeting the tetramerization represents a potential therapeutic option for the future (Beissert *et al.*, 2003).

1.5.7 Allosteric inhibition of BCR/ABL

The activation status of wild-type c-ABL by autophosphorylation is finely regulated by several regulation signals. Myristoylation of the N-terminus of c-ABL is involved in

regulation of the ABL kinase activity. The N-terminus of ABL is myristoylated, and the myristate residue binds to a hydrophobic pocket in the kinase domain (Myristoyl binding pocket, MBP), a process called “capping” (Hantschel *et al.*, 2003). The “capping” leads to conformational changes, that allows the intra-molecular docking of the SH2 domain to the kinase domain. Hence, c-ABL takes on an auto-inhibited conformation. The N-terminal auto-inhibitory ‘Cap’ region is absent in BCR/ABL, and the absence of this ‘Cap’ might allow the fusion protein to “escape” auto-inhibition (Hantschel and Superti-Furga, 2004). This lack of auto-inhibition mainly contributes to the constitutive activation of BCR/ABL (Hantschel and Superti-Furga, 2004). The absence of an N-terminal myristoylated domain activates c-ABL, consistent with its auto-regulatory role (Franz *et al.*, 1989).

In order to discover agents capable of targeting the BCR/ABL kinase via a mechanism distinct from ATP competition, an unbiased differential cytotoxicity screen of a combinatorial kinase-directed heterocyclic library led to the identification of a new class of BCR/ABL inhibitors. One of these compounds, GNF-2, (Figure 8) is a cell-permeable pyrimidine compound that binds to MBP and acts as an allosteric, non-ATP-competitive inhibitor of BCR/ABL. It possesses exclusive anti-proliferative activity against BCR/ABL-expressing factor-independent cells (Adrian *et al.*, 2006). It inhibits BCR/ABL phosphorylation with an IC_{50} of 267 nM, but does not inhibit a panel of 63 other kinases, including native c-Abl, and shows complete lack of toxicity towards cells not expressing Bcr-Abl. Unfortunately; GNF-2 is unable to overcome the resistance of BCR/ABL harboring the T315I mutation (Adrian *et al.*, 2006).

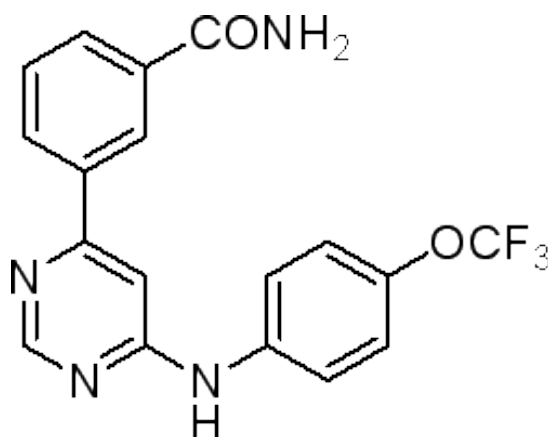


Figure 8: Structure of GNF-2

1.6 Dissertation Hypothesis and Aims

The major oncogenes of Philadelphia chromosome positive (Ph1) leukemia is the BCR/ABL fusion protein. BCR/ABL is characterized by a deregulated and constitutively activated ABL tyrosine kinase (TK) activity (Faderl *et al.*, 1999). Multiple downstream signaling pathways activated by BCR/ABL including RAS, JAK/STAT, phosphatidylinositol-3-kinase (PI3K) and MYC (Deininger *et al.*, 2000; Faderl *et al.*, 1999; Sattler *et al.*, 1996) contribute to the transformation potential of BCR/ABL. The expression of BCR/ABL alone is sufficient to induce a leukemic phenotype in mice (Huettner *et al.*, 2000; Kelliher *et al.*, 1990). Cellular transformation and leukemogenesis are strictly dependent on the TK activity of BCR/ABL (Deininger *et al.*, 1997; Druker *et al.*, 1996; Lugo *et al.*, 1990; Weisberg and Griffin, 2000).

Molecular targeted therapy with the ABL-kinase inhibitor Imatinib Mesylate (Imatinib) induces complete hematological and cytogenetic remissions in the majority of Ph+ leukemia patients (O'Dwyer *et al.*, 2003). A growing concern is that during advanced disease stages, Imatinib-resistant relapse frequently occurs mainly because of point mutations in the ABL-kinase domain that interfere with the binding affinity of Imatinib (Cowan-Jacob *et al.*, 2004; Deininger *et al.*, 2005).

Recently, we have shown that a peptide, representing the CC (a.a 1-63), interferes with BCR/ABL tetramerization and counteracts the kinase activity and transformation potential of BCR/ABL accompanied by an increased sensitivity for Imatinib (Beissert *et al.*, 2003).

Peptide-based molecular targeting is emerging as an important therapeutic approach for treating human cancers (Selivanova *et al.*, 1997). The obvious limitations of using peptides as therapeutics are poor permeability and low selectivity. A potential strategy to overcome these limitations is the peptide transduction (PT) system, which involves conjugating the peptide of interest to a protein transduction domain (PTD), conferring the capacity to pass through the cell membrane of living cells (Fawell *et al.*, 1994). An example of a PTD is HIV-TAT, which is derived from the human immunodeficiency viral protein TAT, and contains an arginine-rich sequence of 11 a.a. (Asoh *et al.*, 2002; Schwarze *et al.*, 1999). Rapid receptor-independent uptake of TAT-conjugated peptides occurs in many cell types and animals (Cao *et al.*, 2002; Denicourt and Dowdy, 2003; Sugioka *et al.*, 2003).

There is increasing evidence that Imatinib-resistant mutations not only interfere with binding affinity to the kinase inhibitors, but also modify the biological functions of BCR/ABL. The observation that additional factors influence the transformation potential of the AKI-resistant BCR/ABL T315I mutant was supported by our recent findings on the inhibition of tetramerization of BCR/ABL and its AKI-resistant mutants. Tetramerization of ABL through

the N-terminal coiled-coil region (CC) of BCR is essential for aberrant ABL-kinase activation. Targeting the CC-domain forces BCR/ABL into a monomeric conformation, abolishes its transformation potential by interfering with its kinase activity, and increases sensitivity to Imatinib (Beissert *et al.*, 2008; Beissert *et al.*, 2003). We showed that factor-dependent hematopoietic progenitors expressing BCR/ABL harboring the Y253F and E255K mutations but not the T315I mutation responded to the inhibition of tetramerization. Together with previous findings, these results led to the hypothesis that BCR/ABL harboring the T315I mutation exhibits additional functions contributing to its leukemogenic potential that are not present in the unmutated BCR/ABL.

Myristoylation of the N-terminus of c-ABL is involved in regulation of the ABL kinase activity. The N-terminus of ABL is myristoylated, and the myristate residue binds to a hydrophobic pocket in the kinase domain (Myristoyl binding pocket, MBP), a process called “capping” (Hantschel *et al.*, 2003; Hantschel and Superti-Furga, 2004). The “capping” leads to conformational changes that allow the intra-molecular docking of the SH2 domain to the kinase domain. Hence, c-ABL takes on an auto-inhibited conformation. The N-terminal auto-inhibitory 'Cap' region is absent in BCR/ABL, and the absence of this 'Cap' might allow the fusion protein to “escape” auto-inhibition (Hantschel and Superti-Furga, 2004). This lack of auto-inhibition mainly contributes to the constitutive activation of BCR/ABL (Hantschel and Superti-Furga, 2004). The absence of an N-terminal myristoylated domain activates c-ABL, consistent with its auto-regulatory role (Franz *et al.*, 1989).

GNF-2 is a cell-permeable pyrimidine compound that binds to MBP and acts as an allosteric, non-ATP-competitive inhibitor of BCR/ABL. It possesses exclusive anti-proliferative activity against BCR/ABL-expressing factor-independent cells (Adrian *et al.*, 2006). Unfortunately, GNF-2 is unable to overcome the resistance of BCR/ABL harboring the T315I mutation (Adrian *et al.*, 2006).

The aims of the study:

- 1- To further develop the CC targeting peptide for effective inhibition
- 2- To determine how the inhibition of oligomerization interferes with the transformation potential of BCR/ABL and its Imatinib-resistant mutants.
- 3- To develop a novel cell based *in vivo* peptides delivery system

- 4- To investigate that why inhibition of oligomerization is ineffective in the case of cells expressing the BCR/ABL-T315I mutant.
- 5- To find Whether T315I confers additional features to the leukemogenic activities of BCR/ABL.
- 6- To investigated whether it is possible to overcome the resistance of the BCR/ABL-T315I mutant against molecular therapeutic approaches by combining the allosteric inhibition of GNF-2 with the competitive peptide Helix-2 to inhibit BCR/ABL oligomerization.

2 Materials

2.1 Instruments and apparatus

3MM Whatman paper	Whatman, Dassel, Germany
Autoclave	Integra Biosciences, Baar, Switzerland
Benchtop gyroory incubator shaker for bacterium	New Brunswick Scientific, Edison N.J. USA
Bacteria incubator	Heraeus, Hanau, Germany
Bandelin Sonopuls HD 2070	South Yorkshire, England
Cell culture flasks/dishes	Greiner, Heidelberg, Germany
Cell culture incubator	Heraeus, Hanau, Germany
CELL locate glass cover slips with grids, - Grid size 55 μm	Eppendorf, Hamburg, Germany
Cell scraper	Corning, Wiesbaden, Germany
Cell strainer (40 μm)	Becton Dickinson, Heidelberg, Germany
FACS (Fluorescence-activated cell sorting) Centrifuge	FACScan, Beckton Dickinson, Heidelberg
Cytocentrifuge	Thermo Shandon, Pittsburgh, USA
Rotina 48 RS Table top centrifuge -Sorvall RC- 5B refrigerated superspeed centifuge and Biofuge 13R	Hettich, Tuttlingen, Germany
Table top centrifuge 5415C	Heraeus, Hanau, Germany
Megafuge 1.0 with Rotor BS4402/A	Eppendorf, Hamburg, Germany
Chemiluminescence detection -Film BioMax	Heraeus, Hanau, Germany
Corning 125 pH meter	Eastman-Kodak, Rochester, USA
Cryotubes	Fisher Scientific, Shwerte, Germany
Cytofunnel	Nalgene, Rochester, NY , USA
Electroporation: Gene Pulser System with electroporation Cuvette 0.4 cm	Shandon, Pittsburgh, USA
Flow Chamber Kit	Bio-Rad Laboratories, Munich, Germany

-Circular parallel plate	GlycoTech, Maryland, U.S.A
Gel electrophoresis system	
-DNA-sub cell and Mini-Sub cell System	Gibco, Bethesda, USA
Power PAC 2000	BioRad, Munich, Germany
Irradiation of mice	
-Betatron 500A	Siemens, Munich, Germany
Lumat LB 9507	Berthold, Bad Wildbad, Germany
Magnetic cell separation	
-MiniMACS separator	Miltenyi, Bergisch Gladbach, Germany
-MidiMACS separator	Miltenyi, Bergisch Gladbach, Germany
-MACS separation columns: LD and LS	Miltenyi, Bergisch Gladbach, Germany
Microscope	
-SZ40 Zoom Stereo Microscope	Olympus, Munich, Germany
Axioplan II-imaging Fluorescence microscope	Zeiss, Goettingen, Germany
Leitz Labovert inverted Microscope	Leitz, Wetzlar, Germany
Zeiss ID03 inverted microscope	Zeiss, Goettingen, Germany
Nitrocellulose membrane (0.45 µm)	Bio-Rad Laboratories, Munich, Germany
PCR	
-Techne TC-312	Kisker, Steinfurt, Germany
Protein transfer	
-Trans-Blot SD Semi-dry Transfer cell	BioRad, Munich, Germany
Spectrophotometer	
-Gene Quant II	Pharmacia Biotech, Freiburg, Germany
-Ultraspec® 2000	Germany
Steril bank	Heraeus, Hanau, Germany
Steril filter	
-0.22µm	Millipore, Eschborn, Germany
-0.45µm	Millipore, Eschborn, Germany
Vortex	Eppendorf, Hamburg, Germany
Water bath	Julabo Labortechnik, Seelbach, Germany

2.2 Chemicals

Acetic acid glacia	Sigma, Steinheim, Germany
Acetone	Roth, Karlsruhe, Germany
Ammonium persulfate	Fluky, Deisenhofen, Germany
Ampicillin	Sigma, Steinheim, Germany
Anti-Sca-1 Microbeads	Miltenyi, Bergisch Gladbach, Germany
Biorad protein dye	Biorad, Munich, Germany
Borax	Sigma, Steinheim, Germany
BrdU	Sigma, Steinheim, Germany
β -Mercaptoethanol	Fluka , Deisenhofen, Germany
Bromophenol blue	Sigma, Steinheim, Germany
Calcium chloride	Sigma, Steinheim, Germany
Chloroform	Fluka , Deisenhofen, Germany
Cumaric acid	Sigma, Steinheim, Germany
ddH ₂ O	Sigma, Steinheim, Germany
DEPC	Sigma, Steinheim, Germany
DMSO	Sigma, Steinheim, Germany
EDTA, disodium, dihydrate	Sigma, Steinheim, Germany
Ethanol	Merck, Darmstadt, Germany
Ethidiumbromid	Sigma, Steinheim, Germany
Formaldehyd	Merck, Darmstadt, Germany
Forene (Isofluran)	Abbott GmbH, Wiesbaden, Germany
Glucose	Sigma, Steinheim, Germany
Glutathione sepharose TM	Amersham/Pharmacia Biotech, Freiburg, Germany
Glycerol	Sigma, Steinheim, Germany
Glycin	Merck, Darmstadt, Germany
Isopropylthio- β -D-Galactoside (IPTG)	Sigma, Steinheim, Germany
HCL	Merck, Darmstadt, Germany
Isobutanol	Sigma, Steinheim, Germany
Isopropanol	Fluka , Deisenhofen, Germany
Kanamycin	Sigma, Steinheim, Germany
Lineage cell depletion kit	Miltenyi, Bergisch Gladbach, Germany
Luminol	Fluka , Deisenhofen, Germany

Methanol	Merck, Darmstadt, Germany
Methylenbla	Sigma, Steinheim, Germany
MgSO ₄	Fluka , Deisenhofen, Germany
NaN ₃	Sigma, Steinheim, Germany
NaCl	Merck, Darmstadt, Germany
NaH ₂ PO ₄	Sigma, Steinheim, Germany
NaOH	Roth GmbH, Karlsruhe, Germany
Natriumacetat	Fluka , Deisenhofen, Germany
Paraformaldehyd	Merck, Darmstadt, Germany
p-Coumaric acid	Sigma, Steinheim, Germany
PD-10 columns	Amersham/Pharmacia Biotec, Freiburg, Germany
Phenol	Fluka , Deisenhofen, Germany
PKH26 Red fluorescence kit	Sigma, Steinheim, Germany
Polybrene	Sigma, Steinheim, Germany
Ponceau S	Sigma, Steinheim, Germany
Propidium iodide	Sigma, Steinheim, Germany
Protease-inhibitors	Roche Basel, Switzerland
Pre-stained SDS-PAGE standards	
-Broad range	Bio-Rad Laboratories, Munich, Germany
Retronectin [®]	Takara Bio Inc., Otsu, Japan
Sca-1 Isolation Kit	Miltenyi, Bergisch Gladbach, Germany
SDS	Sigma, Steinheim, Germany
STREPtactin sepharose [™]	IBA, Goettingen, Germany
Protein elution buffer	IBA, Goettingen, Germany
TEMED	Sigma, Steinheim, Germany
Tritriplex III, 1,1%	University teaching hospital Frankfurt
Trizma HCl	Sigma, Steinheim, Germany
Triton X-100	Sigma, Steinheim, Germany
Tween20	Sigma, Steinheim, Germany
Vivapore (For concentrating protein)	VivaScience, Stonehouse, UK
Xylencyanol	Sigma, Steinheim, Germany

2.3 Special reagents and materials

2.3.1 Cell culture medium and reagents

7-aminoactinomycin D (7-AAD)	Sigma, Steinheim, Germany
BSA, V solution	Sigma, Steinheim, Germany
Chloroquine	Sigma, Steinheim, Germany
DMEM, -High glucose (4.5g/l)	Invitrogen, Karlsruhe, Germany
DMSO	Sigma, Steinheim, Germany
FBS	Gibco BRL, Paisley, Schottland
Ficoll separating solution	Biochrom (# L-6115), Berlin, Germany
Gelatin	Sigma, Steinheim, Germany
GNF-2	Sigma, Steinheim, Germany
HBSS	Gibco, Karlsruhe, Germany
HEPES solution	Gibco, Karlsruhe, Germany
Horse serum	Gibco, Karlsruhe, Germany
Imatinib	Novartis, Basel Switzerland
IMD	Gibco, Karlsruhe, Germany
L-Glutamine	Gibco, Karlsruhe, Germany
Methoculttm GF M3434	StemCell Technologies, Vancouver, Canada
Mycosa	Gibco, Karlsruhe, Germany
PBS	Gibco, Karlsruhe, Germany
Penicillin-Streptomycin solution	Gibco, Karlsruhe, Germany
Retinoic acid	Sigma, Steinheim, Germany
Retronectin	Takara, Shiga, Japan
RPMI 1640	Gibco, Karlsruhe, Germany
Trypan blue stain (0.4%)	Gibco, Karlsruhe, Germany
Trypsin EDTA, 0.25% solution	Gibco, Karlsruhe, Germany

2.3.2 Chemokines and cytokines

rmG-CSF	Peprtech, Offenbach, Germany
rmSCF	Peprtech, Offenbach, Germany
rmIL-6	Peprtech, Offenbach, Germany
rmIL-3	Peprtech, Offenbach, Germany
rmGM-CSF	Peprtech, Offenbach, Germany

2.3.3 Enzymes

Calf intestinal phosphatase (CIP)	NEB, Frankfurt, Germany
Gateway LR clonase enzyme mix	Invitrogen, Karlsruhe, Germany
Klenow-Fragment DNA-polymerase I	NEB, Frankfurt, Germany
Restriction endonucleases	NEB, Frankfurt, Germany
RNase	Sigma, Steinheim, Germany
Superscript II	Invitrogen, Karlsruhe, Germany
T4 DNA-ligase	NEB, Frankfurt, Germany
Taq-DNA-polymerase	Biosystems, Weiterstadt, Germany
Proteinase K	Stratagene, La Jolla, USA

2.3.4 Polymerase Chain Reaction (PCR)

Taq-DNA-polymerase	Biosystems, Weiterstadt, Germany
DNTPs	Fermentas, St. Leon-Rot, Germany
PCR Buffer	Fermentas, St. Leon-Rot, Germany
MgCl ₂	Fermentas, St. Leon-Rot, Germany
PfU turbo polymerase	Stratagene, La Jolla, USA
Primers	Sigma, Steinheim, Germany

2.3.5 Antibodies

2.3.5.1 Primary antibodies used for western blotting

Mouse anti- β -tubulin (Ab-4)	Neo Markers, Asbach, Germany
Mouse lineage panel	PharMingen, San Diego, CA, USA
Rabbit anti-c-ABL (11/24)	Santa Cruz, Heidelberg, Germany
Rabbit anti-p-ABL-Tyr-245	Upstate-Biotechnology, Lake Placid, NY, USA
Rabbit anti-p-ABL-Tyr-412	Cell Signalling, Boston, USA
Rabbit anti-p-BCR-Tyr-177	Cell Signalling, Boston, USA
Rabbit anti-BCR(C-20)	Santa Cruz, Heidelberg, Germany
Mouse anti- GFP	Upstate-Biotechnology, Lake Placid, NY, USA
Mouse anti-phospho-STAT5	Cell Signalling, Boston, USA
Rabbit anti -STAT5	Cell Signalling, Boston, USA
Rabbit anti-phospho-CrkL (Tyr207)	Cell Signalling, Boston, USA

Mouse anti-CrkL	Cell Signalling, Boston, USA
Mouse anti-phosphotyrosine (clone 4G10)	Upstate-Biotechnology, Lake Placid, NY, USA

2.3.5.2 Secondary antibodies

Anti-mouse IgG-HRP	Santa Cruz, Heidelberg, Germany
Anti-rabbit IgG-HRP	Santa Cruz, Heidelberg, Germany

2.3.5.3 FACS antibodies

Mouse-anti-human-PE-LNGFR	BD, San Jose, CA, USA
Rat-anti- mouse-PE-Gr-1	BD, San Jose, CA, USA
Rat-anti- mouse-PE-Mac-1	BD, San Jose, CA, USA
Rat-anti- mouse-PE-B220	BD, San Jose, CA, USA
Mouse-anti-PE-IgG _{2a} , K	BD, San Jose, CA, USA
Mouse-anti-PE-IgG _{2b} , K	BD, San Jose, CA, USA
Rat –anti-Mouse FITC-Sca-1	BD, San Jose, CA, USA
Rat-anti- mouse-PE-Sca-1	BD, San Jose, CA, USA

2.3.6 Buffers

MACS buffer

20% (w/v) BSA	12.5 ml
EDTA	1mmol
Penicillin/Streptomycin	5ml
Add PBS up to	500ml

2M CaCl₂ solution

The component was dissolved in ddH₂O and sterile filtered with 0.22 µm filter and stored at -20°C in aliquots until use.

2X HBS solution

Na ₂ HPO ₄	0.315g (1.5 mM final)
HEPES	19.5g (0.05M final)
NaC	24g (0.28M final)

Water added up to 1200ml, three clean bottles were filled with exactly 400 ml of the solution, the pH to 6,95/ 7,0 / 7,05 was adjusted respectively, each bottle was filled to 500 ml, pH was controlled again. The buffer was filter-sterilized and stored at -20°C in aliquots.

1x TAE Electrophoresis buffer

Tris-Acetate 0,04M

EDTA 1 mM

Buffer W for lysis of bacteria

Tris-HCl pH 8.0 100 mM

NaCl 150 mM

EDTA 1 mM

Tween 0.1%

Protease inhibitor 1x

1X SDS gel-loading buffer

Tris-HCl, pH 6.8 50mM

SDS 2 % (w/v)

Glycerol 10% (v/v)

β -mercaptoethanol 100mM

Bromophenol blue 0.1 % (v/v)

1X SDS gel-loading buffer lacking dithiothreitol was stored at room temperature. β -mercaptoethanol from a 14 M stock was added just before the buffer is used.

For protein electrophoresis (Invitrogen life technologies, Germany)

NuPAGE Novex Bis-Tris

Tris-Acetate Pre-Cast Gels

NuPAGE Novex MES and Tris-Acetate SDS Running Buffers

NuPAGE Transfer Buffer

Precision plus protein (PPP)

NuPAGE LSD Sample Buffer

NuPAGE Reducing Agent

NuPAGE Antioxidant

10X TBS

Trizma HCl, pH 7.5 24.23 g

NaCl 80.06 g

Above materials were mixed in 800 ml water, and pH was adjusted to 7.6 with pure HCL. The volume was adjusted to 1 L with wate.

TBST

1X TBS+ 0.05% Tween 20

Blocking Buffer for immunoblot

5% Carnation non-fat dry milk in TBST

Protein transfer buffer

TrisHCl	48 mM
Glycine	39 mM
SDS	0,038 % (w/v)
Methanol	20 % (v/v)

Coomassie staining solution

Coomassie brilliant blue R250	0.1 % (w/v)
Methanol	50 % (v/v)
Glacial acetic acid	10 % (v/v)

Coomassie destaining Solution

Methanol	50 % (v/v)
Glacial acetic acid	10 % (v/v)

Ponceau S staining solution

Ponceau S	2 % (w/v)
Trichloroacetic acid	30 % (v/v)
Sulfosalicylic acid.	30 % (v/v)

ECLsolution I:

1 M TrisHCl, pH 8,5	10ml
90mM p-Coumaric acid (in DMSO)	0.44ml
250mM Luminol (in DMSO)	1ml

Water was added up to 100ml; aliquots were made and stored in the dark at -20°C.

ECLsolution II:

30 % H ₂ O ₂	64µl
1 M TrisHCl, pH 8,5	10 ml

Water was added up to 100ml, aliquot solution and store in the dark at -20°C.

Stripping buffer

Tris-HCl, pH8.0	62.5 mM
2-mercaptoethanol	100 mM
SDS	2 % (w/v)

FACS Wash Buffer

PBS + 1%FCS + 1% NaN₃

FACS Fixative Solution

PBS + 2% formaldehyde solution

Phosphate-Buffered Saline (PBS)

NaCl	137 mM
KCl	2.7 mM
Na ₂ HPO ₄	10 mM
KH ₂ PO ₄	2 mM

The above components were dissolved in water and adjusted pH to 7.4 with HCl.

Tris-HCl (1M)

121.1g of Tris base was dissolved in 800ml of water. The pH was adjusted to the desired value by adding concentrated HCl as follows:

pH	HCl
7.4	70 ml
7.6	60 ml
8.0	42 ml

The solution was allowed to cool to room temperature before making final adjustments to the pH. The volume of the solution was adjusted to 1 liter with water.

10X Tris EDTA (TE)

pH 7.4	100 mM Tris-Cl (pH 7.4)
	10 mM EDTA (pH 8.0)
pH 7.6	100 mM Tris-Cl (pH 7.6)
	10 mM EDTA (pH 8.0)
pH 8.0	100 mM Tris-Cl (pH 8.0)
	10 mM EDTA (pH 8.0)

SDS (20% w/v)

200 g of electrophoresis-grade SDS was dissolved in 900 ml of water. The mixture was heated to 68°C and stirred with a magnetic stirrer to assist dissolution. The pH was adjusted to 7.2 by adding a few drops of concentrated HCl. The volume was adjusted to 1 liter with water.

EDTA (0.5 M, pH 8.0)

186.1 g of disodium EDTA was added to 800 ml of H₂O. The mixture was stirred vigorously on a magnetic stirrer. The pH was adjusted to 8.0 with NaOH. The disodium salt of EDTA did not go into solution until the pH of the solution was adjusted to ~ 8.0 by the addition of NaOH.

Solutions for plasmid minipreparation

Resuspension solution (*Sol I*)

Glucose	50 mM
Tris-HCl pH 8.0	25 mM
EDTA pH 8.0	10 mM

Autoclaved and stored the solution at 4°C

Alkaline lysis solution (*Sol II*)

NaOH	0.2 M
SDS	1 % (w/v)

Sol II was prepared fresh and used at room temperature

Neutralization solution (*Sol III*)

5 M Potassium acetate	60 ml
Glacial acetic acid	11.5 ml
ddH ₂ O	28.5 ml

The solution was stored at 4°C and transferred to ice before use

0.1% Diethylpyrocarbonate (DEPC)

1 g DEPC was dissolved in 1 L water and mixed it vigorously. It let stand with loose lid overnight at room temperature or at 37°C for 1h and autoclaved for 15 minutes at 15 psi on liquid cycle. DEPC cannot be used to treat Tris buffer.

2.3.7 Plasmids and vectors

pCDNA 3.1 vector	Invitrogen GmbH, Karlsruhe, Germany
pEntr1A	Invitrogen GmbH, Karlsruhe, Germany
PINCO	Retroviral hybrid vector with LTR derived from Moloney murine Leukemia virus. The main characteristics of this vector is the presence of the EBV origin of replication and the EBNA-1 gene and the presence of the cDNAs that encodes for the EGFP, controlled by a cytomegalovirus promoter. This vector allows high-efficiency gene transfer (Grignani <i>et al.</i> , 1998).
PAULO	This vector is a modified pinco vector in which GFP is replaced by LNGFR
PIDE	This vector is based on pinco vector in which GFP is deleted and Hind III site can be used for cloning gene instead of GFP
PincoΔCMV	Retroviral pinco based vector without any reporter gene

pPRIBA2	IBA, Gottingen , Germany
pGEX4T3	Amersham Biosciences, Freiburg, Germany

2.3.8 Bacterial *E.Coli* Strain and genotype

E. coli – HB101, BL21, JM83, DB 3.1, Invitrogen, Karlsruhe, Germany

2.3.9 Medium for bacterium

LB medium

Bacto-Tryptone	1 % (w/v)
Bacto-Yeast-Extrac	0.5 % (w/v)
NaCl	1.5 % (w/v)

Adjuted pH to 7.4 with NaOH and autoclaved

LB agar plates

Bacto-Agar	1.5 % (w/v)
------------	-------------

Bacterium freezing solution

Glycerin	65 % (v/v)
MgSO ₄	0.1 M
TrisHCl, pH 8.0	0.025M
SOC	Invitrogen, Karlsruhe, Germany

2.3.10 Cell lines

2.3.10.1 Ph+ cells

CML blast cell lines

In CML cells, the translocation product encodes for p210^{BCR/ABL}.

BV173: Human B cell precursor leukaemia cell line, established from the peripheral blood of a patient with chronic myeloid leukaemia (CML) in lymphoid blast crisis. Contains the t(9;22) b2-a2 fusion gene. Obtained from DSMZ, Germany

K562: Established from the pleural effusion of a patient with chronic myeloid leukaemia (CML) in myeloid blast crisis. Cells carry the Ph chromosome with the Bcr-Abl b3-a2 fusion gene. Obtained from DSMZ, Germany

Ph+ ALL

In Ph+ cells, the translocation product encodes for p185^{BCR/ABL}.

Sup-B15: Human B cell precursor leukemia cell line, established from the bone marrow of a patient with acute lymphoblastic leukemia, carrying the ALL-variant (m-bcr) of the BCR/ABL fusion gene (e1-a2). Obtained from DSMZ, Germany

Tom-1: human B cell precursor leukemia. Established from the bone marrow of a patient with refractory Ph chromosome acute lymphoblastic leukemia (ALL); described to carry the ALL-variant (m-BCR) of the BCR/ABL fusion gene (e1-a2) obtained from DSMZ, Germany.

2.3.10.2 Other Cell lines

Nalm-6: Human lymphoblastic B cell line; Ph-

Ba/F3: IL-3 dependent murine pro B cell line established from peripheral blood; apparently derived from BALB/c mouse.

32D: IL-3 dependent murine myeloid cell line established from peripheral blood.

Rat-1: Rat fibroblast cells line

293T: Transformed human embryonal kidney cell line

Phoenix: Based on the 293T cell line (transformed human embryonal kidney cell line). Expresses the retroviral structural genes *gag*, *pol* und *env*. It is also known as a packaging cell line. The ecotropic packaging cell line delivers genes only to dividing murine or rat cells.

All cells were obtained from the “Deutsche Sammlung von Mikroorganismen und Zellkulturen GmbH” (DSMZ) (German Collection of Microorganisms and Cell Cultures), with the exception of the ecotrophic Phoenix cells which were obtained from Nolan lab, Standford, USA.

2.3.11 Medium for Cell culture

L-glutamine 1 % (v/v)

FBS 10 % (v/v)

Penicillin/Streptomycin 1 % (v/v)

Added to DMEM and RPMI medium for adherent and suspension cells respectively

Medium for 32D/Baf3 cells

L-glutamine 1 % (v/v)

FBS 10 % (v/v)

Penicillin/Streptomycin 1 % (v/v)

mIL-3 10 ng /ml

Added the above to RPMI medium

Medium for Nalm-6, BV-173 and K562

L-glutamine 1 % (v/v)

FBS 10 % (v/v)

Penicillin/Streptomycin 1 % (v/v)

Added the above to RPMI medium

Medium for Tom-1

L-glutamine 1 % (v/v)

FBS 20 % (v/v)

Penicillin/Streptomycin 1 % (v/v)

Added the above to RPMI medium

Medium for Sup-B15

L-glutamine 1 % (v/v)

FBS 20 % (v/v)

Penicillin/Streptomycin 1 % (v/v)

Added the above to Mycosa medium

Medium for Sca1+/lin- mouse BM cells

L-glutamine 1 % (v/v)

FBS(Hyclon) 10 % (v/v)

Penicillin/Streptomycin 1 % (v/v)

mIL-3 20 ng /ml

mIL-6 20 ng /ml

mSCF 100 ng /ml

Added the above to ISCOVE medium

Cell freezing medium

Solution I

RPMI/DMEM 70 % (v/v)

FBS 30 % (v/v)

Solution II

RPMI/DMEM 80 % (v/v)

DMSO 20 % (v/v)

2.3.12 Materials for animal experiments

2.3.12.1 Mice

The C57BL/6N mice (age between 6-8 weeks, all female) were purchased from Charles River Laboratories GmbH in Munich, Germany and served as the recipient mice for all the animal experiments.

2.4 Miscellaneous

Nucleospin ^R Mini plasmid DNA isolation Kit	Macherey-Nagel, Dueren Germany
Nucleospin ^R Maxi plasmid isolation kit	Macherey-Nagel, Dueren Germany
Gel cleaning kit	Macherey-Nagel, Dueren Germany
PCR cleaning kit	Macherey-Nagel, Dueren Germany
Qiagen gel extraction Kit	Qiagen, Duesseldorf, Germany
Qiagen Plasmid kit Mini, Midi and Maxi	Qiagen, Duesseldorf, Germany
Qiagen PCR purification Kit	Qiagen, Duesseldorf, Germany
Quick change site mutagenesis kit	Stratagene, La Jolla, USA
Endo Toxin removal kit	Profos AG, Regensburg, Germany
Cell proliferation (XTT) kit	Amersham/Pharmacia Biotech, Freiburg, Germany
Protein concentrator (Vivapore)	VivaScience, Hannover, Germany

3 Methods

3.1 Preparation of plasmid DNA

3.1.1 Transformation of *E.coli*

A frozen vial of competent *E.coli* bacteria was thawed on ice. The transforming DNA (up to 25ng per 50ul competent bacterium or 10ul ligation product) was pipetted directly to competent *E.coli* bacteria and mixed by swirling the tubes gently several time. Bacteria were left on ice for 30 minutes and then exposed to 42°C heat shock for exactly 2 minutes. The vial was removed from 42°C immediately and put on ice for 2min, 500µl of SOC medium (without antibiotic) was added and the tube was transferred to a shaking incubator set at 37°C. The culture was incubated for 45min to allow the bacterium to recover and express antibiotic resistant marker encoded by plasmid. 1/10 of the transformed cells were spread on a LB agar plate containing antibiotics. The plate was incubated for 16 hours at 37°C and individual colonies were identified.

3.1.2 Bacterium growth in liquid media

3.1.2.1 Growing an overnight culture

To make an overnight saturated culture of *E. coli*, inoculate 2ml liquid LB medium containing antibiotics with a single colony quickly to minimize contact of the tube with the possibly contaminated air. Grow the culture at 37°C with vigorous agitation (~220 rpm) until the culture is freshly saturated which normally takes at least 6 hours.

3.1.2.2 Growing larger cultures

Larger cultures are generally inoculated with overnight cultures diluted 1:100. Use an Erlenmeyer or baffle flask whose volume is at least 5 times the volume of the culture. Grow the culture at 37°C with vigorous agitation (~300 rpm) to ensure proper aeration.

3.1.3 Miniprep: a small scale preparation of plasmid DNA

Mini preparation of the plasmids was performed with Nucleobond® AX Mini preparation kit according to the manufacturer's instructions. The Nucleobond® AX Miniprep procedure are based on a modified alkaline lyses procedure, followed by binding of plasmid DNA to Nucleobond Anion-Exchange Resin under appropriate salt concentrations and pH conditions.

3.1.4 Maxi prep: a large scale preparation of plasmid DNA

Maxi preparation of the plasmids was performed with Nucleobond® AX Maxi preparation kit according to the manufacturer's instructions. The Nucleobond® AX Maxiprep procedure are based on a modified alkaline lysis procedure, followed by binding of plasmid DNA to Nucleobond Anion-Exchange Resin under appropriate salt concentrations and pH conditions.

3.1.5 Determining of DNA yield and quality

Plasmid yield is measured by UV spectroscopy using the following relationship: 1 OD at 260 nm (1 cm path length) is equivalent to 50 µg plasmid DNA/ml. Plasmid quality is checked initially by running a 1% agarose gel. This will give information on percentage of super coiled form of isolated plasmid DNA. Plasmid quality is further checked by UV spectroscopy (quotient 260 nm/ 280 nm). A ratio of 1.80-1.90 is an indication for pure plasmid DNA.

3.1.6 Enzymatic Modification of Nucleotide Acids

3.1.6.1 Restriction digestion of Plasmid DNA

The restriction endonucleases used for restriction of plasmid DNA belong to the type II endonucleases, which can recognize short DNA sequences and cleave double stranded DNA at specific sites. Thereby either blunt ends or sticky ends can be obtained. Restriction endonuclease cleavage is accomplished simply by incubating the enzymes with DNA in the appropriate reaction conditions. 0.5 µg – 1 µg plasmid-DNA was used for one restriction reaction. The DNA was incubated together with 5-fold excess of enzyme (5-10U enzyme/µg DNA) and appropriate restriction buffer for 1-2 hours at 37° C.

3.1.6.2 Dephosphorylation of Linear Plasmid-DNA by Alkaline Phosphatase CIP (Calf Intestinal Phosphatase)

This method was used to decrease self-ligation of the cut plasmid DNA. The CIP-treated fragments lack the 5' phosphoryl-termini, which are required by ligases for proper ligation.

The reaction was performed by incubating cut plasmid DNA with CIP-buffer and 1 µl (0.5 U/µg vector) CIP at 37° C for 1 hour. The following phenol-chloroform extraction or gel extraction was performed to purify the DNA fragments.

3.1.6.3 Fill-in of 5'-Overhangs to form blunt ends by Klenow-Reaction

The 5' overhang of DNA ends were filled up by Klenow-fragment, a large subunit of the DNA polymerase I of *E. coli*. The enzyme is active in all the NEB buffers and was incubated with the restricted DNA (1 U/µg DNA) and dNTPs for 15 minutes at 25° C. The enzyme activity

was stopped by adding EDTA to a final concentration of 10 mM and heating at 75° C for 20 minutes.

3.1.6.4 Ligation of DNA Fragments

DNA fragments and vector were ligated with T4 DNA ligase. T4 DNA ligase catalyses the formation of a phosphor-diester bonds between juxtaposed 5' phosphate and 3' hydroxyl termini in duplex DNA. 15 µl reaction was done with 25-50 ng vector, 3-5 fold molar excess of insert, 1.5 µl 10x ligase buffer and 1 U T4 DNA ligase overnight at 16°C and 7,5 µl of the reaction was used for the transformation with chemically competent *E.Coli* .To control for the self-ligation an additionally vector-only ligation reaction was included.

3.1.6.5 Quick change site-directed mutagenesis

The *in vitro* site-directed mutagenesis protocol used is a modification of *Stratagene's* Quick-change site-directed mutagenesis Kit protocol. This technique was used for vector modifications. With this technique, point mutations were introduced. The mutagenic polymerase chain reactions were performed using *PfuTurbo* DNA polymerase.

3.1.6.6 Recombination („gateway LR clonase enzyme kit“from Invitrogen)

This technique is based on the recombination reactions of the bacteriophage λ vector and makes use of a special Enzyme Mix (Integrase and Excisionase of the bacteriophage λ; and Integration Host Factor from *E. coli*). The Gateway cloning mechanism includes a BP Reaction (PCR fragment (contains attB sites) + Donor vector (contains attP sites) = Entry Clone (gene of interest flanked by attL sites), followed by an LR reaction (Entry Clone ,gene of interest flanked by attL sites) + Destination Vector (contains attR sites) = Expression Clone). Sequences known as attachment sites (att sites) are the points where excision and integration occurs.

The recombination reaction generates two molecules. One molecule contains the DNA segment of interest, the other molecule is a by-product.

The Recombination reactions are carried out with the Gateway LR-clonase enzyme kit (Invitrogen, Karlsruhe, Germany). 4 µl of LR-reaction buffer was pipetted (composition not mentioned by manufacturer), 300 ng Entry clone DNA (pEp185^{BCR/ABL} or mutant plasmids), 300 ng Destination vector DNA (PINCO) and made up to 16µl with TE-buffer (10 mM Tris-HCl, pH7,4; 1 mM EDTA, pH8,0), mixed by pipetting.4 µl LR-Clonase Enzyme Mix was added, mixed and incubated for 1 hour at room temperature. Finally, *E. coli* HB101 competent cells were transformed using 4µl of the reaction mixture and plasmid DNA was prepared for transfection and infection.

3.1.6.7 Cloning of Gateway Destination vector

For the recombination reaction, the pinco, paulo, PIDE, pPRIBA2 or pGEX4T3 vectors were converted into a Destination vector using the gateway reading frame cassettes i.e. RFA, RFB or RFC (Invitrogen, Karlsruhe, Germany).

3.1.7 Electrophoretic separation of DNA

DNA was separated electrophoretically on agarose gels for the following reasons: to control the progression of a restriction enzyme digestion, determine the yield and purity of the DNA preparation, check the products of the PCR reaction, or purify the DNA fragments. Concentration of agarose gels ranged from 0.5% to 3%, depending on the size of a desired fragment. Agarose was mixed with 1X TAE buffer and heated in a microwave until completely dissolved. This solution was cooled down to 50°C, added ethidium bromide to a final concentration of 1 µg/ml, and poured into a gel tray. Samples were mixed with 6X DNA loading buffer and electrophoresis was carried out in 1X TAE buffer at 5 V/cm. Following electrophoresis, gel was exposed to UV light ($\lambda=320\text{nm}$) to visualize the ethidium bromide-stained DNA fragments, and fragment length determined by comparing to DNA marker (Sambrook and Russel, 1989).

3.1.8 Cloning of the used Plasmids

3.1.8.1 Cloning of Eukaryotic expression plasmids

All cDNAs encoding p210^{BCR/ABL} as well as p185^{BCR/ABL} and its mutants have been described previously (Beissert *et al.*, 2008; Beissert *et al.*, 2003; Puccetti *et al.*, 2000). All retroviral expression vectors used in this study were based on the bi-cistronic vectors PINCO or PAULO converted into Gateway[®]-destination vectors by the introduction of a Gateway[®] cassette according to the manufacturer's instructions (Invitrogen, Karlsruhe, Germany). All related inserts were available in the Gateway[®] entry-vector (pENTR1A) for recombination into the destination vectors using the "LR-clonase" enzyme kit (Invitrogen). The mutant constructs were prepared using the following strategies and the modular organization of these constructs is shown in figure 9.

Δ CC constructs

Δ CCp185-Y253F, Δ CCp185-E255K, Δ CCp185-T315I, Δ CCp185-T315I, Δ CCp210 and Δ CCp210-T315I were generated by substituting the sequence encoding the first 63 aa of p185^{BCR/ABL} by a Kozak-consensus by using the following primers: 5'-ATCTACCTGCAGACGACGATGGCCAAG-3' and 5'-ATGGCCCTTGCGGATCCGCTCG-3' (the Kozak

consensus at the start codon and the BamHI site are underlined). The resulting fragments were cloned into BamHI-digested p185-Y253F, p185-E255K, and p185-T315I and p210BCR^{/ABL} sequences.

BCC/ABL-T315I

BCC/ABL-T315I was cloned by “megaprimer” PCR. First, PCR was performed with the primers Pr1 5′-CCACCATGGTGGACCCGGTGGGCTTC-3′ (start-codon underlined) and Pr2 5′-CGCTGAAGGGCTTCTTCAGCAACGTCTGCAGGT-3′ (ABL sequences, *BCR-sequences*). The resulting “megaprimer” and the primer Pr3 5′-AGGCCCATGGTACCAGGAGTG-3′ were used in a second PCR round, and the resulting fragment was cloned into a KpnI-digested pEp185-T315I.

#ABL and #ABL-T315I

For constructing the ABL part of BCR-ABL (#ABL and #ABL-T315I), the start codon and Kpn1 sites were introduced at the ABL-part by PCR using the primers Pr4 5′-AAGGTACCACCATGGAAGCCCTTCAGCGGCCAGTAGCATCTGACTTTGAGC-3′ (Start-codon and Kpn1 underlined) and Pr3 5′-AGGCCCATGGTACCAGGAGTG-3′ (Kpn1 site underlined). The resulting PCR products were controlled by sequencing and cloned into the KpnI-digested p185 and p185-T315I sequences, respectively.

ΔSH3-ABL and ΔSH3-ABL-T315I

ΔSH3-ABL and ΔSH3-ABL-T315I were constructed by digesting the constructs pEΔCCp185 and pEΔCCp185 -T315I with HincII followed by recircularization. Linker 5′-gaccaccatggagaaacactcctgtac was ligated to the recircularized plasmids with Kpn1 and HincII to introduce a Kozak consensus sequence.

BCR (1-196)/ABL and BCR(1-196)/ABL-T315I

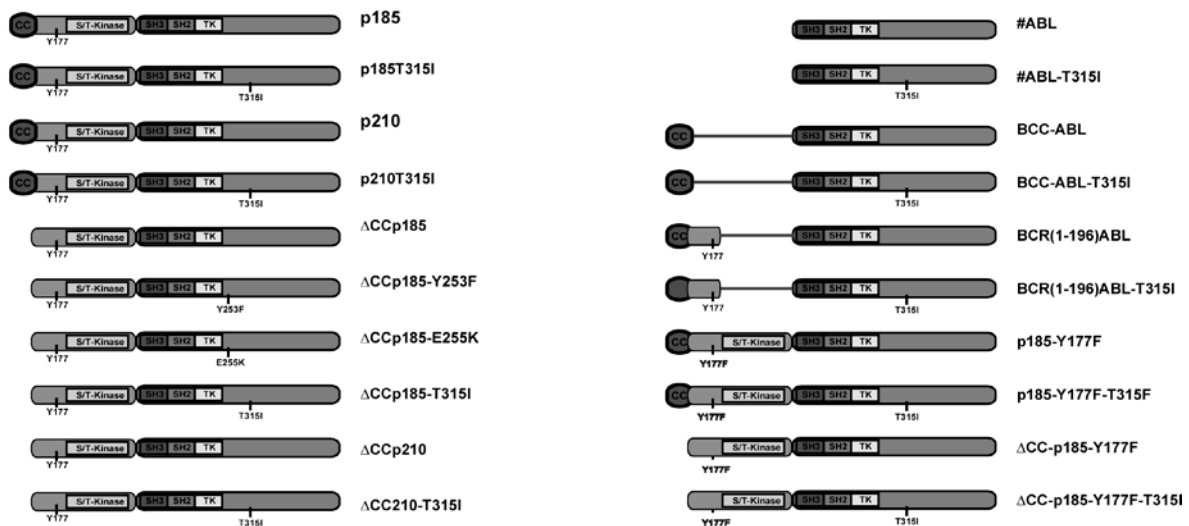
In order to construct BCR(1-196)/ABL and BCR(1-196)/ABL-T315I, two PCR rounds were performed, first with primers pr5 5′-TTCTAAAGCTTCACCTCTTTGTCGTTGACC-3′ and pr6 5′-AAATGGATCCGGTACCATGGTGGACCCGGTGG-3′ and then with pr7 5′-ATCATGAAGCTTGAAGAAGCCCTTCAGCGG-3′ and Pr3 5′-AGGCCCATGGTACCAGGAGTG-3′ (Kpn1 site underlined). The resulting products were controlled by sequencing and ligated and subcloned into KpnI-digested pEp185 and pEp185-T315I.

p185Y177F and p185Y177F-T315I

In order to construct p185Y177F and p185Y177F-T315I, three PCR rounds were performed: first with the primers pr8 5′-CCTGTTAGTTAGTTACTTAAGCTCG-3′ and pr9 5′-TGAAACTCGACGTTACGAAGAAGGGCTTCTCG-3′, second with the primers pr10 5′-AGAAGCCCTTCTTCGTGAACGTCGAGTTTACC -3′ and Pr3 5′-AGGCCCATGGTACCAGGAGTG-3′,

and finally, PCR products 1 and 2 were used as primers without a template. The full-length p185Y177F and p185Y177F-T315I products were completed by ligating the third PCR products using the KpnI-site of p185^{BCR/ABL} p185-T315I cDNA.

A



B

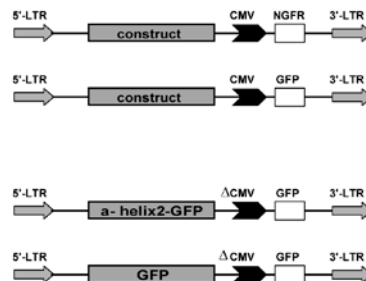


Figure 9 – Different constructs used in the study: A Modular organization of the p185^{BCR/ABL} and p210^{BCR/ABL} and their mutants lacking different functional domains. B Schematic presentation of different retroviral constructs

ΔCCp185-Y177F and ΔCCp185 Y177F-T315I

To construct double mutant ΔCCp185-Y177F and ΔCCp185 Y177F-T315I, pEΔCC p185 was cloned into BamHI-digested p185Y177F and p185Y177F-T315I. All other constructs have been described previously (Beissert *et al.*, 2008; Beissert *et al.*, 2003).

3.1.8.2 Cloning of prokaryotic expression plasmids

All expression vectors used in this study were based on pPRIBA2, which provides an in-frame Strep Tag as well as a His-tag (IBA - BioTAGnology, Goettingen, Germany). pPRIBA2 was converted into a Gateway®-destination vector by the introduction of a

Gateway® cassette, according to the manufacturer's instructions (Invitrogen, Karlsruhe, Germany). All related inserts were available in the Gateway® entry-vector (pENTR1A), and were shuttled into the destination vectors using the "LR-clonase" enzyme kit (Invitrogen). The pENTR1A with GFP and the Hfelix-2-GFP fusion peptide (pE-GFP and pE-H2-GFP, respectively) have been previously described [13]. For the generation of the HIV-TAT-H2GFP fusion peptides (here referred to as MPH-2), the following linkers were used 5'-GCGCCTACGGCCGCAAGAAGCGACGTCAGAGACGACGCGTCAAC-3' and 5'-TATCGTTGACGCGTCGTCTCTGACGTCGCTTCTTGCGGCCGTAG-3'. Retro-HIV-TAT-H2GFP fusion peptides were generated using the linkers 5'-GCGCCCGAAGACGCCAACGAAGGAAGAAACGGGTCAAC-3' and 5'-TATCGTTGACCCGTTTCTTCCTTCGTTGGCGTCTTCGG-3'. The resulting PCR products were all confirmed by sequencing, and were cloned into the pPRIBA2 vector using a BsaI site, and recombined with pE-GFP and pE-H2GFP. The pPRIBA2-GFP and pPRIBA2-H2-GFP vectors were constructed by directly shuttling pE-GFP and pE-H2GFP into the pPRIBA2 vector.

3.2 Immunoblot

3.2.1 Lysis of cells (Sambrook *et al.*, 1989)

Cells were washed twice with cold PBS, collected by centrifugation (2000 x g for 10 minutes at 4°C) and lysed by adding approximately 100µl of SDS lyses buffer per million cells. In the case of primary mouse bone marrow cells, SDS lysis buffer at 80°C can be used. After 10 minutes incubation on ice, lysates were cleared by centrifugation at 14000 x g for 15 minutes at 4°C. The supernatants were transferred to the fresh tubes and stored by -80°C.

3.2.2 Determining of protein concentration

Protein concentrations were determined by Bradford-assay with Bio-Rad protein detection kit according to the manufacturer's instruction and quantified with a spectrophotometer at 595 nm. The standards for protein concentration were prepared with different concentrations of BSA (0.5 to 10mg/ml).

3.2.3 SDS-polyacrylamide gel electrophoresis (SDS-PAGE)

A very common method for separating proteins by electrophoresis uses a discontinuous polyacrylamide gel as a support medium and SDS to denature the proteins. The method is called sodium dodecyl sulfate polyacrylamide gel electrophoresis (SDS-PAGE). SDS is an anionic detergent. A polypeptide chain binds amounts of SDS in proportion to its relative

molecular mass. The negative charges on SDS destroy most of the complex structure of proteins, and are strongly attracted toward an anode (positively-charged electrode) in an electric field. Their net migration through gel is determined not by the electrical charge but by molecular weight,

Mini Protean II® (8.5cm X 6.5cm) apparatus was assembled by using two glass plates and side spacers. The resolving gel was mixed in acrylamide-bisacrylamide concentration that matches protein weight (Sambrook *et al.*, 1989), and poured between the two glasses. Isobutanol saturated with ddH₂O was laid over to ensure a flat surface and prevent trapping of air bubbles. After the gel has polymerized, isobutanol was washed out and stacking gel laid over. Samples were prepared by mixing 50µg of total protein with sample buffer in the 25µl end volume, heated for 5 minutes at 80⁰C and briefly collected to the bottom.

Electrophoresis was run for approximately 1 hour, at a constant voltage of 150V. After the electrophoresis, gel was stained in Coomassie-blue for visualizing separated proteins.

3.2.4 Transfer of proteins onto a nitrocellulose membrane (Western blot)

Following electrophoresis, proteins were transferred to the 0.2µm nitrocellulose membranes in a process called Western blotting. This transfer was carried out between the two horizontal metal plates in a Semidry System (Bio-Rad). The membrane was soaked in a transfer buffer for 10 minutes, placed on top of the 3MM

Whatman® paper immersed in the same buffer, and laid the gel over. This was covered by another sheet of wet 3MM Whatman® paper, all dimensions being slightly brighter than the gel. Transfer was carried out in excess of blotting buffer for 2 hour, by electric density of 0.3mA/cm² and a 300- 400 mA current (45 V). Following Western blotting, membranes were usually stained with Ponceau-S for 5 minutes and protein bands were visualized. The dye was removed by washing with TBST, and membrane stored at 4⁰C until further analysis.

3.2.5 Immunodetection of specific proteins

Proteins immobilized on a membrane were identified by using highly specific antibodies. The membrane was first incubated in TBS-T containing 5% (w/v) Carnation milk in order to saturate nonspecific protein binding sites, and after one hour or overnight incubation by 4⁰C on a rocking platform the membrane was washed three times for 5 minutes in TBS-T. Primary antibody was diluted to appropriate concentration (1:200-1:10000) in TBS-T and membrane was incubated for 3 hours to overnight. Incubation was followed by three washing steps for 10 minutes in TBS-T and secondary antibody added (as recommended). After one hour, membrane was again repeatedly washed in TBS-T to remove unbound secondary antibody.

Signals were detected in the dark by rinsing the membrane shortly in water and then incubating with ECL (enhanced chemo luminescence system) I and II solutions in 1:1 ratio for one minute. Membranes were exposed to X-OMAT film for 30 seconds to 5 minutes depending on the intensity of the signal detected and antibody-bound proteins visualized.

3.3 Characterization of high molecular weight complexes (HPLC)

The formation of HMW was detected as previously described (Minucci *et al.*, 2000). Both COS-1 cells expressing p185^{BCR/ABL} and GFP or Helix-2- GFP, respectively, and IL-3-independent Ba/F3 cells expressing p185^{BCR/ABL} and GFP or Helix-2-GFP were used. Cytosolic extracts were prepared from 1 to 5 X 10⁸ cells and fractionated at 4⁰C by HPLC using a Superose 6 HR 10/30 size exclusion column (Amersham/Pharmacia Biotech). The flow rate was 0.4 ml/min. Fractions of 0.4 ml were pulled, concentrated and analyzed by Western blotting as described above.

3.4 Production of GST-Fusion protein in bacteria

3.4.1 Protein mini preparation

E. coli JM-83 cells were transformed with the required PGEX4T3 fusion protein constructs and PGEX empty vector as control. The transformed bacteria were plated on Agar/Amp plates and incubated over night at 37⁰C. Single colony was inoculated into 2 mL LB/Amp liquid medium and shaken at 37⁰C over night. The culture was diluted as 1:10 in LB/Amp medium and shaken for 3 hours. Finally the protein induced with 0.1 mM IPTG shaken for more 3 hours. The bacteria were centrifuged at 3000 rpm for 2 mints. The pallet was lysed in 200 µl E1A buffer (150mM) and sonicated. 10 µl of lysate was mixed with 10 µl 2X SDS/PAGE sample buffer and separated the lysates with SDS-PAGE. The gel was stained in coomassie solution for 3 hours. The gel was destained by incubation over night in distilled water. The expression was observed by comparing the bands with un-induced samples and empty vector.

3.4.2 Protein maxi preparation

E. coli JM-83 cells were transformed with the required PGEX4T3 fusion protein constructs and PGEX empty vector as control. The transformed bacteria were plated on Agar/Amp plates and incubated over night at 37⁰C. Single colony was inoculated into 2 mL LB/Amp liquid medium and shaken at 37⁰C over night. The culture was diluted as 1:10 in LB/Amp medium and shaken for 3 hours. Finally the protein induced with 0.1 mM IPTG shaken for more 3 hours. Bacterial growth was stopped by incubation the culture on ice for 10 mints. The

bacteria were centrifuged on 4°C at 4000 rpm for 15 mins. The pellet was lysed in 20 ml E1A buffer (150 mM NaCl, 1% Triton X-100) and sonicated. The lysates were centrifuged at 1000g on 4°C for 10 minutes. The supernatant was collected. 1 ml of GST sepharose beads were mixed with 10 ml of lysate and rotated on 4°C at low speed for 3 hours or more. The mixture was centrifuged for 1 minute at 4000 rpm and the protein bound sepharose were collected. The sepharose were washed 4 times with 10 ml E1A buffer (150 mM without detergents). At the end the sepharose beads were resuspended in E1A buffer (50 mM NaCl, 0.1% NP-40) and stored at 4°C. 10 µl of lysate was mixed with 10 µl 2X SDS/PAGE sample buffer and separated the proteins with SDS-PAGE. The gel was stained in coomassie solution for 3 hours. The gel was destained by incubation over night in distilled water. The expression was observed by comparing the bands with empty vector.

3.5 GST “Pull-down” assays

The glutathione *S*-transferase (GST)–BCC, Helix-2 and Helix-1 fusion proteins were expressed in *Escherichia coli* BL21 cells by induction with isopropyl thiogalactoside (IPTG) for 3 hours at 37°C. Extracts were prepared after cell lysis by sonication/detergent treatment. Cell lysates were cleared by centrifugation (10 minutes at 10 000g) and incubated for 2 hours at 4°C with glutathione- Sepharose beads (Amersham/Pharmacia Biotech, Freiburg, Germany). The beads were washed twice with E1A buffer (HEPES 50 mM, pH 7.8, NaCl 150 mM, EDTA 5 mM, DTT [dithiothreitol] 1 mM, NP40 0.1%) and quantified on sodium dodecyl sulfate–polyacrylamide gel electrophoresis (SDS-PAGE) by comparison to a standard curve of bovine serum albumin (BSA). For the pull-down experiments cells were resuspended in E1A buffer (NaCl, 150 mM). Cell extracts were prepared after cell lyses by sonication and clarification by centrifugation (10 minutes at 10 000g). Total protein (1 mg) was then incubated with GST or GST-Helix-2 fusion protein (approximately 10µg) bound to glutathione Sepharose for 1 hour at 4°C. The bound proteins were eluted by boiling in 30 µL 2 X SDS-PAGE loading buffer, resolved by SDS-PAGE, and visualized by Western blotting with the α -ABL antibody described earlier.

3.6 Cell biology techniques

3.6.1 Cell cultures

Eukaryotic cells were grown in culture flasks in a humidified atmosphere at 37°C and by 5% CO₂.

3.6.1.1 Used Cell lines

Nalm-6, BV-173 and K562 suspension cells were cultivated in RPMI 1640, supplemented with 10% FCS (Gibco), 2mM L-glutamine, 40µg/ml penicillin and 40µg/ml streptomycin medium, cultures were seed out in 1:4 to 1:10 ratio every 2-3 days in order to keep constant log phase population growth at about 1×10^6 cells/ml.

Sup-B15 were cultivated in Mycosa medium, supplemented with 10% FCS (Gibco), 2mM L-glutamine, 40µg/ml penicillin and 40µg/ml streptomycin medium, cultures were seed out in 1:3 to 1:5 ratio every 2-3 days in order to keep constant log phase population growth at about 1×10^6 cells/ml.

Tom-1 were cultivated in RPMI 1640, supplemented with 20% FCS (Gibco), 2mM L-glutamine, 40µg/ml penicillin, 40µg/ml streptomycin medium .

BaF/3 and 32D cells were cultivated in RPMI 1640, supplemented with 10% FCS (Gibco), 2mM L-glutamine, 40µg/ml penicillin, 40µg/ml streptomycin medium and 10 ng/ml of recombinant murine–interleukin 3

Adherent Rat-1, Phoenix and 293T cells were grown in DMEM medium supplemented with 10% FCS (Hyclone), 2mM L-glutamine, 40U/ml Penicillin and 40µg/ml Streptomycin. Upon reaching sub confluent state (~80% surface occupied), cells were washed with PBS and 1ml of trypsin-EDTA (PAN Biotech) added. After 1-2 minutes, trypsin was inactivated by addition of FCS-containing medium and detached cells reseeded in the fresh plates at approximately 1:7 ratios.

3.6.1.2 Cell counting and determination of cell viability

Cell number and viability were controlled by trypan blue exclusion. 10µl cell suspension was mixed with 40µl of 0.4% trypan blue in 0.9% NaCl. Only unstained cells were considered viable, and their number was calculated as follows: Cell concentration [10^6 /ml] = Number of counted cells in 5 quadrants $\times 10^4$ / ml

3.6.1.3 Freezing and thawing

Freezing

For storing in liquid nitrogen, approximately 1×10^7 cells were collected at 1200 x g for 5 minutes and washed with PBS. After centrifugation, the cells were resuspended in 0.9 ml freezing Solution I, transferred into cryovials, and mixed with drop wise added 0.9 ml of freezing Solution II. This suspension was immediately placed in cryobox containing isopropanol at -80°C, and after 3-5 hours stored in a liquid nitrogen freezer.

Thawing

Cryo-preserved cells were taken out of the liquid nitrogen, thawed rapidly in a 37°C incubator and resuspended in a 5 ml culture medium. Following one washing step to remove residual DMSO, cells were transferred into culture flasks and resuspended with fresh medium.

3.6.2 Genetic modification of mammalian cell**3.6.2.1 Transfection of mammalian cells**

A day prior to transfection, Phoenix cells were plated in fresh medium. After 14-16 hours, cells were sub confluent (70-80% of plate occupied), which is the stage when they are most transfectable and give the highest possible virus titre.

For transfection, following premix was made:

2M CaCl 62 µl

DNA 5 µg

Add H₂O to make final volume as 500µl

While vortexing the premix, 0.5 ml of 2xHBS were added drop wise. The mix was kept for 10-20 minutes at room temperature. Next, medium was aspirated, DNA/HBS solution was gently spread across the cell layer and plates were transferred to 37°C incubator. After 30 minutes, fresh pre-warmed medium with 25 µM chloroquine was added, and incubation continued for the next 8-12 hours (DNA delivered by CaCl₂ transfection is believed to transit through lysosomes, and chloroquine acts as to inhibit lysosomal DNases by neutralizing vesicle pH). Following this time, medium was replaced and cells were left overnight. Next day medium was changed and incubated the cells for next 24 hours. Transfection efficiency was estimated according to the level of expression of green fluorescence protein (GFP) on FACS (Fluorescence Activated Cell Sorter). Only after reaching the transfection efficiency of at least 80%, experiment was preceded and retroviral supernatant were collected, filtered and cry frozen in liquid nitrogen. Next day again the virus supernatant was collected, stored and used for further infection of target cells.

3.6.2.2 Retroviral infection

For infection of target cells, retronectin1 (Takara Bio, Otsu, Japan) was used to enhance infection efficiencies following the manufacturer's instructions. Non tissue culture 24-well plates were coated with 0.2mg retronectin per well in 100µL volume. The plate was incubated at 4°C overnight. Retronectin were removed, washed with PBS and blocked with 0.2% BSA for 30 minutes. 200µL of viral supernatant were plated in each well and centrifuged at 4000 rpm for 15 minutes on 15°C. Viral supernatant were discarded and repeated the procedure 2-3

times. The wells were washed with PBS and Ba/F3, 32D or Rat-1 target cells (100 000 cells/ml) were plated in the viral coated plate. Infection efficiency was measured by fluorescence-activated cell sorting (FACS) analysis of GFP-positive cells after 48 hours.

3.6.3 Cell growth and proliferation assay

Cell growth was assessed by dye exclusion using Trypan-blue. Ba/F3, 32D harboring p185 and p185 T315I and loss of function mutants of BCR/ABL were plated at 10^5 cells/ml. IL3 independent growth was monitored for 4 days with dye exclusion assay. Proliferation was assessed with proliferation kit XTT (Amersham) according to the manufacture instructions. Similarly, cells growth and proliferation was measured for human Philadelphia chromosome positive and negative cell lines like Nalm- 6, BV-173, Sup-B15, Tom-1 and K562 either retrovirally transduced or with cell permeable TAT-fusion peptides.

3.6.4 Proliferation-competition assays (PCA)

For modified proliferation-competition assays (PCA) (Griswold *et al.*, 2006)), Ba/F3 and 32D cells were infected with PAULO vectors harboring unmutated and mutant p185^{BCR/ABL}. IL-3 was removed from the media of infected Ba/F3 cells by washing the cells twice with phosphate buffered saline (PBS). The cells were continuously cultivated in absence of IL-3 and superinfected with GFP and Helix-2-GFP. Day 4 GFP-expression levels were used to normalize the expression levels of different GFP expression. Proliferation- competition between single and double infected cell fractions was monitored by FACS analysis of the GFP expression (Fig. 12A).

Similarly, GFP expression was followed in Nalm-6, SupB15 and BV173 cells infected with GFP, and Helix-2-GFP.

3.6.5 Apoptosis measurement by 7-aminoactinomycin D (7-AAD)

7-AAD is used in the staining of apoptotic cells, whereby it binds to the DNA. The 7AAD staining was carried out as described elsewhere (Schmid *et al.*, 1994). Briefly, 2.5 to 5×10^5 cells were taken in 1 ml FACS buffer and centrifuged for 5 minutes at 1500 rpm. Supernatant was completely discarded. The pellet resuspended in 200 μ l of 7AAD solution (diluted in PBS at a ratio of 1: 10 to have a final concentration of 20 μ g/ml). The cells were then incubated in the dark for 20 minutes at 4°C. The Tubes were filled with PBS and pelleted cells by centrifugation. Supernatant was discarded, and cells were resuspended in an appropriate volume (200 to 500 μ l) of FACS fixing solution. Cells were analyzed immediately by FACS scanning.

3.6.6 Transformation assays

3.6.6.1 Focus formation assay

For focus-formation assays in a 24-well plate format 40,000 per well infected Rat-1 cells were plated. Foci were stained after 15 days using 1% crystal violet (Sigma-Aldrich, Steinheim, Germany) and photographed.

3.6.6.2 Soft agar anchorage-independent growth assay

For soft-agar assays Rat-1 fibroblasts were co-transduced with GFP or Helix-2-GFP and PAULO vectors harbouring unmutated and mutant p185(BCR/ABL). Six-well-plates were filled with 2ml/well DMEM/10%FCS/0.5% bactoagar (DIFCO Laboratories, Detroit, USA). 5000 Rat-1 cells were plated in 1 ml/well topagar (DMEM/10% FCS/ 0.25% bactoagar). Rat-1 colonies were counted after 15 days incubation at 37⁰C, 5% CO₂.

3.7 Production of recombinant TAT- fusion proteins

The strep-tagged H2-GFP, TAT-GFP and MPH-2 peptides were produced in E.coli BL21 using pPRIBA2 vectors upon induction with 0.5 mM isopropyl thiogalactoside (IPTG) overnight at 25°C. Bacterial lysates were prepared in buffer W (100 mM Tris-HCl pH 8.0, 150 mM NaCl, 1 mM EDTA, 0.1% Tween) containing a complete protease inhibitor cocktail (Roche Basel Switzerland), sonicated, and cleared by centrifugation (10.000 g for 10 min.). Further purification of the STREP-tagged peptides was performed using a STREPtactin Matrix (IBA, Gottingen, Germany). The beads were washed 4 times with buffer W, and the proteins were eluted with elution buffer at room temperature for 15 min. The buffer was exchanged with PBS using PD-10 columns (Amersham/Pharmacia Biotec, Freiburg, Germany), and the endotoxin was removed using endotoxin free columns (Profos AG, Regensburg, Germany). The amount of protein was quantified by comparing the samples to a bovine serum albumin (BSA) standard curve. Samples were stored at -20°C in 15-20% glycerol for further use. Quantification of proteins was performed using SDS-PAGE followed by coomassie-staining.

3.8 Determination of TAT-fusion protein uptake

To determine the uptake efficiency of the fusion proteins, 1x 10⁵ cells/well of 293T, Rat-1, Nalm-6, BV-173, K562 and Tom-1 were plated in a 12-well plate for 12-16 hr. Cells were then incubated with H2-GFP, TAT-GFP or MPH-2 (1 µM each) for 3 hours. The cells were washed with PBS, harvested, and the uptake efficiency was measured by quantification of the GFP-positivity by fluorescent activated cell sorting (FACS).

3.9 „Pull-down-assays“for TAT-fusion protein

BV173 cells were exposed to 1 μ M H2-GFP, TAT-GFP and MPH-2. After 3 hr, the cells were washed, trypsinized and lysed in E1a buffer. The cell lysates were clarified by centrifugation (10 min at 10.000g). An aliquot of total protein (1 μ g) was incubated with 10 μ L STREPtactin Matrix (IBA) overnight at 4° C. The mixture of sepharose and protein was washed 4 times with E1A buffer (150 mM, NaCl, 5mM, HEPES 50 mM pH 7.0, EDTA 5mM pH 8.0, 1% Triton, NaVO₄ 2 mM and 1X protease inhibitor cocktail Roche, Mannheim, Germany). The bound protein was eluted with elution buffer (IBA), resolved by SDS-PAGE, and visualized by staining the blots with an α -ABL antibody.

3.10 Animal experiments

3.10.1 *In vivo* peptide transduction

3.10.1.1 Raring of mices

C57 BL/6N female mice (Harlan Winkelmann, Borchon, Germany) 6 to 8 weeks old were kept on sterile bedding in filter-top cages. They were provided with sterile food and water ad libitum.

3.10.1.2 Delivery of peptides to the mices

Membrane permeable Helix-2 (MPH-2) peptides dissolved in PBS at a dosage of 2.5 mg/kg were inoculated i.v. into recipient mice. Negative control mice received the same volume of phosphate-buffered saline (PBS).

3.10.1.3 Analysis of the mices

Animals were sacrificed by CO₂-asphyxiation after 15 min, 2 hr, 6 hr, and 24 hr of treatment. Peripheral blood (PB) was obtained from the heart, and bone marrow (BM) was harvested from the femur and tibiae by flushing the bones with a syringe and 26-gauge needle. Spleen cells were isolated by passing the tissue through a 40 μ M Nylon cell strainer (Beckton-Dickinson, Le Pont de Claix, France). For analysis of GFP expression, the mono nucleic cells (MNCs) were enriched using a Ficoll density gradient and GFP expression was measured by fluorescence activated cells sorting (FACS).

3.11 Statistical Analyses

All statistical analyses were performed using Student-t-Tests and $p \leq 0.05$ was considered as significant. The data were presented as mean values from three independent experiments with corresponding standard error.

4 Results

4.1 Targeting of the N-terminal coiled-coil (CC) oligomerization interface by a Helix-2 peptide inhibits BCR/ABL

4.1.1 The Helix-2 but not Helix-1 of coiled-coil (CC) interacts with 185^{BCR/ABL}

It is previously shown by our group that a peptide of the amino acid (a.a. = 1-63 representing the N-terminal BCR coiled-coil oligomerization interface (CC) interacts with p185^{BCR/ABL}. This CC inhibits kinase activity and growth of p185^{BCR/ABL} (Beissert *et al.*, 2003). The CC domain is composed of two α -helices, Helix-1 and 2 (Figure 10A). Previous data on deletion mutants and crystal structures suggest that Helix-2 mediates the protein-protein interaction by the CC domain (Smith *et al.*, 2003; Zhao *et al.*, 2002). To definitively determine the relevant protein-protein interaction interface in the CC domain, we investigated the capacity of peptides encompassing Helix-1 (a.a.1–17) and Helix-2 (a.a. 23–72), respectively, to bind with p185^{BCR/ABL}. Therefore, recombinant GST-Helix-1 and GST-Helix-2 fusion proteins were purified from *E.coli* JM-83 by high affinity chromatography (Figure 10B). These Immobilized peptides on glutathione-sepharose beads were used as a bait to precipitate p185^{BCR/ABL} from lysates of Ba/F3 cells expressing p185^{BCR/ABL}. GST alone and the previously described GST-CC (Beissert *et al.*, 2003) were used as a negative and positive control, respectively.

Sepharose-bound protein complexes were separated by SDS-PAGE and analyzed by α -ABL Western blotting. As depicted in figure 10C, only GST-Helix-2 was able to precipitate p185^{BCR/ABL} from the cell lysates to the same extent as GST-CC.

These data indicate that Helix-2 represents the oligomerization interface of BCR and thus mediates the interaction between p185^{BCR/ABL} monomers.

4.1.2 Co-expression of Helix-2 disrupts p185^{BCR/ABL} tetramers

The tetramerization of p185^{BCR/ABL} is reflected by the formation of intracellular HMW complexes. In fact, the size of complexes formed by a deletion mutant lacking the N-terminal CC domain is markedly reduced as compared to unmutated p185^{BCR/ABL} (Beissert *et al.*, 2003).

To investigate whether it is possible to disrupt the p185^{BCR/ABL} HMW-complexes by the presence of Helix-2, we co-expressed p185^{BCR/ABL} with either GFP or Helix-2-GFP in Cos-1 cells (Figure 11A). Cell lysates were separated by size-exclusion-HPLC. The single HPLC-elution fractions were then subjected to α -ABL Western blot analysis. Upon co-expression

with GFP, p185^{BCR/ABL} was found in complexes with an apparent MW between 670 and 1,070 kDa (Figure 11B), whereas the presence of Helix-2 led to the detection of p185^{BCR/ABL} complexes with apparent MW between 440 and 1,070, with a marked peak at 670 kDa.

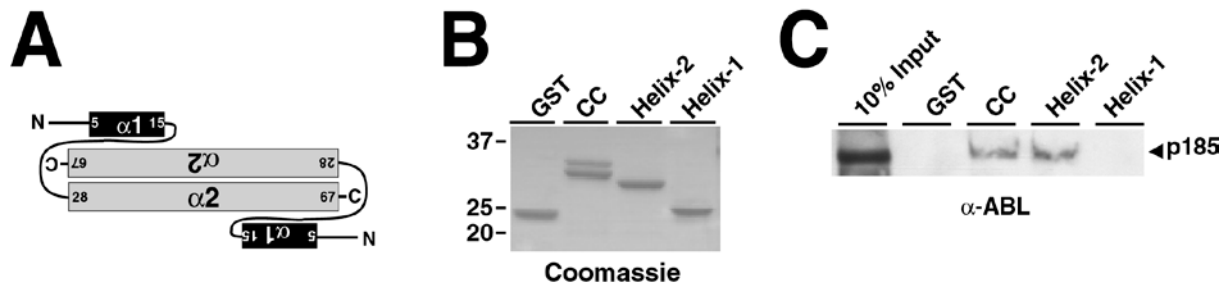


Figure 10- Interaction of Coiled-Coil Subdomains with p185 BCR/ABL . (A) Modular organization of the BCR-coiled-coil domain adapted from Zhao *et al.* Helix-1 spans from a.a.5-15, Helix-2 spans from a.a. 28-67¹⁹. (B) Expression of recombinant proteins in *E. coli* and ‘pull-down’ experiment: the coomassie staining (left side) shows the purity and integrity of the indicated constructs expressed in *E. coli* BL21. Lysates from p185^{BCR/ABL} expressing Ba/F3 cells were incubated with the indicated GST-fusion constructs immobilized on GST-sepharose beads. The precipitation of interacting p185^{BCR/ABL} was detected by Western blotting using an α -ABL antibody.

Endogenous c-ABL complexes displayed an apparent MW of 440–670 kDa, which was not influenced by the presence of GFP or Helix-2-GFP (Figure 11B).

In summary, these data suggest that binding to Helix-2 interferes with the oligomerization of p18^{BCR/ABL} as revealed by the reduction of the size of its HMW-complexes.

4.1.3 Helix-2 reduces the autophosphorylation of p185^{BCR/ABL}

The fact that Helix-2 interact with p185^{BCR/ABL} disrupts the p185^{BCR/ABL} HMW-complexes prompted us to investigate whether the Helix-2 peptides have inhibitory effects on p185^{BCR/ABL} expressing cells as compared to the known effects of the CC-peptides (Beissert *et al.*, 2003).

Hence, we investigated the autophosphorylation of p185^{BCR/ABL} in the presence of CC-GFP and Helix-2-GFP. Therefore, we analyzed Ba/F3 cells stably co-expressing p185^{BCR/ABL} in the presence of GFP, CC-GFP or Helix-2-GFP by Western blotting with an α -phospho-ABL antibody (α -P-ABL-Y245) and an α -ABL antibody. As depicted in Figure 11C the presence of Helix-2 reduced the level of p185^{BCR/ABL} autophosphorylation to the same extent as CC.

Taken together, these results show that the Helix-2 peptide inhibits the p185^{BCR/ABL} kinase activity to the same extent as the previously described CC-peptide.

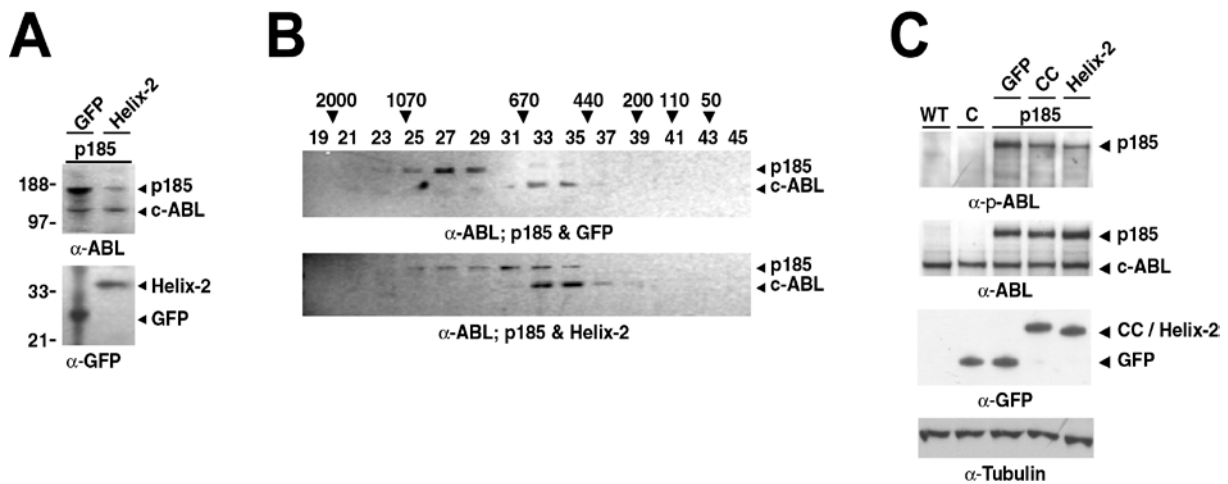


Figure 11- Disruption of p185BCR/ABL High Molecular Weight Complexes and Reduction of p185 BCR/ABL autophosphorylation by Helix-2. (A) Western blot analysis of cytoplasmic extracts of transfected Cos-1 cells. The cells were co-transfected as indicated either with GFP and p185^{BCR/ABL} or Helix-2-GFP and p185^{BCR/ABL}. The expression of the transgenes was determined by α -GFP and α -ABL antibodies. (B) The cytoplasmic extracts of co-transfected Cos-1 cells were fractionated by size-exclusion HPLC. p185^{BCR/ABL} was detected in the fractions by an α -ABL Western blot. The blots show the presence of p185^{BCR/ABL} in fractions corresponding to the molecular weight (MW) indicated at the top. (C) Ba/F3 cells stably expressing the indicated transgenes were lysed and phosphorylation at ABL-tyrosine residue 245 was analyzed by Western blot using an α -ABL(Tyr-245) specific antibody. The membrane was repeatedly stripped and probed with the indicated antibodies. One representative experiment out of three is given.

4.1.4 Helix-2 inhibits growth of p185BCR/ABL positive cells and increases its sensitivity towards Imatinib

To assess whether the inhibited autophosphorylation of p185^{BCR/ABL} by Helix-2 interferes with the survival of cells transformed by p185^{BCR/ABL}, we performed proliferation competition experiments on p185^{BCR/ABL} expressing Ba/F3 cells. The principle of the assay is depicted in Figure 12A. Ba/F3 cells transduced with the retroviral vector PAULOp185^{BCR/ABL} were selected by IL-3 withdrawal for 7 days, resulting in bulk populations that uniformly coexpress p185^{BCR/ABL} and Δ LNGFR. Thereafter, these cells were transduced with retroviral vectors harboring GFP, CC-GFP or Helix-2-GFP. The resulting double infected cell populations were then exposed to a sub-apoptotic Imatinib concentration (0.4 μ M) for p185^{BCR/ABL} expressing Ba/F3 cells. The effect of the transduced peptides was assessed by the detection of GFP positive cells for 1 week by FACS. The GFP-expression on day 4 was taken as a reference for normalization.

As shown in Figure 12B, the expression of GFP did not alter the proliferation of p185^{BCR/ABL} expressing Ba/F3 cells as revealed by the constant percentage of GFP positive cells. In contrast, CC and Helix-2 inhibited the growth of p185^{BCR/ABL} expressing Ba/F3 cells as shown by the fact that the percentage of CC-GFP or Helix-2-GFP expressing cells decreased over time with comparable kinetics (Fig. 12B). The addition of Imatinib accelerated the decrease of CC-

GFP- or Helix-2-GFP expressing cells, but had no influence on GFP controls (Fig. 12B). To exclude effects of the peptides not related to their binding to p185^{BCR/ABL} and to prove the specificity of their effects, we performed the same experiments with Ba/F3 cells expressing a constitutively activated murine c-Kit, the mutant c-KitD814H.21 The c-KitD814H mediates factor independence to the same extent as p185^{BCR/ABL}, which was also reverted by 2 μ M Imatinib (Zheng *et al.*, 2009). The co-expression of Helix-2- or CC-GFP-fusion peptides did not inhibit the growth of c-KitD814H-expressing IL-3 independent cells either in the absence or presence of Imatinib (Figure 12C).

Taken together, these results show that the Helix-2 peptide inhibits the p185^{BCR/ABL} kinase activity to the same extent as the previously described CC-peptide inducing both growth suppression of p185^{BCR/ABL}-dependent cells and an increased sensitivity for Imatinib.

4.1.5 Helix-2 specifically inhibits Ph+ human cell lines

To confirm the effects of Helix-2 on human Ph+ patient derived cells, we performed the proliferation competition experiments on human Ph+ cell lines derived from ALL or CML patients. We used SupB15 (Ph+ ALL) expressing p185^{BCR/ABL}, BV-173 (lymphatic CML blast crisis) expressing p210^{BCR/ABL} and as a BCR/ABL-negative control the Ph- Nalm-6 cells, because all these cells exhibited a nearly identical pre-B lymphatic differentiation level (Puccetti *et al.*, 2000). These cells were retrovirally infected with GFP, CC-GFP or Helix-2-GFP. The GFP-expression was determined for 12 days after infection with the day 4 expression as a reference. In contrast to the Ph- Nalm-6 cells which exhibited a constant GFP, CC-GFP or Helix-2 expression, in the Ph+ SupB15 and BV173 cells the percentages of CC-GFP and Helix-2-GFP positive cells decreased over time, whereas the GFP expression was constant. The kinetics of the outgrowth of Helix-2-GFP positive cells was accelerated with respect to that of CC-GFP positive cells (Figure 12D).

To obtain 100% infected human cells, we sorted CC-GFP and Helix-2-GFP expressing cells. While Nalm-6 cells transduced with GFP, Helix-2-GFP or CC-GFP rapidly proliferated after sorting, BV173 and SupB15 cells only infected with GFP but not with CC-GFP or Helix-2-GFP grew up after sorting.

Taken together these data show that patient derived Ph+ cell lines are specifically inhibited by peptides targeting the N-terminal oligomerization interface of BCR/ABL and that Helix-2 seems to be more effective than CC in the inhibition of BCR/ABL.

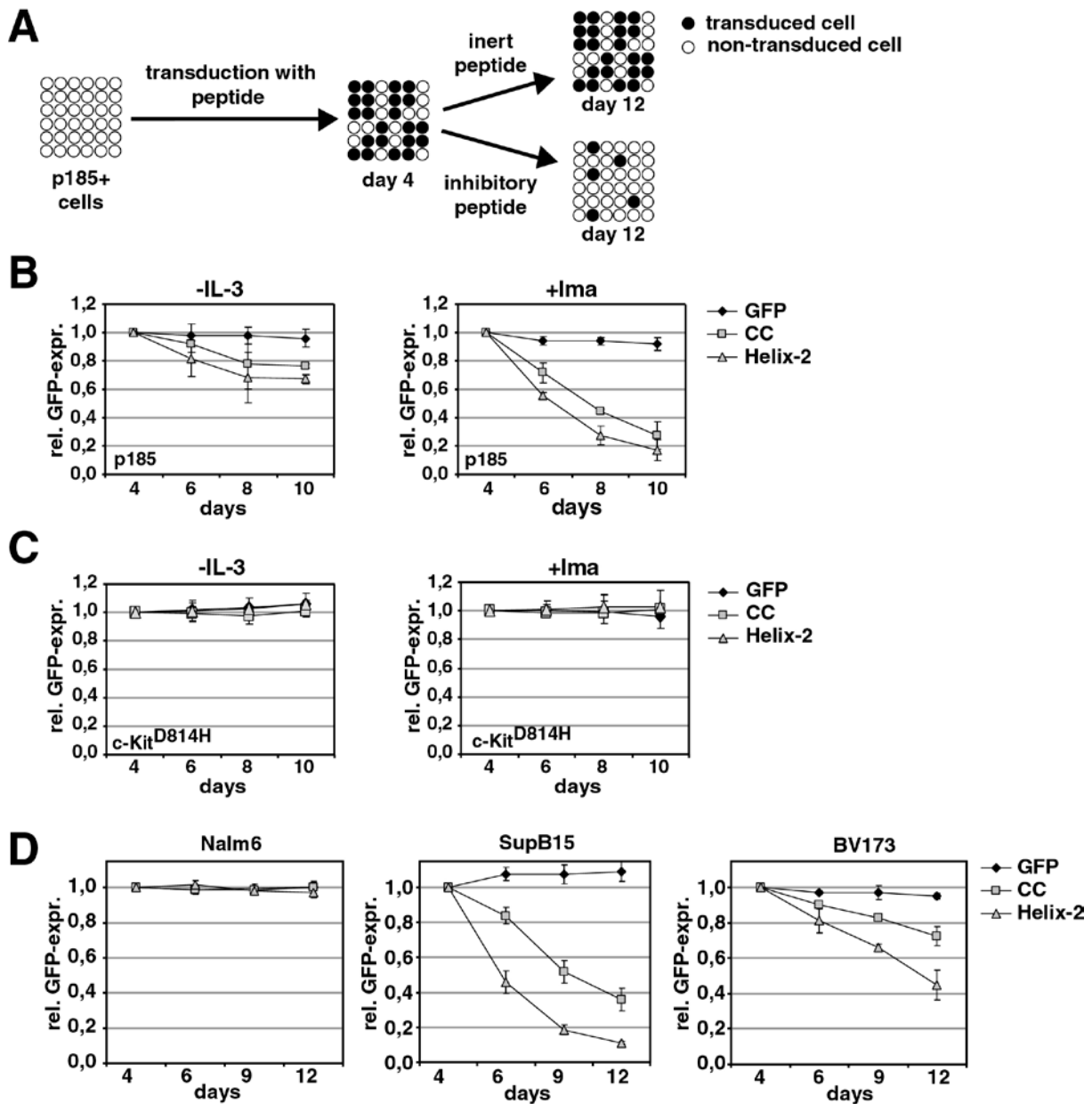


Figure 12- Growth Inhibition of p185BCR/ABL Expressing Ba/F3 Cells and Philadelphia Chromosome positive human cell lines. (A) Schematic representation of a proliferation-competition assay. Factor independent cells (e.g. p185^{BCR/ABL} expressing Ba/F3 cells) are retrovirally infected with inert control peptides (GFP) or inhibitory peptide-GFP fusions (CC-GFP or Helix-2-GFP). In the case of the inert GFP control the percentage of GFP-positive cells remains constant from day 4 to day 12. In contrast, the expression of inhibitory peptides results in an outgrowth of peptide expressing cells revealed by a progressive loss of Helix-2-GFP expression. (B and C) For proliferation-competition experiments p185^{BCR/ABL} or c-Kit^{D814H} transduced Ba/F3 cells adapted to factor independence were infected with GFP, CC-GFP or Helix-2-GFP expressing retroviruses and replated 4 days after infection in the presence or absence of sub-apoptotic Imatinib (Ima) concentrations (0,4 μ M). The proportion of the GFP-positive cell fraction was followed by flow cytometry for 10 days and normalized to the GFP expression at day 4. Graphs show mean values \pm SD of three independent experiments. (D) Proliferation competition assays were performed with the human B-cell precursor cell lines Nalm-6 (Ph-), SupB15 (Ph+) and BV173 (Ph+). These cells were infected with GFP, CC-GFP or Helix-2-GFP expressing retroviruses. The proportion of GFP-positive cell fraction was followed by FACS for 10 days and normalized to the GFP expression at day 4. Graphs show mean values \pm SD of three independent experiments.

Based on our present results, Helix-2 efficiently inhibits BCR/ABL positive cells. The next goal was to establish an efficient method for the delivery of Helix-2 peptides to Ph⁺ cells.

4.2 Targeting the oligomerization of BCR/ABL by membrane permeable competitive peptides inhibits the proliferation of Philadelphia chromosome positive leukemic cells

4.2.1 HIV-TAT-fusion peptides were efficiently delivered to fibroblasts

To determine the most efficient peptide transduction system, we compared the HIV-TAT with the Retro-HIV-TAT-sequences fused to Helix-2. We created fusion peptides containing a Strep-tag (for efficient immunoprecipitation), HIV-TAT or Retro-HIV-TAT as the peptide transduction tag, the Helix-2 sequence, and GFP as reporter (Figure 13A). A construct lacking the Helix-2 sequence (TAT-GFP) was used as the control in experiments. These fusion peptides were expressed in the *E.coli* strain BL21, and purified by high affinity chromatography (Figure 13B). Peptide transduction was performed in the presence/absence of chloroquine, which facilitates the up-take of membrane permeable peptides. Here, we show a higher efficiency of peptide transduction of Helix-2 upon fusion with the HIV-TAT (MPH-2), as compared to Retro-HIV-TAT in untransformed Rat-1 fibroblasts (Figure 13C). Due to its high efficiency, HIV-TAT was used as transduction tag for the remaining studies.

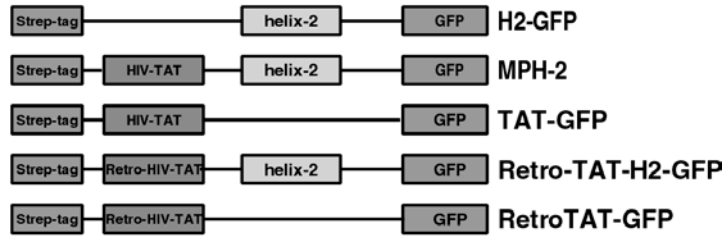
4.2.2 HIV-TAT mediates the efficient cellular uptake of Helix-2 fusion proteins

To confirm that the HIV-TAT fused membrane permeable Helix-2 (now referred to as MPH-2) is able to enter leukemic cells, we exposed Ph⁺ (Tom-1, BV173 and K562) and Ph⁻ (Nalm-6) leukemic cells to the HIV-TAT-fusion peptides. Peptides without the TAT-domain (H₂-GFP) or TAT-GFP were used as controls. The uptake rate was assessed by determining the percentage of GFP-positive cells by FACS. As reported in figure 14A, both the Ph⁺ and Ph⁻ leukemic cell populations were nearly 100% positive for GFP in the presence of the transduction tag, whereas the cells incubated with control peptides were completely negative. Interestingly, the uptake of MPH-2 was more efficient than the TAT-GFP peptide. To exclude that the GFP-positivity was due to peptides binding to the outer side of the cell membrane without penetrating the cell, we exposed Nalm-6 and BV-173 to H₂-GFP, TAT-GFP or MPH-2, and performed immunoblots on cell lysates that excluded the membrane fraction. Both of the cell lines expressed the peptides corresponding to the HIV-TAT tag, which clearly confirmed greater uptake of MPH-2 compared to the TAT-GFP control (Figure 14B).

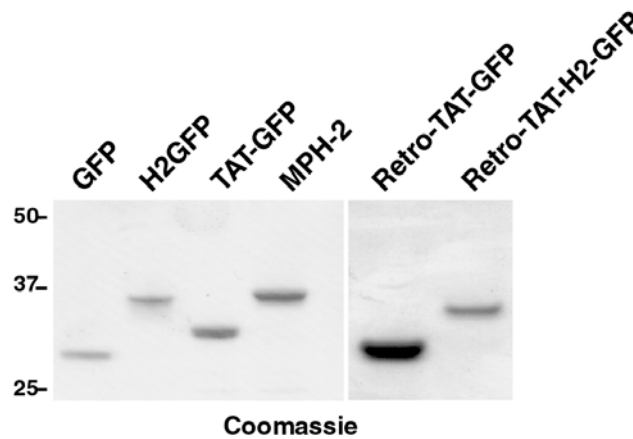
To determine the stability of MPH-2, Rat-1 fibroblasts were exposed to TAT-GFP, MPH-2 and H₂-GFP for 3 hr. Then the cells were extensively washed, trypsinized, and seeded in fresh media. GFP expression was measured after 30, 60 and 120 min, 6 hr and 24 hr. As

depicted in figure 14C, GFP was detectable for at least 6 hr, showing that the TAT-fusion peptides were stable for at least 6 hr.

A



B



C

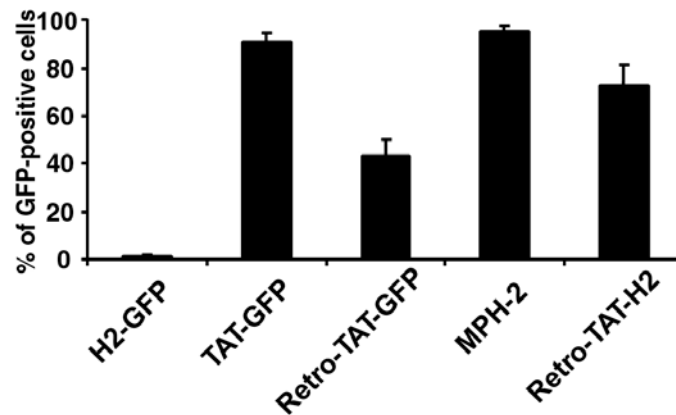


Figure 13 - Recombinant membrane permeable peptides. (A) Schematic representation of the fusion peptides used in this study with the indicated tags. (B) Recombinant peptides on a coomassie-stained SDS-PAGE Gel. (C) Peptide transduction efficiency with the indicated peptide transduction tag fused to Helix-2 in Rat-1 fibroblasts, provided as percentage of GFP-positive cells. The data represent the mean of 3 independent experiments with SD.

Taken together, these data provide evidence that MPH-2 transduces several different cell types with high efficiency, and remains stable for several hours.

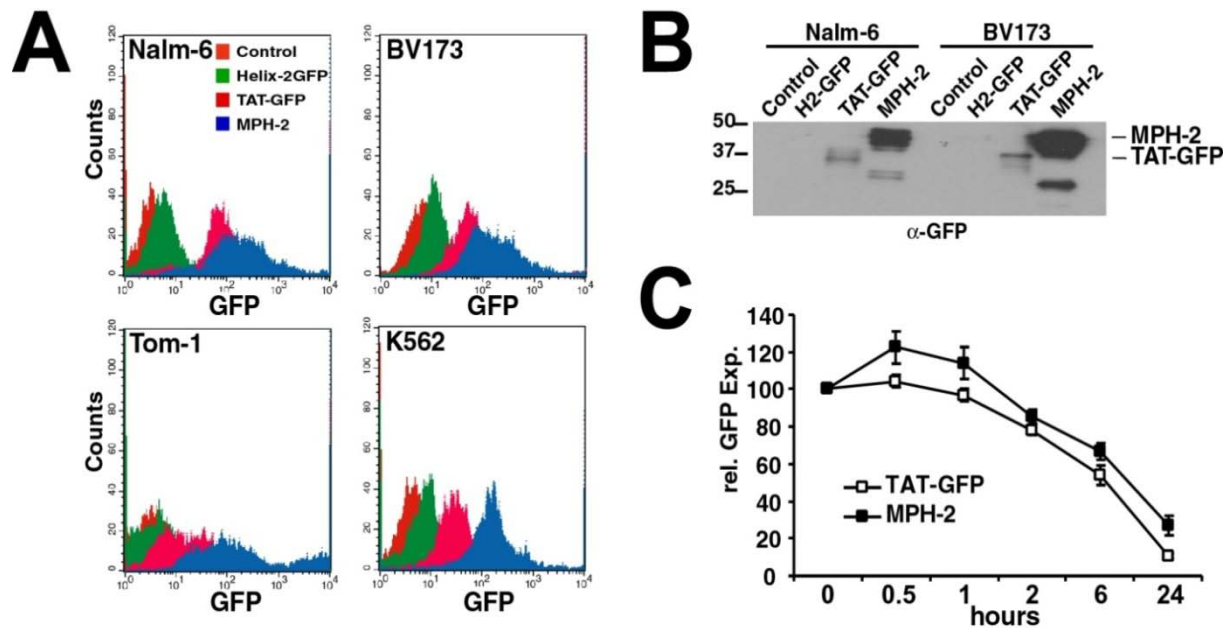


Figure 14 - Uptake of HIV-TAT fusion peptides by leukemic cell lines and primary stem cells. (A) Ph⁺ cell lines; Tom-1 (Ph⁺ ALL), BV173 (CML lymphatic blast crisis) and K562 (CML - myeloid blast crisis), and the Ph- Nalm-6 cells (ALL) were exposed to 1 μ M of the indicated peptides. GFP expression was determined using FACS. (A) one representative of 3 independent experiments is provided, as all yielded nearly identical results. (B) Intracellular uptake of MPH-2. Western blot analysis of the cell lysates cleared from the membrane fraction, and probed with an α -GFP-antibody. D Stability of MPH-2. Rat-1 cells were exposed to 1 μ M of the indicated peptides. GFP expression was determined using FACS at indicated time points.

4.2.3 MPH-2 interacts with BCR/ABL

To be therapeutically effective, MPH-2 has to inhibit the oligomerization of BCR/ABL by competing for the binding to the N-terminal CC-domain of BCR/ABL. We investigated whether MPH-2 could bind BCR/ABL. We exposed Ph⁺ BV173 cells to MPH-2, and to H2-GFP and TAT-GFP, which were negative controls. As shown in Figure 13A, all of the recombinant peptides used in the experiments had a Strep-tag. Lysates were incubated with strep-tactin sepharose to pull down the strep-tagged peptides. Strep-tactin sepharose-bound protein complexes were separated by SDS-PAGE, and blotted on a methyl cellulose membrane, which was probed with an α -ABL antibody (Figure 15).

Here, we show that MPH-2 was able to precipitate BCR/ABL from the cell lysates, which confirms that MPH-2 and BCR/ABL directly interact.

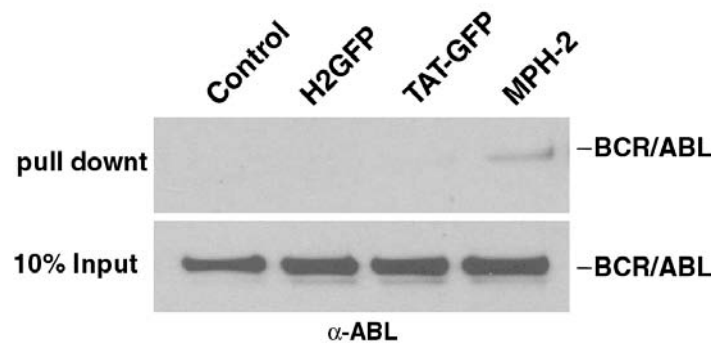


Figure 15 - Interaction between MPH-2 and BCR/ABL. Pull-down of BCR/ABL from BV173 cells exposed to TAT fusion proteins. BV173 were exposed for 3 hr to 1 μ M of MPH-2 or the indicated control peptides. All fusion peptides harbored the Strep-tag (Figure 1A) and were pulled down by the STREPTactin Matrix. They were analyzed for the presence of bound BCR/ABL by probing with the α -ABL antibody. As a control, 10% of the inputs are shown.

4.2.4 MPH-2 efficiently reduces the autophosphorylation of BCR/ABL

The capacity of MPH-2 to interact with BCR/ABL *in vivo* prompted us to study its inhibitory effects on the aberrant BCR/ABL kinase-expressing cells. We investigated the autophosphorylation status of BCR/ABL at the phospho-tyrosine residue Y245, which is critical for ABL-kinase activation in the Ph⁺ cell lines, Tom-1 (Ph⁺ ALL) and BV-173 (lymphatic CML blast crisis), upon exposure to MPH-2. Tom-1 and BV-173 cells were transduced with MPH-2 and TAT-GFP as negative controls. After 3 hr, cells were lysed, and a western blot was performed with antibodies directed against the c-ABL and phosphorylated ABL (Y245). As depicted in Figure 16, in contrast to TAT-GFP, MPH-2 inhibited the autophosphorylation of BCR/ABL, showing that MPH-2 targets BCR/ABL in patient derived Ph⁺ leukemic cell lines.

4.2.5 MPH-2 selectively inhibits Ph⁺ leukemic cell lines

To definitively establish the inhibitory effects of MPH-2 on the transformation potential of BCR/ABL, we assessed the growth of human Ph⁺ patient derived cells. We exposed Tom-1, BV-173, and K562 (myeloid CML blast crisis), and the BCR/ABL negative Nalm-6 cells to 1 μ M of MPH-2, and the negative controls, TAT-GFP and Helix-2-GFP. Cell viability was monitored by Trypan blue dye exclusion. As shown in Figure 17A, the growth of Tom-1, BV-173 and K562 were inhibited by MPH-2 in comparison to the controls, but MPH-2 did not exert any influence on the growth of Nalm-6 cells. The inhibitory effects of MPH-2 on the growth of Ph⁺ leukemic cell lines were confirmed by XTT-proliferation assays. The human Ph⁺ cell lines Tom-1, BV-173, K562, and the Ph⁻ cell line Nalm-6 were transduced with 1 μ M of MPH-2, and the proliferation rate was measured after 48 hr of exposure. As depicted in Figure 36B, the proliferation of Tom-1 and BV-173 BCR/ABL expressing cells was

significantly inhibited by MPH-2, whereas the proliferation of K562 was only slightly reduced. No non-specific activity of MPH-2 on Nalm-6 cells was observed (Figure 17B).

Taken together, these data indicate that MPH-2 specifically inhibits Ph⁺ human cell lines.

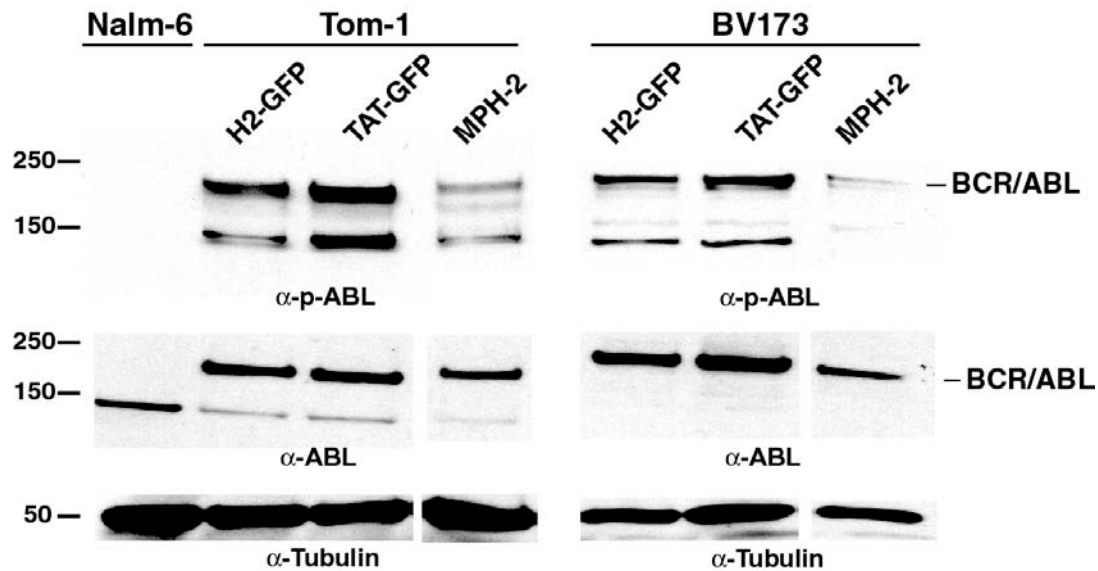


Figure 16 - MPH-2 inhibits the autophosphorylation of BCR/ABL. TOM-1 and BV173 cells were exposed for 3 hr to 1 μ M of MPH-2. Autophosphorylation was assessed by Western blotting with the α -ABL and α -p-ABL antibodies directed against whole and phosphorylated ABL, respectively.

4.2.6 TAT-fusion protein are efficiently delivered *in vivo*

To investigate whether the MPH-2 is efficiently transduced into primary cells we exposed primary Sca1⁺/lin⁻ murine hematopoietic stem cells (HSCs) to MPH-2 for 3 hr. We found that these cells were transduced to a similar extent than the above described leukemic cell lines (Figure 18A). To determine to what extent the TAT fusion peptides are actively transduced *in vivo* and to assess their *in vivo* stability, we inoculated i.v. 250 μ g of TAT-GFP and MPH-2 peptides into recipient mice. MNCs from the peripheral blood and bone marrow and spleen cells were isolated after 15 mins, 2 hr, 6 hr and 24 hr of treatment. GFP expression was measured using FACS. As shown in figure 18B, the GFP expression level peaked at 15 mins, was maintained until 6 hr, and was completely abolished after 24 hr in the peripheral blood and bone marrow cells. Consistent with peripheral blood, the GFP expression was maximal after 15 min and maintained until 24 hr in the bone marrow cells (Figure 18B). In contrast, the spleen cells exhibited maximal GFP expression after 6 hr of treatment, which was completely lost after 24 hr (Figure 18B). Control mice had no detectable GFP expression in any organ.

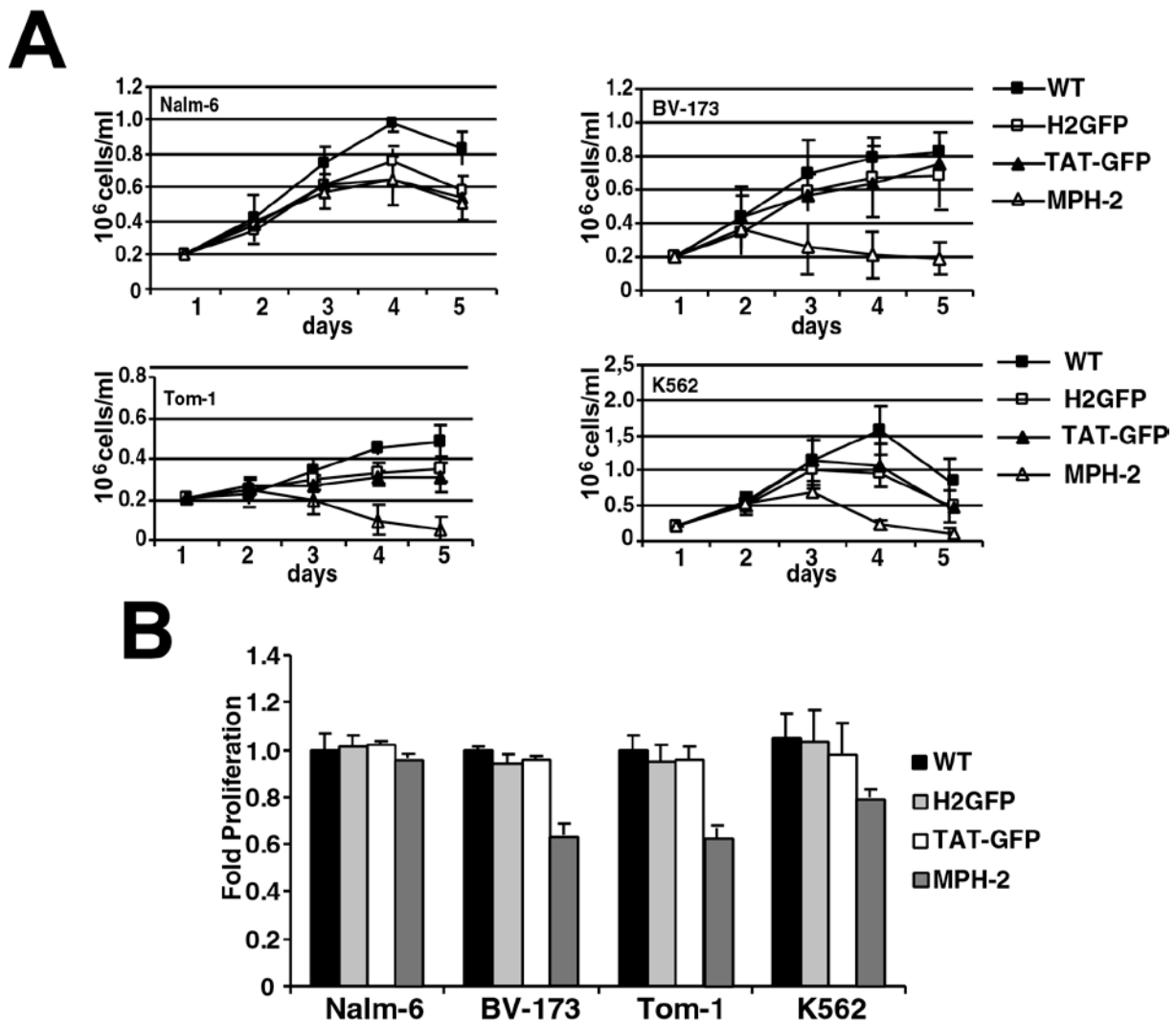


Figure 17 - Growth inhibition of Ph⁺ leukemic cell lines upon exposure to MPH-2. Ph⁺ cell lines; Tom-1 (Ph⁺ ALL), BV173 (CML lymphatic blast crisis) and K562 (CML - myeloid blast crisis), and the Ph⁻ Nalm-6 cells (ALL) were exposed to 1 μ M of the indicated peptides. A Proliferation was assessed by either the Trypan blue dye exclusion (A) or XTT (B) assay.

In summary, these results demonstrate that TAT-fusion proteins are efficiently delivered to the hematopoietic organs and are pharmacologically stable for a pharmacologically reasonable period of time.

Ph⁺ cell lines are specifically inhibited by Helix-2 peptides targeting the N-terminal oligomerization interface of BCR/ABL and these peptides were efficiently delivered to Ph⁺ cell lines.

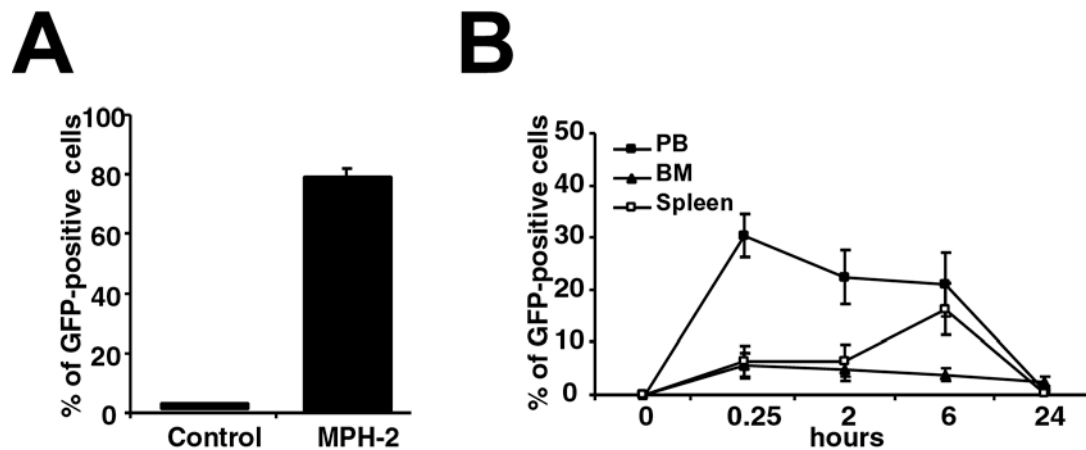


Figure 18 - In vivo transduction of MPH-2. (A) Transduction efficiency in primary $Sca1^{+}/lin^{-}$ murine hematopoietic stem cells. (B) Transduction efficiency *in vivo*. 25 $\mu\text{g}/\text{kg}$ of body weight of MPH-2 were injected i.v., and after the indicated time points, 3 mice/group were sacrificed. GFP expression was determined in the MNCs from PB, spleen and BM.

The most frequent and clinical important resistant BCR/ABL mutations are the “P-loop” mutations Y253F and E255K, the “activation loop” mutation H396P, the “catalytic domain” mutation M351T, and the “gatekeeper” mutation T315I (Shah *et al.*, 2002). The aim was to find out strategies for overcoming resistance towards kinase inhibitors by targeting the tetramerization domain of BCR/ABL.

4.3 Mechanism of the resistance of “gatekeeper” mutation T315I and strategies to overcome this resistance

4.3.1 Helix-2 interacts with mutant $p185^{BCR/ABL}$ and disrupts the HMW-complexes of these mutants

The acquisition of point mutations, which decrease the affinity of competitive TK-inhibitors such as Imatinib, Dasatinib or Nilotinib to the ATP-binding site of BCR/ABL, is the best studied mechanism for resistance against kinase inhibitors (Hantschel and Superti-Furga, 2004; O'Hare *et al.*, 2005a; von Bubnoff *et al.*, 2005). To assess whether the inhibition of tetramerization by Helix-2-peptides is able to inhibit Imatinib-resistant $p185^{BCR/ABL}$ we evaluated the effects of Helix-2 on three clinically relevant mutations responsible for Imatinib resistance - two P-loop mutations Y253H and E255K, and the “gatekeeper” T315I mutation. As the interaction of Helix-2 with mutant $p185^{BCR/ABL}$ and its capacity to disrupt the $p185^{BCR/ABL}$ tetramerization are required for its inhibitory effects, we first investigated whether Helix-2 interacts with mutant $p185^{BCR/ABL}$ and disrupts the HMW-complexes of mutant $p185^{BCR/ABL}$. Therefore, lysates of IL-3 independent Ba/F3 cells co-expressing either WT

p185^{BCR/ABL} or its mutants together with GFP or Helix2-GFP were used for co-immunoprecipitation as well as for size-exclusion HPLC as described above.

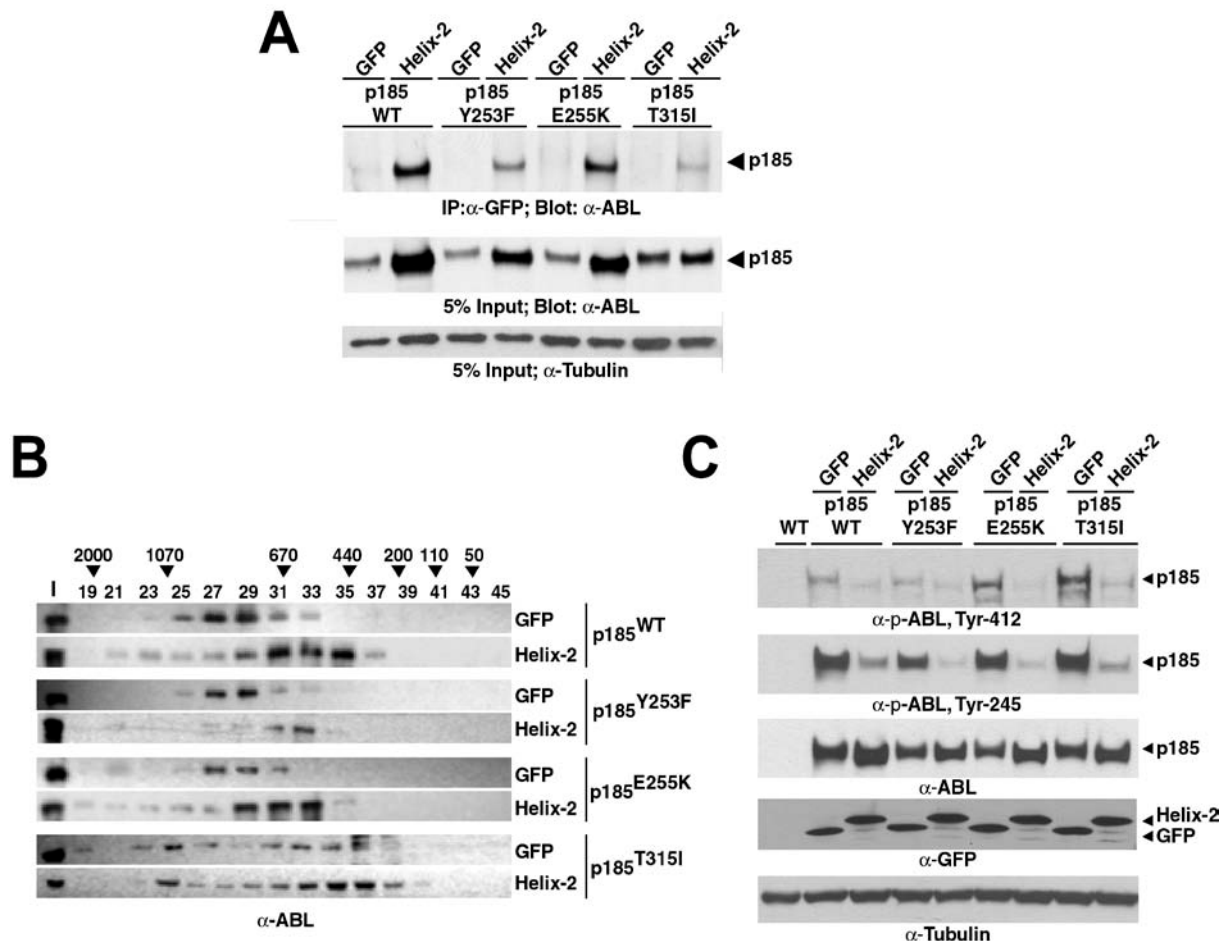


Figure 19 - Helix-2 Interacts with Mutant p185 BCR/ABL, Disrupts HMW-Complexes and Inhibits Auto-phosphorylation of WT and Mutant p185 BCR/ABL. (A) A GFP specific antibody was used to co-precipitate WT or mutant p185^{BCR/ABL} from lysates of IL-3 independent Ba/F3 cells co-expressing WT or mutant p185^{BCR/ABL} and either GFP or Helix-2-GFP. Co-precipitated p185^{BCR/ABL} was detected by Western blot with an α -ABL antibody. 5% of the protein amount used is given as input. (B) Cytoplasmic extracts of IL-3 independent Ba/F3 cells coexpressing the indicated p185^{BCR/ABL} constructs and either GFP or Helix-2-GFP were fractionated by size-exclusion HPLC. p185^{BCR/ABL} was detected in the fractions by an α -ABL Western blot. (C) Autophosphorylation of Mutant p185^{BCR/ABL} in presence of Helix-2 peptides. Lysates of GFP or Helix-2-GFP Ba/F3 cell clones infected with WT or mutant p185^{BCR/ABL} were blotted and probed with an α -ABL(Tyr-245) specific antibody, stripped and re-probed with an α -ABL(Tyr-412) specific antibody. The membrane was repeatedly stripped and probed with the indicated antibodies. One representative experiment out of three is given.

The co-immunoprecipitation by an α -GFP antibody and subsequent α -ABL Western blotting showed that the p185^{BCR/ABL} mutants bind to Helix-2 like wt p185^{BCR/ABL} (Figure 20A)

Noteworthy, in contrast to GFP, the presence of Helix-2 in these factor-independent cell populations seemed to select high expression of p185^{BCR/ABL}, p185^{BCR/ABL-Y253F} and p185^{BCR/ABL-E255K}, but not p185^{BCR/ABL-T315I} (Figures 19A).

The analysis of p185^{BCR/ABL} HMW-complex formation by size-exclusion-HPLC revealed no differences between WT p185^{BCR/ABL}, and the mutants p185^{BCR/ABL-Y253F} and p185^{BCR/ABL-E255K}, in the presence of GFP. In fact, all these p185^{BCR/ABL} forms were found in HMW fractions corresponding to an apparent MW between 670 and 1070 kDa (Figure 19B). In general p185^{BCR/ABL-T315I} forms HMW-complexes of similar sizes as WT p185^{BCR/ABL}. In addition to this p185^{BCR/ABL-T315I} predominantly forms a complex of about 1070 kDa (fraction no. 25). In the presence of Helix-2-GFP we observed a similar size reduction of the HMW-complexes of WT p185^{BCR/ABL}, p185^{BCR/ABL-Y253F} and p185^{BCR/ABL-E255K} as observed before in transfected Cos-1 cells (Figure 11B). Similarly, Helix-2 influenced the HMW-complex pattern of p185^{BCR/ABL-T315I}. Helix-2 led to the elution of p185^{BCR/ABL-T315I} in fractions corresponding to lower MWs than GFP. In contrast, the predominant 1070 kDa fraction (no. 25) formed by the mutant T315I was not influenced by Helix-2 (Figure 19B).

In summary, these data suggest that Helix-2 interacts with p185^{BCR/ABL}, notwithstanding the presence of point mutations related to the resistance against kinase inhibitors. Contrary to this, the presence of T315I mutations seems to interfere with the capacity of Helix-2 to disrupt HMW-complexes of p185^{BCR/ABL}.

4.3.2 Helix-2 inhibits the factor independence and overcomes Imatinib resistance of hematopoietic cells expressing mutant p185^{BCR/ABL} with exception of T315I

To assess whether the interaction of Helix-2 peptides with p185^{BCR/ABL} is able to overcome p185^{BCR/ABL}-mediated factor independence of hematopoietic cells and the Imatinib-resistance conferred by point mutations, we performed proliferation competition assay (PCAs) as described earlier. Retrovirally transduced IL-3 independent Ba/F3 bulk populations expressing either Δ LNFR and unmutated p185^{BCR/ABL} or Δ LNFR and p185^{BCR/ABL} “p-loop” mutants Y253H, E255K and “gatekeeper” mutant T315I were super infected with GFP or Helix-2-GFP. GFP and Helix-2-GFP expression levels were followed for 8 days and expression at day 4 was taken as a reference. Half of the cells were exposed to sub-apoptotic Imatinib concentrations (0.4 μ M for unmutated p185^{BCR/ABL}, 3 μ M for mutant p185^{BCR/ABL}). As shown in Figure 20A, the growth of cells expressing unmutated p185^{BCR/ABL}, p185^{BCR/ABL-Y253F} or p185^{BCR/ABL-E255K}, but not p185^{BCR/ABL-T315I} was inhibited by Helix-2-GFP, whereas no effect of GFP was seen. This effect was enhanced by Imatinib with the exception of p185^{BCR/ABL-T315I} (Figure 20A). To exclude cell line specific effects we extended the on the IL-3 dependent murine myeloid cell line 32D with identical results (Figure 20B).

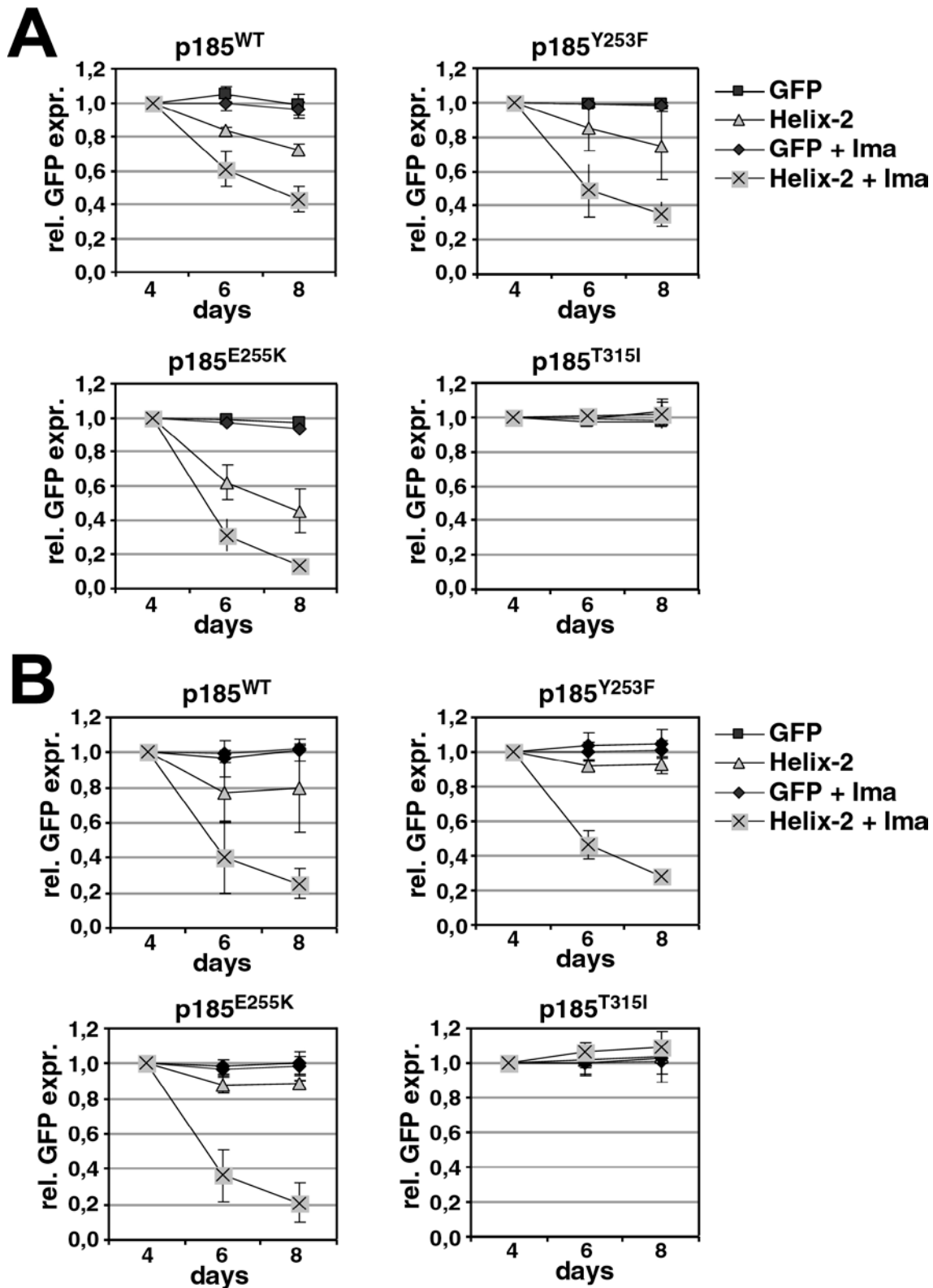


Figure 20 - Effect of Helix-2 on BCR/ABL mutants resistant to Imatinib. For proliferation competition experiment WT or mutant p185^{BCR/ABL} transduced Ba/F3 cells (A) or 32D cells (B) adapted to factor independence were infected with GFP or Helix-2-GFP expressing retroviruses. The cells were replated 4 days after infection in the presence or absence of sub-apoptotic Imatinib (Ima) concentrations (0.4 μ M for WT and 3 μ M for mutant p185^{BCR/ABL}). The proportion of the GFP-positive cell fraction was followed by FACS for 10 days and normalized to the GFP expression at day 4. Graphs show mean values \pm SD of three independent experiments.

In summary, these results demonstrated that Helix-2 is able to inhibit the proliferation of Ba/F3 and 32D cells expressing p185^{BCR/ABL-E255K} and p185^{BCR/ABL-Y253F}, but not p185^{BCR/ABL-T315I}. Except for p185^{BCR/ABL-T315I} the co-expression of Helix-2 increases the sensitivity of mutant p185^{BCR/ABL} towards Imatinib.

4.3.3 Helix-2 reduces the transforming activity of unmutated and mutant p185^{BCR/ABL}

We have shown before that the BCC-GFP peptides inhibit the transformation potential of BCR/ABL, as revealed by the inhibition of the anchorage independent growth of p185^{BCR/ABL}-expressing Rat-1 fibroblasts (Beissert *et al.*, 2003). To investigate whether Helix-2 peptides exhibit similar inhibitory effects on the transformation potential of mutant p185^{BCR/ABL} we co-expressed GFP or Helix-2-GFP and unmutated or mutant p185^{BCR/ABL} in Rat-1 cells. The transduction efficiency was assessed by the detection of GFP and Δ LNGFR, respectively. For each construct triplicates of 5,000 double infected Rat-1 cells were plated in soft agar and the colonies were counted after 15 days. As shown in Figure 21A Helix-2 inhibited the colony formation of Rat-1 cells that express either unmutated or mutant p185^{BCR/ABL}. To assess whether Helix-2 restores the contact inhibition of Rat-1 fibroblasts expressing unmutated or mutant p185^{BCR/ABL} we performed focus-formation assays with these double-infected Rat-1 bulks in the presence and absence of Imatinib. At day 15, foci were stained with crystal violet. The expression of Helix-2 restored the contact inhibition of unmutated and less pronounced that of mutant p185^{BCR/ABL}. With the exception of the mutant T315I, the addition of Imatinib to the growth medium enhanced the restoration of the contact inhibition (Figure 21B). These data indicate that Helix-2 peptides inhibit the transforming capacity of Imatinib-resistant p185^{BCR/ABL} mutants and increase the sensitivity towards Imatinib except for the mutant T315I.

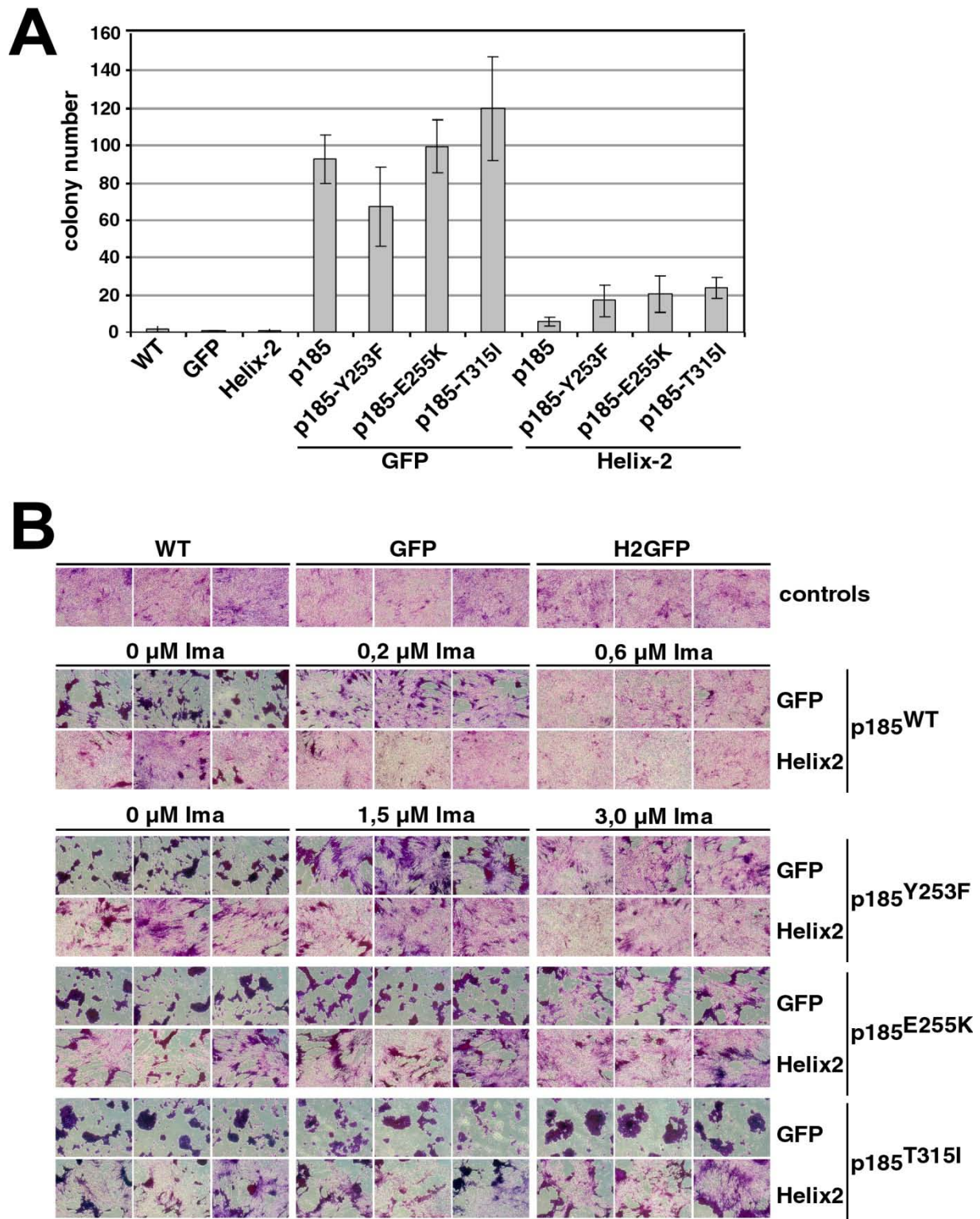


Figure 21 - Fibroblast Transformation Assays. Rat-1 cells were retrovirally transduced with GFP or Helix-2-GFP and overinfected with retroviruses encoding WT or Mutant p185^{BCR/ABL} as indicated. (A) 5000 double infected Rat-1 cells per well were plated in soft-agar in 6-well-plates as described in the material and methods section. After 15 days incubation at 5% CO₂ and 37°C the colonies were counted. Means ±SD of triplicates of two representative experiments are given. (B) Triplicates of 40000 double infected Rat-1 cells per well were plated in 24-well-plates. 72h later cells reached confluency and were subsequently incubated for additional 12 days in absence or presence of the indicated concentrations of Imatinib. Thereafter the adherent cells were washed twice with PBS, dried and stained with 1% crystal violet. One representative experiment of three is given (40x magnification).

4.3.4 ABL kinase inhibitor (AKI)-resistance mutations restore both transformation potential and the capacity to mediate factor independence of oligomerization-deficient p185^{BCR/ABL}

Targeting the oligomerization interface of p185^{BCR/ABL} using competitive peptides reduced the factor independence of hematopoietic progenitors expressing either unmutated p185^{BCR/ABL} or p185^{BCR/ABL} harboring the Y253F or E255K but not the T315I mutations. Furthermore, it restored Imatinib-sensitivity to p185^{BCR/ABL} harboring the Y253F and E255K mutations but not to p185^{BCR/ABL-T315I} (Beissert *et al.*, 2008). To determine whether T315I and the other two most clinically relevant mutations Y253F and E255K influence the leukemogenic potential of p185^{BCR/ABL}, we created oligomerization-deficient p185^{BCR/ABL} lacking the N-terminal CC-domain (Δ CCp185) (Beissert *et al.*, 2003) and harboring the Y253F, the E255K, or the T315I mutations. The aberrant kinase activity of unmutated BCR/ABL induces signaling pathways able to replace factor-induced survival signaling of hematopoietic precursors such as the IL-3 signaling in the Ba/F3 cell line. We first investigated the capacity of the mutated Δ CCp185 to mediate factor independence of Ba/F3 cells. Therefore we retrovirally expressed the indicated constructs (Figure 22A) in Ba/F3 cells and controlled the transgene expression by Western blotting (Figure 22B). As reported in figure 22C, “unmutated” Δ CCp185 did not grow upon factor withdrawal, in contrast to Δ CCp185 harboring Y253F and T315I, which exhibited growth curves identical to unmutated p185^{BCR/ABL}. The Δ CCp185-E255Y cells showed a delay in growth of two days (Figure 22C). To avoid cell specific effect we did the same experiments using myeloid hematopoietic cells (32D). As shown in figure 22D, in “unmutated” p185^{BCR/ABL} deletion of the coiled-coil domain completely inhibited the growth of p185^{BCR/ABL} after factor withdrawal but Δ CCp185 harboring T315I exhibited growth curves identical to unmutated p185^{BCR/ABL}. The Δ CCp185-E255Y and Δ CCp185-Y253F cells showed a delay in growth (Figure 22D).

To investigate the influence of the mutations on the transformation potential of p185^{BCR/ABL}, we performed classical transformation assays: focus formation assays for the determination of contact inhibition and colony assays in semi-solid medium for the determination of

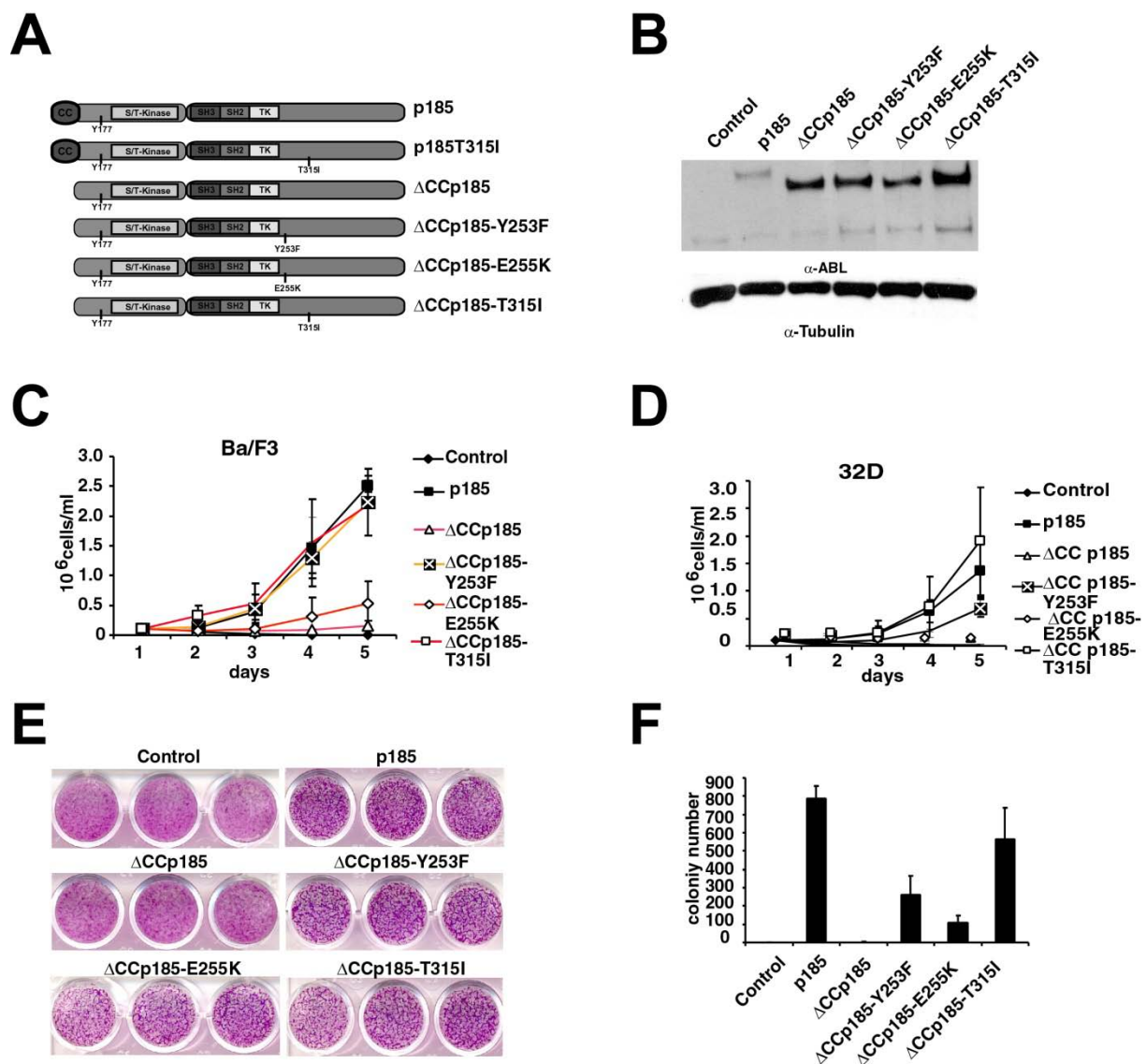


Figure 22 - The influence of the resistance mutations on the transformation potential of oligomerization-deficient p185^{BCR/ABL}. (A) Modular organization of the p185^{BCR/ABL} mutants lacking the CC oligomerization interface. (B) Expression of the transgenes in Ba/F3 cells. Tubulin was used as a loading control. (C) Factor-independent growth of Ba/F3 cells expressing the indicated transgenes; the graph shows the means \pm SDs (standard deviations) of three independent experiments. (D) Factor-independent growth of 32D cells expressing the indicated transgenes; the graph shows the means \pm SDs (standard deviations) of three independent experiments. (E) Focus formation assay - 4×10^4 infected Rat-1 cells/well were plated in 24-well-plates, grown for 72h to confluence, and incubated for additional 12 days. The plates were then washed, dried, and stained with crystal violet. One representative of each of 3 experiments performed in triplicate is given (34x magnification). (F) Colony formation - Rat-1 cells were retrovirally transduced with the indicated constructs and seeded at 5×10^3 cells/well in soft-agar in 6-well-plates. After 15 days, the colonies were counted and the means \pm SDS of triplicates of 2 representative experiments are given.

anchorage-dependent growth. We retrovirally transduced Rat-1 fibroblasts with the constructs indicated in figure 22A. As shown in Figure 22 E and F, the inhibition of the oligomerization by the deletion of the CC-domain completely abolished both focus and colony formation of p185^{BCR/ABL}, whereas the presence of Y253F, E255K, or T315I restored the transformation

potential of Δ CCp185 as shown by the formation of foci and colonies, respectively (Figure 22E and F).

Taken together, these data indicate that the "p-loop mutations" Y253F and E255K and the "gatekeeper" mutation T315I are not only responsible for AKI-resistance but also confer additional properties to the oligomerization-deficient Δ CCp185, which allow the transformation potential and the capacity to mediate factor independence to be restored. Notably, the T315I mutation exhibited the most prominent effects. We focused our study on the "gatekeeper" mutation T315I which confers resistance against virtually all ATP competitors and oligomerization inhibition.

4.3.5 The "gatekeeper" mutation T315I restores the capacity to mediate factor independence of oligomerization-deficient CML-associated p210^{BCR/ABL}

T315I confer additional properties to the oligomerization-deficient Δ CCp185, which allow the transformation potential and the capacity to mediate factor independence.

To determine whether T315I influences the leukemogenic potential of p210^{BCR/ABL} also, we created oligomerization-deficient p210^{BCR/ABL} lacking the N-terminal CC-domain (Δ CCp210) and harboring the T315I mutation. The aberrant kinase activity of unmutated BCR/ABL induces signaling pathways able to replace factor-induced survival signaling of hematopoietic precursors such as the IL-3 signaling in the Ba/F3 cell line. We first investigated the capacity of the mutated Δ CCp210 to mediate factor independence of Ba/F3 cells. Therefore we retrovirally expressed the indicated constructs (Figure 23A) in Ba/F3 cells and controlled the transgene expression by Western blotting (Figure 23B). As reported in Figure 23C, "unmutated" Δ CCp210 did not grow upon factor withdrawal, in contrast to Δ CCp185 harboring T315I, which exhibited growth curves identical to unmutated p185^{BCR/ABL}.

Collectively these data show that in CML-associated p210^{BCR/ABL}, T315I restored the factor independent growth of the oligomerization deficient Δ CCp210 in similar way as p185^{BCR/ABL}. Therefore, we focused our study on the Ph+ ALL-associated p185^{BCR/ABL} because there is no difference in the response to oligomerization inhibition between CML-associated p210^{BCR/ABL} and p185^{BCR/ABL}.

4.3.6 Deletion of BCR AA 64-412 (BCC/ABL) sensitizes T315I towards inhibitory peptides

To determine the mechanisms i.) of the resistance of T315I mutants against the inhibition of oligomerization and ii.) of how the T315I mutation influences the biology of BCR/ABL itself, we investigated the effects of T315I on BCR/ABL mutants that have no capacity or a reduced

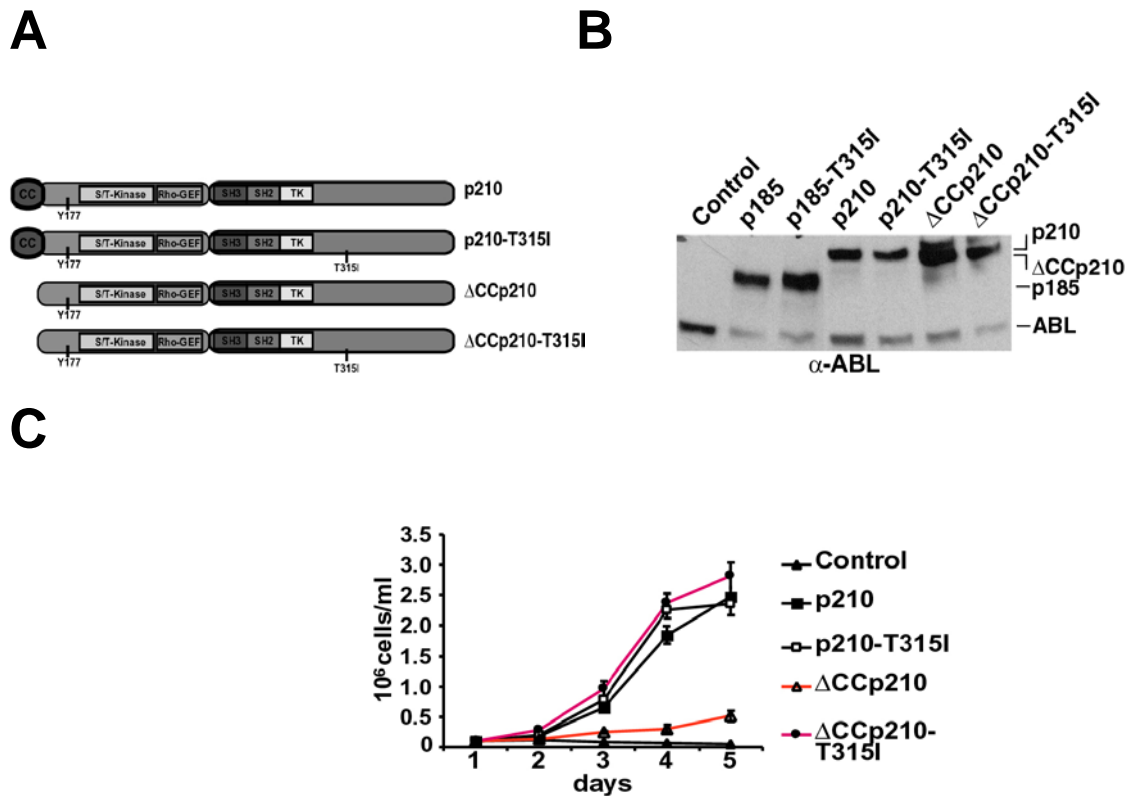


Figure 23 - The influence of the resistance mutations on the transformation potential of oligomerization-deficient p210^{BCR/ABL}. (A) Modular organization of the p210^{BCR/ABL} and its T315I mutant lacking the CC oligomerization interface. (B) Expression of the transgenes in Ba/F3 cells in comparison to p185^{BCR/ABL} and p185-T315I. The detection of endogenous ABL allows us to evaluate equal loading. (C) Factor-independent growth of Ba/F3 cells expressing the indicated transgenes; the graph shows the means \pm SDs of three independent experiments.

capacity to mediate factor-independent growth of hematopoietic progenitors. First we focused on mutations interfering with functional domains in the BCR-portion of the fusion protein. We investigated the effects of T315I on BCC/ABL, in which the CC-domain is directly fused to the ABL-portion of the fusion protein (Beissert *et al.*, 2003). Thus; we retrovirally transduced Ba/F3 and 32D cells with the indicated constructs (Figure 24A) and the expression of the transgenes was controlled by Western blotting (Figure 24B). We investigated cell growth upon factor withdrawal (Figure 24C-F). As shown in Figure 24C, T315I strongly improved the capacity of BCC/ABL to mediate factor-independent growth of Ba/F3. In fact, BCC/ABL-T315I grew to the same extent as unmutated p185^{BCR/ABL}, whereas BCC/ABL showed the expected delay in growth (Figure 24C). To study the response of these mutants to the inhibition of the oligomerization, we performed proliferation competition assays upon exposure to either the Helix-2 peptide fused to GFP or to GFP alone as a control as described previously (Beissert *et al.*, 2008).

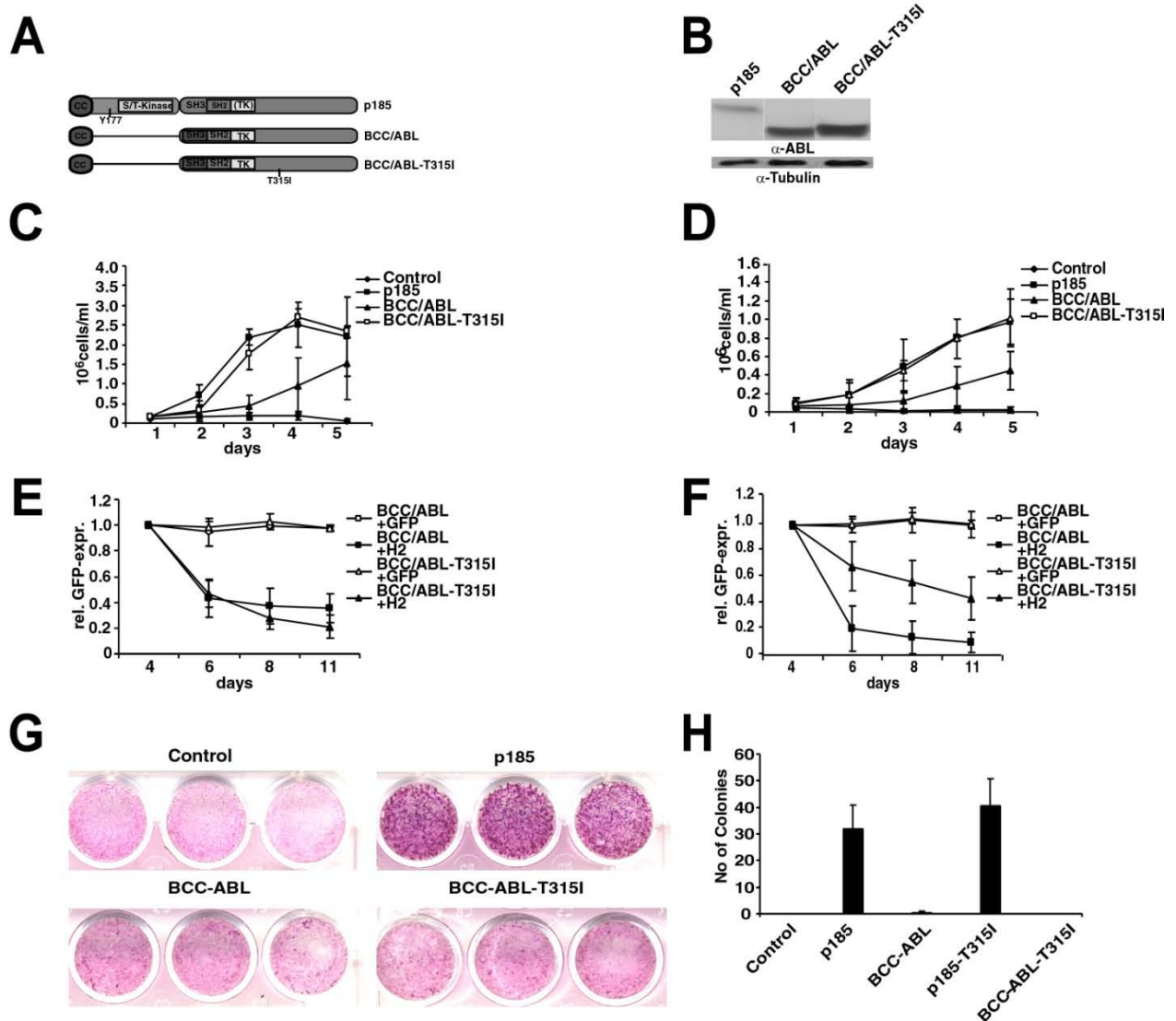


Figure 24 - Role of serine/threonine and Grb-2 binding domains in the resistance of T315I mutants against the oligomerization inhibition by Helix-2. For the determination of factor-independent growth and for the proliferation competition assays (CPAs) and transformation assays, Ba/F3, 32D and Rat-1 cells were retrovirally transduced with the indicated constructs. **(A)** BCC/ABL - the N-terminal CC-domain of BCR/ABL directly fused to the ABL-portion of the fusion protein +/- T315I. **(B)** Transgene expression was confirmed by Western blotting with the indicated antibodies. Molecular mass references (KDa) are given, and α -Tubulin was used as a loading control. **(C)** factor-independent growth Ba/F3 cells and **(D)** factor-independent growth 32D cells. The number of viable cells was daily determined by Trypan blue dye-exclusion. **(E)** CPAs for Ba/F3 and **(F)** for 32D cells. The cells were adapted to factor independence, infected with GFP or Helix-2-GFP, and seeded. The proportion of the GFP-positive cell fraction was followed by FACS for 10 days and normalized to the GFP expression at day 4 (rel. GFP expression). The graphs show the means \pm SD of three independent experiments. **(G)** Focus formation assay - 4×10^4 infected Rat-1 cells/well were plated in 24-well-plates, grown for 72h to confluence, and incubated for additional 12 days. The plates were then washed, dried, and stained with crystal violet. One representative of each of 3 experiments performed in triplicate is given (34x magnification). **(H)** Colony formation - Rat-1 cells were retrovirally transduced with the indicated constructs and seeded at 5×10^3 cells/well in soft-agar in 6-well-plates. After 15 days, the colonies were counted and the means \pm SDS of triplicates of 2 representative experiments are given.

The capacity of both BCC/ABL and BCC/ABL-T315I to mediate factor-independent growth was completely abolished by the inhibition of the BCC-mediated oligomerization through the

competitive Helix-2 peptide (Figure 24E). Similar results were obtained in 32D cells (Figure 24D and F)

Regarding the transformation potential of p185^{BCR/ABL}, we performed focus formation assays for the determination of contact inhibition and colony assays in semi-solid medium for the determination of anchorage-dependent growth. We retrovirally transduced Rat-1 fibroblasts with the constructs indicated in figure 24A. As shown in figure 24G and H, deletion of the S/T and Grb-2 binding (Y177) domains completely abolished both focus and colony formation of p185^{BCR/ABL} and p185^{BCR/ABL-T315I}.

Collectively these data show that deletion of serine/threonine and Grb-2 binding domains sensitize T315I towards inhibitory peptides and the cells are no more transformed.

4.3.7 In case of Δ S/T (BCR 1-196ABL) construct: T315I enhances factor independence while transformation of fibroblast is not changed

Further we constructed mutants BCR(1-196) ABL and BCR(1-196) ABL-T315I, in which the Y177 phosphorylation is present in addition to the CC-domain. We retrovirally transduced Ba/F3 cells with the indicated constructs (Figure 25A) and controlled the expression of transgene by western blotting (Figure 25B). We investigated cell growth upon factor withdrawal by dye exclusion using Trypan-blue (Figure 25C). As show in (Figure 26B) the T315I mutation improved the capacity to mediate factor-independent growth to the level of unmutated p185^{BCR/ABL}, while unmutated BCR/ABL showed a delay in growth.

To study the response of the above mutants to the inhibition of the oligomerization, we performed proliferation competition assays upon exposure to either the Helix-2 peptide fused to GFP or to GFP alone as a control as described previously (Beissert *et al.*, 2008). Notably, the presence of T315I rendered the BCR (1-196)/ABL resistant against the inhibition of oligomerization by Helix-2 (Figure 25D).

To determine transformation potential, focus formation assay and colony formation in semi-solid medium were performed with retrovirally transduced Rat-1 cells. As depicted in figure 25E and F deletion of serine/threonine domain did not change the transformation potential of fibroblast.

Take together these data show that serine/ threonine domain has no important role in transformation of fibroblast and the resistance of T315I towards inhibitory peptides.

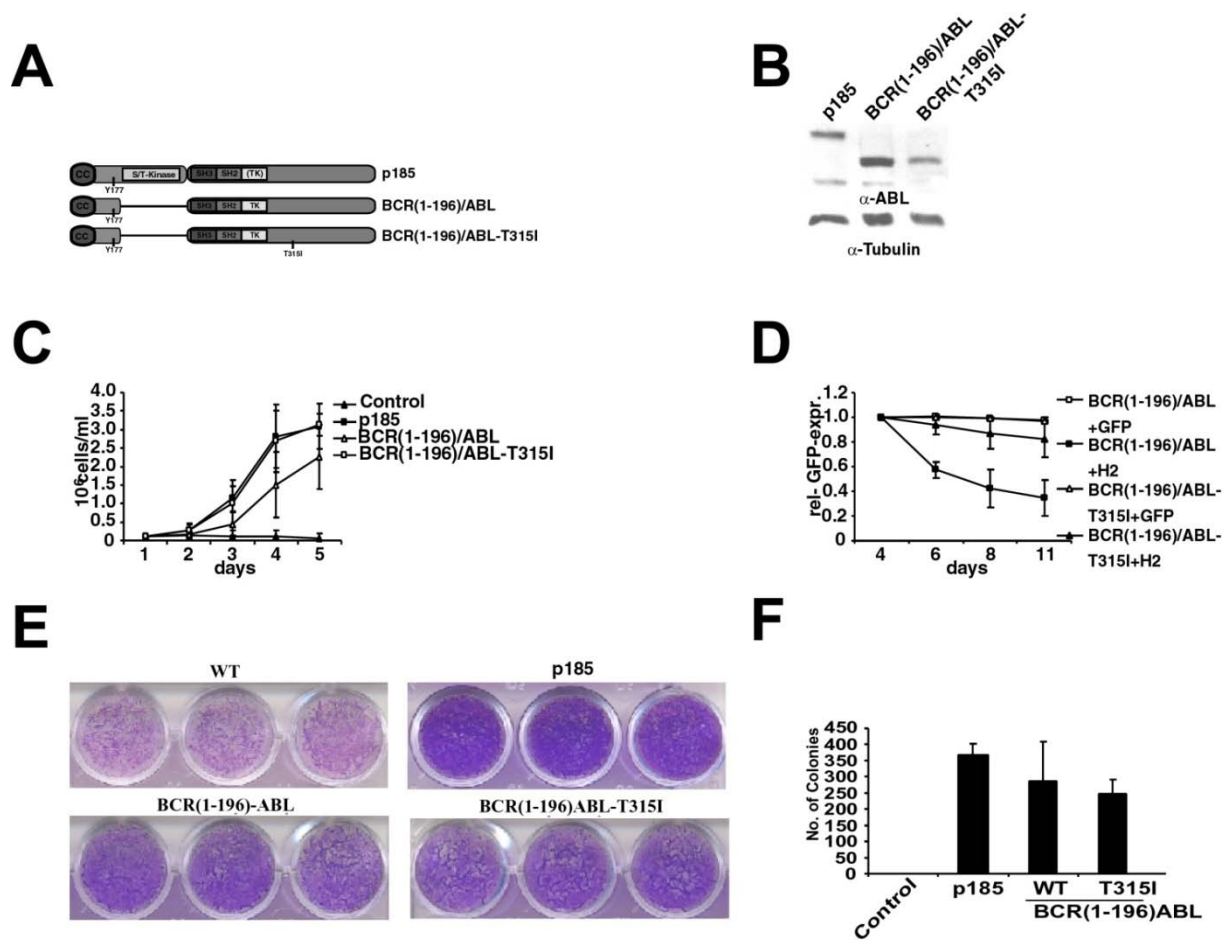


Figure 25 - Role of serine/threonine domain in the resistance of T315I mutants against the oligomerization inhibition by Helix-2. For the determination of factor-independent growth and for the proliferation competition assays (CPAs) and transformation assays, Ba/F3 and Rat-1 cells were retrovirally transduced with the indicated constructs. **(A)** Δ S/T-ABL or BCR(1-196)/ABL - the N-terminal CC-domain to Grb-binding sites of BCR/ABL directly fused to the ABL-portion of the fusion protein +/- T315I. **(B)** Transgene expression was confirmed by Western blotting with the indicated antibodies. Molecular mass references (KDa) are given, and α -Tubulin was used as a loading control. **(C)** factor-independent growth Ba/F3 cells. The number of viable cells was daily determined by Trypan blue dye-exclusion. **(D)** CPAs for Ba/F3 cells. The cells were adapted to factor independence, infected with GFP or Helix-2-GFP, and seeded. The proportion of the GFP-positive cell fraction was followed by FACS for 10 days and normalized to the GFP expression at day 4 (rel. GFP expression). The graphs show the means +/- SD of three independent experiments. **(E)** Focus formation assay - 4×10^4 infected Rat-1 cells/well were plated in 24-well-plates, grown for 72h to confluence, and incubated for additional 12 days. The plates were then washed, dried, and stained with crystal violet. One representative of each of 3 experiments performed in triplicate is given (34x magnification). **(F)** Colony formation - Rat-1 cells were retrovirally transduced with the indicated constructs and seeded at 5×10^3 cells/well in soft-agar in 6-well-plates. After 15 days, the colonies were counted and the means +/- SD of triplicates of 2 representative experiments are given.

4.3.8 Resistance of $p185^{BCR/ABL-T315I}$ against inhibition of the oligomerization depends on the phosphorylation at Y177

To confirm the hypothesis that the phosphorylation of Y177 is indispensable for the resistance of $p185^{BCR/ABL}$ harboring the T315I mutation against the Helix-2, we studied a $p185$ -T315I mutant in which phosphorylation at Y177 was abolished by a point mutation to phenylalanine ($p185$ -Y177F-T315I). We retrovirally transduced Ba/F3 cells with the indicated constructs

and confirmed the expression of transgene by western blotting (Figure 26A and B). We investigated cell growth upon factor withdrawal by dye exclusion using trypan-blue. As shown in figure 26C, the absence of phosphorylation at Y177 strongly delayed growth upon factor withdrawal, which was completely restored by the presence of T315I. To study the response of these mutants to the inhibition of the oligomerization, we performed proliferation competition assays upon exposure to either the Helix-2 peptide fused to GFP or to GFP alone as a control as described previously (Beissert *et al.*, 2008). Factor-independent growth of p185^{BCR/ABL} which was reduced by mutating Y177 to Y177F was completely abolished by the inhibition of oligomerization through the competitive Helix-2 peptides. Furthermore, the p185-Y177F-T315I turned sensitive to the oligomerization inhibition by Helix-2 (Figure 26D).

To study transformation potential of the fibroblast, focus formation and semi-solid colony formation assays were performed. As shown in figure 26E, mutation of Y177 to phenylalanine impaired colony formation in unmutated BCR/ABL but not in T315I, while no difference was observed foci formation (Figure 26E and F).

In summary, our results show that i.) the phosphorylation of Y177 is critical for the resistance of p185^{BCR/ABL} against the inhibition of the oligomerization ii.) the phosphorylation of Y177 is for colony formation but has no role in foci formation iii.) the effects of the T315I mutation are not limited to oligomerization-deficient p185^{BCR/ABL} mutants.

4.3.9 Autophosphorylation at Y177 is not affected by the oligomerization inhibition, but phosphorylation at Y177 of endogenous BCR parallels the effects of T315I

The differences between unmutated p185^{BCR/ABL} and p185-T315I regarding the apparent importance of the phosphorylation at Y177 for the resistance against the inhibition of oligomerization prompted us to investigate the tyrosine phosphorylation at Y177 in the presence/absence of T315I. We used a specific antibody directed against BCR phosphorylated at Y177 on lysates of Ba/F3 cells expressing the different p185^{BCR/ABL} mutants with or without the T315I mutation. To avoid the interference of stress signalling induced by the selection factor withdrawal, we performed these experiments on newly transduced cells in the presence of IL-3. We showed that unmutated p185^{BCR/ABL} and all mutants in which Y177 was present (Δ CCp185, Δ CCp185-T315I, BCR(1-196)/ABL, BCR(1-196)/ABL-T315I) were fully phosphorylated at the Y177 (Figure 27A-C) independently of the inhibition of oligomerization through either the Helix-2 or the deletion of the CC-domain (Figure 27A and B).

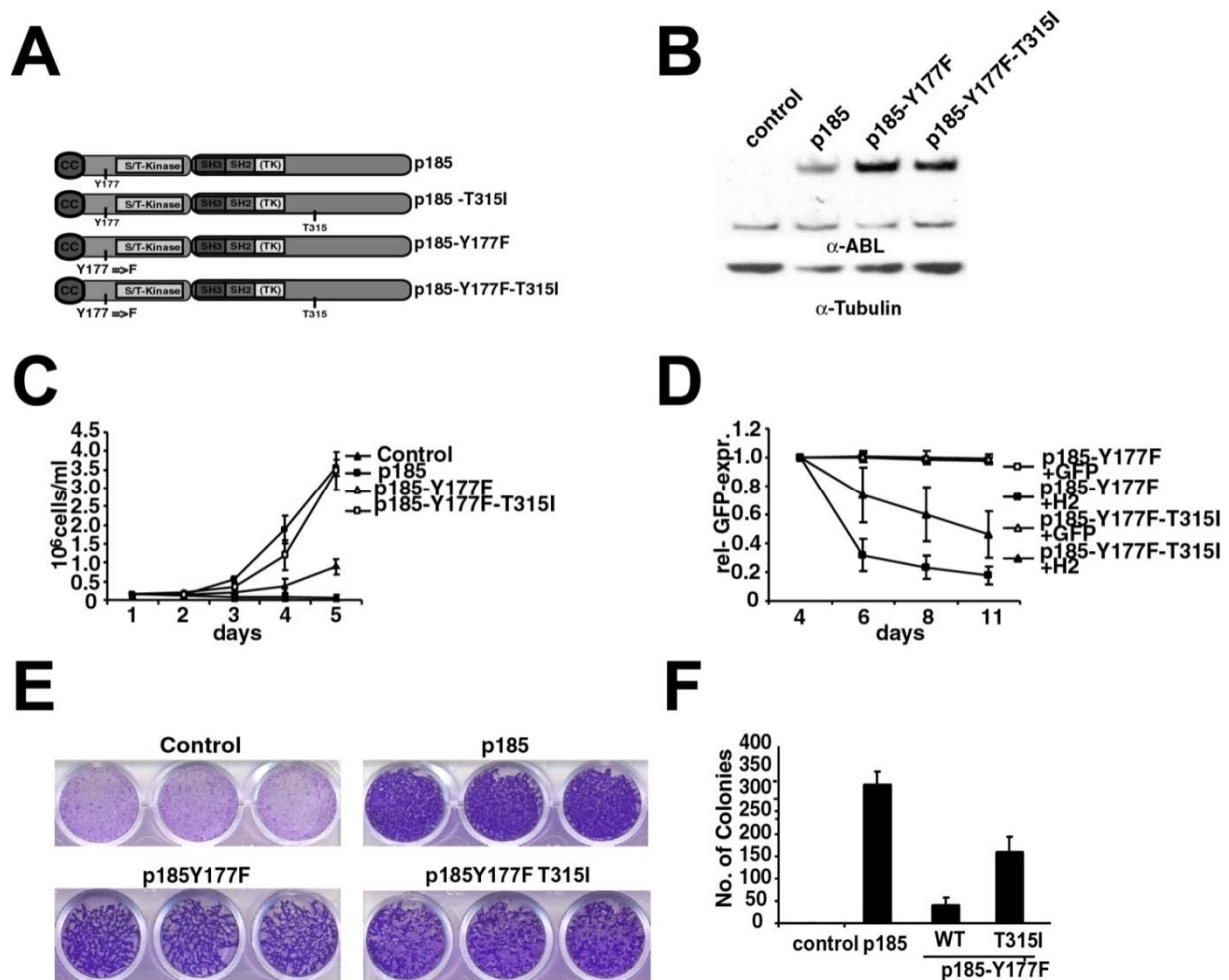


Figure 26 - Role of Y177 in the resistance of T315I mutants against the oligomerization inhibition by Helix-2. For the determination of factor-independent growth and for the proliferation competition assays (CPAs) and transformation assays, Ba/F3 and Rat-1 cells were retrovirally transduced with the indicated constructs. **(A)** Grb-2-binding site Y177 of BCR/ABL was mutated to phenylalanine +/- T315I. **(B)** Transgene expression was confirmed by Western blotting with the indicated antibodies. Molecular mass references (kDa) are given, and α -Tubulin was used as a loading control. **(C)** factor-independent growth Ba/F3 cells. The number of viable cells was daily determined by Trypan blue dye-exclusion. **(D)** CPAs for Ba/F3 cells. The cells were adapted to factor independence, infected with GFP or Helix-2-GFP, and seeded. The proportion of the GFP-positive cell fraction was followed by FACS for 10 days and normalized to the GFP expression at day 4 (rel. GFP expression). The graphs show the means \pm SD of three independent experiments. **(E)** Focus formation assay - 4×10^4 infected Rat-1 cells/well were plated in 24-well-plates, grown for 72h to confluence, and incubated for additional 12 days. The plates were then washed, dried, and stained with crystal violet. One representative of each of 3 experiments performed in triplicate is given (34x magnification). **(F)** Colony formation - Rat-1 cells were retrovirally transduced with the indicated constructs and seeded at 5×10^3 cells/well in soft-agar in 6-well-plates. After 15 days, the colonies were counted and the means \pm SDS of triplicates of 2 representative experiments are given.

The antibody also revealed the Y177-phosphorylation of endogenous BCR. The inhibition of oligomerization either by the deletion of the CC-domain or by the competitive Helix-2 peptides reduced or abolished Y177 phosphorylation of endogenous BCR in cells expressing

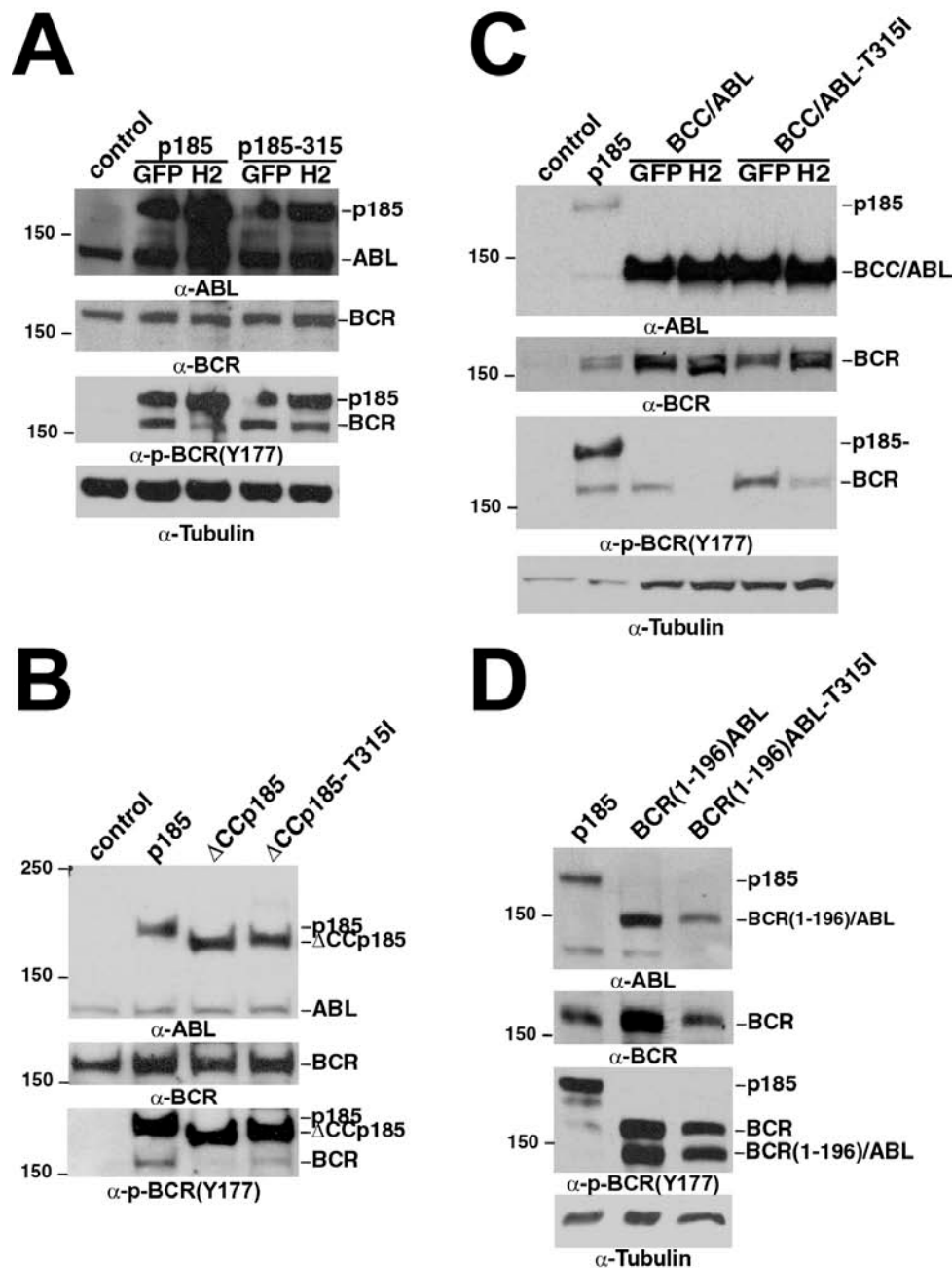


Figure 27 - Y177-phosphorylation in the autophosphorylation of p185BCR/ABL and its mutants and the transphosphorylation of endogenous BCR in relationship to the presence of T315I upon the inhibition of oligomerization. Western blotting using antibodies directed against BCR (which did not detect BCR/ABL) (α -BCR) and BCR phosphorylated at Y177 (α -p-BCRY177). p185^{BCR/ABL} and its mutants were detected by an α -ABL-antibody. Molecular mass references (KDa) are given. Tubulin or endogenous ABL was used as a loading control. (A) Ba/F3 cells expressing p185^{BCR/ABL} or p185-T315I in the presence of either Helix-2 (H2) or control GFP. (B) Ba/F3 cells expressing p185^{BCR/ABL} p185-T315I lacking the N-terminal CC-oligomerization interface (Δ CCBCR/ABL) in the presence of either Helix-2 (H2) or control GFP. (C) Ba/F3 cells expressing BCC/ABL +/- T315I in the presence of either Helix-2 (H2) or control GFP. (D) Ba/F3 cells expressing BCR(1-196)/ABL +/- T315I.

unmutated p185^{BCR/ABL}, BCR(1-196)/ABL, or BCC/ABL (Figure 27A-C). Notably, in all mutants, the T315I mutation restored the phosphorylation of BCR at Y177 independently of targeting the oligomerization (Figure 27A-C and D).

Taken together, these data indicate that the biological effects of the T315I mutation may be mediated through an aberrant trans-phosphorylation of endogenous BCR as an expression of a restored or increased substrate phosphorylation by the ABL-kinase in the presence of the T315I mutation.

4.3.10 The effects of T315I are associated with an intact ABL-kinase activity

Our data suggest a direct relationship between positive effects of T315I on p185^{BCR/ABL}-mutants and the phosphorylation of endogenous BCR. To confirm this hypothesis and to disclose whether the effects of T315I depend on an intact ABL-kinase activity, we first explored the effects of T315I on the isolated ABL portion of the BCR/ABL fusion proteins (#ABL) regarding factor-independent growth. Ba/F3 cells were retrovirally transduced with the indicated constructs the expression of the transgenes was controlled by Western blotting (Figure 28A and B). As shown in Figure 28C, T315I was unable to confer to #ABL the capacity to induce factor-independence. To investigate transformation potential of fibroblast of #ABL constructs, we performed focus formation and semi-solid colony assay using retrovirally transduced RAT-1 cells. As show in figure 28E and F, T315I could not confer transformation potential to the deleted construct #ABL. In these cells, endogenous BCR was not phosphorylated (Figure 28B). Same results were obtained from 32D cells (Figure 28D). These data show that T315I exerts its effects in the presence of an intact ABL-kinase activity and confirm the relationship between the phosphorylation of endogenous BCR and the capacity of BCR/ABL and ABL-mutants to mediate factor-independent growth induced by the presence of T315I.

4.3.11 Deletion of regulatory SH3 domain (Δ SH3-ABL) restores factor-independent growth of T315I

In the past, it has been described that the deletion or inactivation of the SH3 domain of ABL by point mutations confers transformation potential to c-ABL (Barila and Superti-Furga, 1998; Zheng *et al.*, 2004). The SH3 domain seems to be responsible for the functional inactivity of the ABL-portion of BCR/ABL. Hence, we created a mutant that lacks a functional SH3 domain (Δ SH3-ABL) alone and in combination with the T315I and retrovirally transduced Ba/F3 cells with these constructs (Figure 29A). As shown in Figure 29C, upon factor-withdrawal, Δ SH3-ABL allowed the survival of the cells but the cells did not proliferate. In contrast, cells expressing Δ SH3-ABL-T315I proliferated to the same extent as p185^{BCR/ABL}. In both Δ SH3-ABL- and Δ SH3-ABL-T315I-expressing cells, endogenous BCR was phosphorylated (Figure 29B).

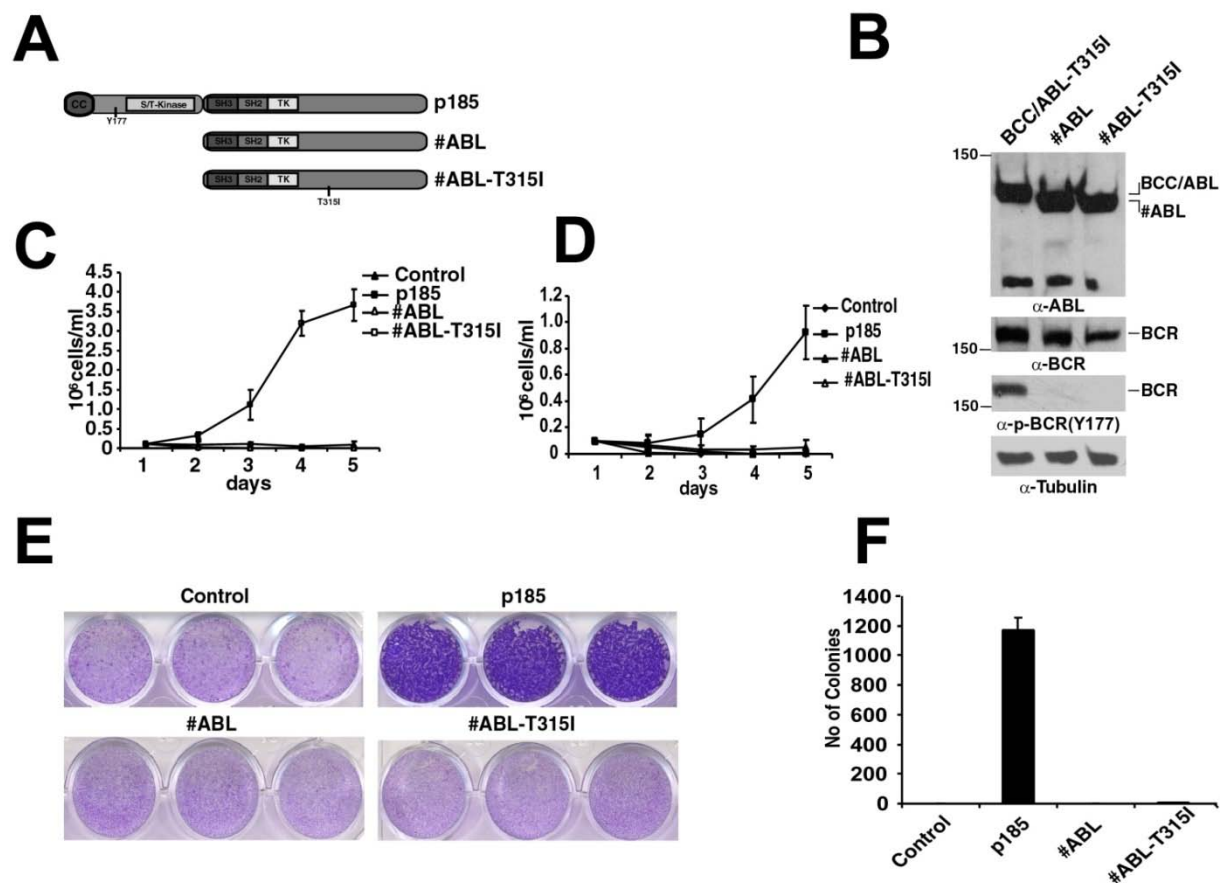


Figure 28 - Role of the ABL-kinase in the activity of T315I in p185BCR/ABL and its mutants. For the determination of factor-independent growth and transformation assay, Ba/F3 and Rat-1 cells were retrovirally transduced with the indicated constructs and grown upon factor withdrawal. **(A)** Constructs #ABL - the ABL-portion of the BCR/ABL fusion protein +/- T315I. **(B)** Transgene expression was confirmed by Western blotting with the indicated antibodies against ABL and BCR and BCR phosphorylated at Y177. α -Tubulin was used as a loading control. **(C)** factor-independent growth Ba/F3 cells. The number of viable cells was daily determined by Trypan blue dye-exclusion. **(D)** CPAs for Ba/F3 cells. The cells were adapted to factor independence, infected with GFP or Helix-2-GFP, and seeded. The proportion of the GFP-positive cell fraction was followed by FACS for 10 days and normalized to the GFP expression at day 4 (rel. GFP expression). The graphs show the means \pm SD of three independent experiments. **(E)** Focus formation assay - 4×10^4 infected Rat-1 cells/well were plated in 24-well-plates, grown for 72h to confluence, and incubated for additional 12 days. The plates were then washed, dried, and stained with crystal violet. One representative of each of 3 experiments performed in triplicate is given (34x magnification). **(F)** Colony formation - Rat-1 cells were retrovirally transduced with the indicated constructs and seeded at 5×10^3 cells/well in soft-agar in 6-well-plates. After 15 days, the colonies were counted and the means \pm SDS of triplicates of 2 representative experiments are given.

Collectively these data show that deletion of SH3 domain restores factor-independent growth of T315I which is accompanied with endogenous BCR phosphorylation.

4.3.12 Oligomerization domain & GRB-2 binding site double deletions (Δ CCp185-

Y177F): T315I enhances factor-independence

To definitively prove the effects of T315I on functionally completely inactive BCR/ABL mutants, we created an oligomerization-deficient mutant lacking the phosphorylation site at

Y177 (Δ CCp185-Y177F). We retrovirally transduced Ba/F3 cells for factor-independent growth and Rat-1 for transformation potential with the indicated constructs (Figure 30A).

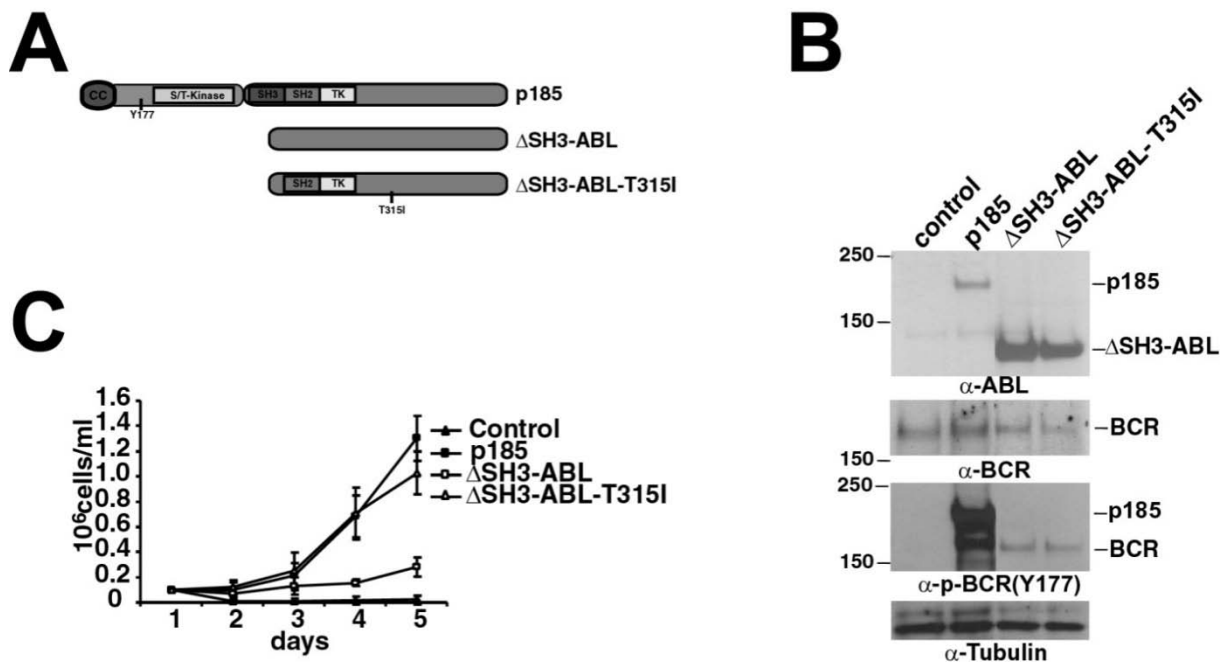


Figure 29 - Role of the SH3 domain in the activity of T315I in p185BCR/ABL. For the determination of factor-independent growth, Ba/F3 cells were retrovirally transduced with the indicated constructs and grown upon factor withdrawal. **(A)** Constructs Δ SH3-ABL - ABL lacking the N-terminal SH3 domain +/-T315I. **(B)** Transgene expression was confirmed by Western blotting with the indicated antibodies against ABL and BCR and BCR phosphorylated at Y177. α -Tubulin was used as a loading control. **(C)** factor-independent growth Ba/F3 cells. The number of viable cells was daily determined by Trypan blue dye-exclusion.

Interestingly, even in this mutant, which lacks two functions considered indispensable for the activity of BCR/ABL, in the presence of T315I the capacity to mediate factor independent growth was almost completely restored (Figure 30B). The same results were observed for transformation potential of fibroblast (Figure 30D and E). Also, the presence of T315I was accompanied by the Y177 phosphorylation of endogenous BCR (Figure 30C).

These data show that T315I exerts its effects in the presence of an intact ABL-kinase activity and confirm the relationship between the phosphorylation of endogenous BCR and the capacity of BCR/ABL and ABL-mutants to mediate factor-independent growth induced by the presence of T315I. Furthermore, it seems that activation of the ABL-kinase activity is enough to ensure survival of cells upon factor withdrawal but not to make them proliferate.

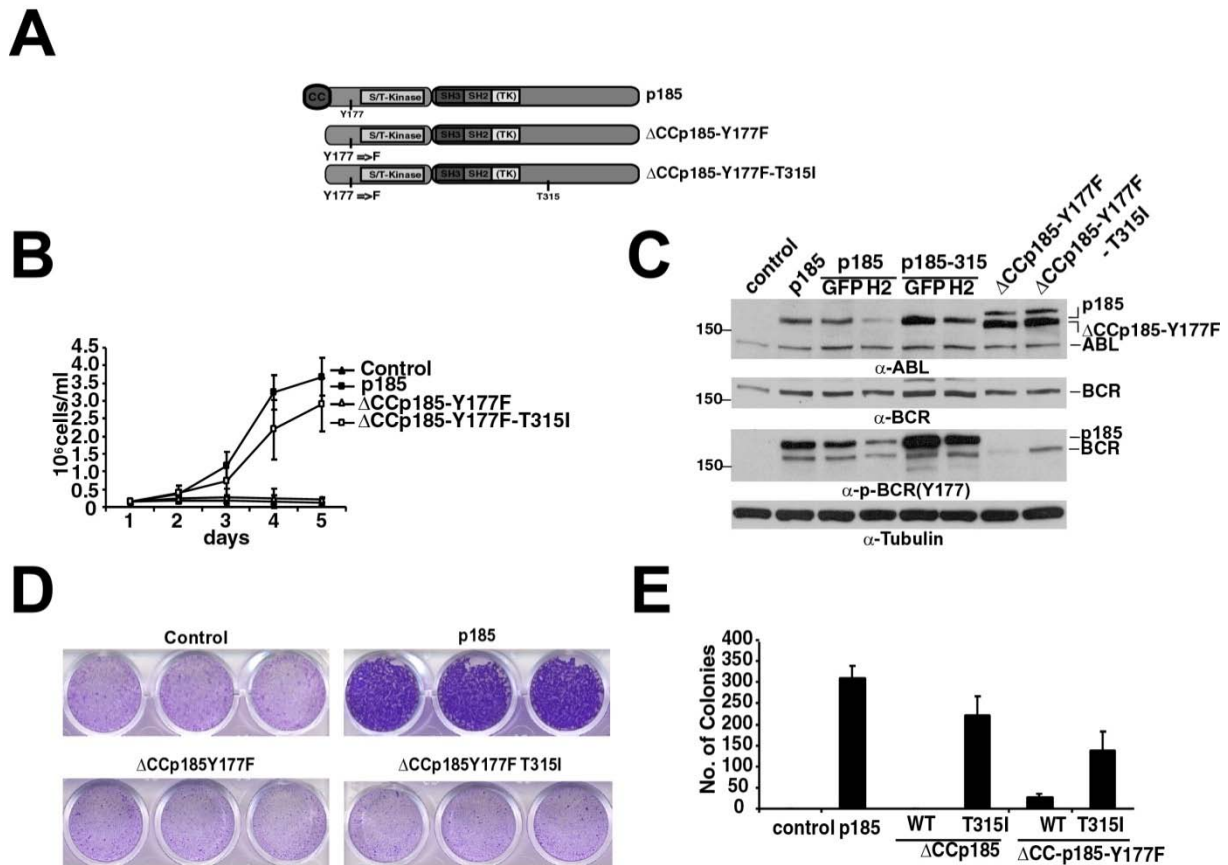


Figure 30 - The influence of the resistance mutations on the transformation potential of oligomerization-deficient & GRB-2 binding site (Y177F) double mutant BCR/ABL. (A) Modular organization of the p185^{BCR/ABL} mutants lacking the CC oligomerization interface and point mutation in the Grb-2 binding site Y177. (B) Factor-independent growth of Ba/F3 cells expressing the indicated transgenes; the graph shows the means \pm SDs (standard deviations) of three independent experiments. (C) Transgene expression was confirmed by Western blotting with the indicated antibodies against ABL and BCR and BCR phosphorylated at Y177. α -Tubulin was used as a loading control. (D) Focus formation assay - 4×10^4 infected Rat-1 cells/well were plated in 24-well-plates, grown for 72h to confluence, and incubated for additional 12 days. The plates were then washed, dried, and stained with crystal violet. One representative of each of 3 experiments performed in triplicate is given (34 x magnifications). (E) Colony formation - Rat-1 cells were retrovirally transduced with the indicated constructs and seeded at 5×10^3 cells/well in soft-agar in 6-well-plates. After 15 days, the colonies were counted and the means \pm SDs of triplicates of 2 representative experiments are given.

4.3.13 The presence of T315I is associated with increased ABL-kinase activity also in mutants unable to induce Y177 phosphorylation of endogenous BCR

To determine whether the Y177 phosphorylation in the presence of T315I is due to increased substrate phosphorylation of the ABL-kinase, we investigated whether the T315I was able to interfere with the ABL-kinase activity. Therefore, we studied the autophosphorylation at Y245 in the different mutants used in this study. As shown in Figure 31, T315I increased the autophosphorylation in all mutants as revealed by the specific antibody. Interestingly, T315I induced a slight increase in kinase activity in the #ABL mutant, which was unable to rescue

the capacity of this mutant to mediate factor independent growth or the Y177 phosphorylation of endogenous BCR (32 A and B).

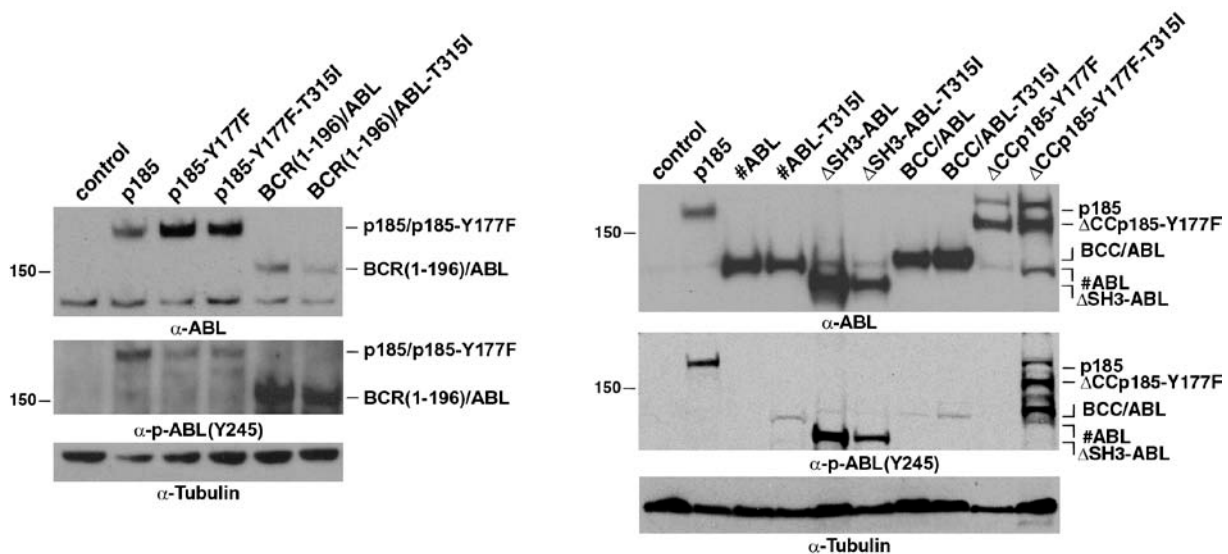


Figure 31 - Influence of T315I on the kinase activity p185^{BCR/ABL} and its mutants – autophosphorylation. Western blotting on lysates of Ba/F3 cells expressing the indicated transgenes using antibodies directed against c-ABL and ABL Y245 (α -p-ABLY245). Molecular mass references (kDa) are given and Tubulin was used as a loading control.

These data show that T315I induces increased ABL-kinase activity, an effect that is probably masked in the unmutated forms of BCR/ABL. Interestingly; there is no direct relationship between the ABL-kinase activity and the capacity to mediate factor-independence as revealed by the #ABL-T315I mutant, which was unable to induce Y177 phosphorylation of BCR.

Oligomerization inhibition and allosteric inhibition (GNF-2) are unable to overcome the resistance of BCR/ABL harboring the T315I mutation (Beissert *et al.*, 2008). we investigated whether it was possible to overcome the resistance of the BCR/ABL-T315I mutant against molecular therapeutic approaches by combining the allosteric inhibition of GNF-2 with the competitive peptide Helix-2 to inhibit BCR/ABL oligomerization.

4.4 Oligomerization inhibition combined with allosteric inhibition abrogates the transformation potential of T315I-positive BCR/ABL

4.4.1 Targeting the oligomerization of BCR/ABL increases the efficacy of GNF-2 against unmutated p185^{BCR/ABL} and p185^{BCR/ABL} harboring the T315I mutation

In order to determine whether or not the inhibition of oligomerization improved the response to allosteric inhibition of cells that depend on the functionality of BCR/ABL for their survival, we performed proliferation competition assay (PCA) on p185^{BCR/ABL} expressing

Ba/F3 cells. The principle of the assay is depicted in Figure 32A: Ba/F3 cells transduced with the retroviral vector PAULOp185. The resulting in bulk populations that uniformly coexpress p185^{BCR/ABL} and Δ LNGFR, were transduced with retroviral vectors harboring GFP and Helix-2-GFP. The resulting double infected cell populations were then exposed to GNF-2 at a concentration of 2 μ M, which was the IC50 for growth inhibition in our system. The effect of the transduced peptides was assessed by the detection of GFP positive cells for 10 days by FACS. The GFP-expression on day 2 was taken as a reference for normalization. As shown in figure 32B, the expression of GFP did not alter the proliferation of p185^{BCR/ABL} expressing Ba/F3 cells as revealed by the constant percentage of GFP positive cells. In contrast, Helix-2 inhibited the growth of p185^{BCR/ABL} expressing Ba/F3 cells as shown by the fact that the percentage of Helix-2-GFP expressing cells decreased over time with comparable kinetics (Figure 32B). The addition of GNF-2 accelerated and intensified the decrease of Helix-2-GFP expressing cells, but had no influence on GFP controls, suggesting a reciprocal interaction between the two compounds in blocking the BCR/ABL-dependent survival signaling upon factor withdrawal in these cells (Figure 32B).

Given the fact that PCA cannot reveal the effects of GNF-2 alone, we investigated the effects of GNF-2 alone or in combination with Helix-2 in comparison to the effects of Helix-2 on the proliferation of p185^{BCR/ABL}-expressing Ba/F3 cells by measuring the reduction of the tetrazolium salt XTT to formazan (XTT-assay). As a control, the cells were exposed to 0.5 μ M Imatinib. Imatinib and GNF-2 reduced the metabolic activity of the p185^{BCR/ABL}-expressing Ba/F3 cells to the same extent independently of the presence of helix-2 (Figure 32C).

Both GNF-2 and Helix-2 are known to have no effect on cells that express p185-T315I (Adrian *et al.*, 2006; Beissert *et al.*, 2008). To investigate whether the combination of these two approaches are able to inhibit p185-T315I, the experiments described above were repeated using Ba/F3 cells that express p185-T315I. The known resistance of these cells against GNF-2 and Helix-2 alone was confirmed in the PCA and the XTT assay (Figure 32D and E). Interestingly, in combination, the two compounds were nearly able to completely abolish the capacity of the p185-T315I mutant to mediate factor-independent growth (Figure 32D and E).

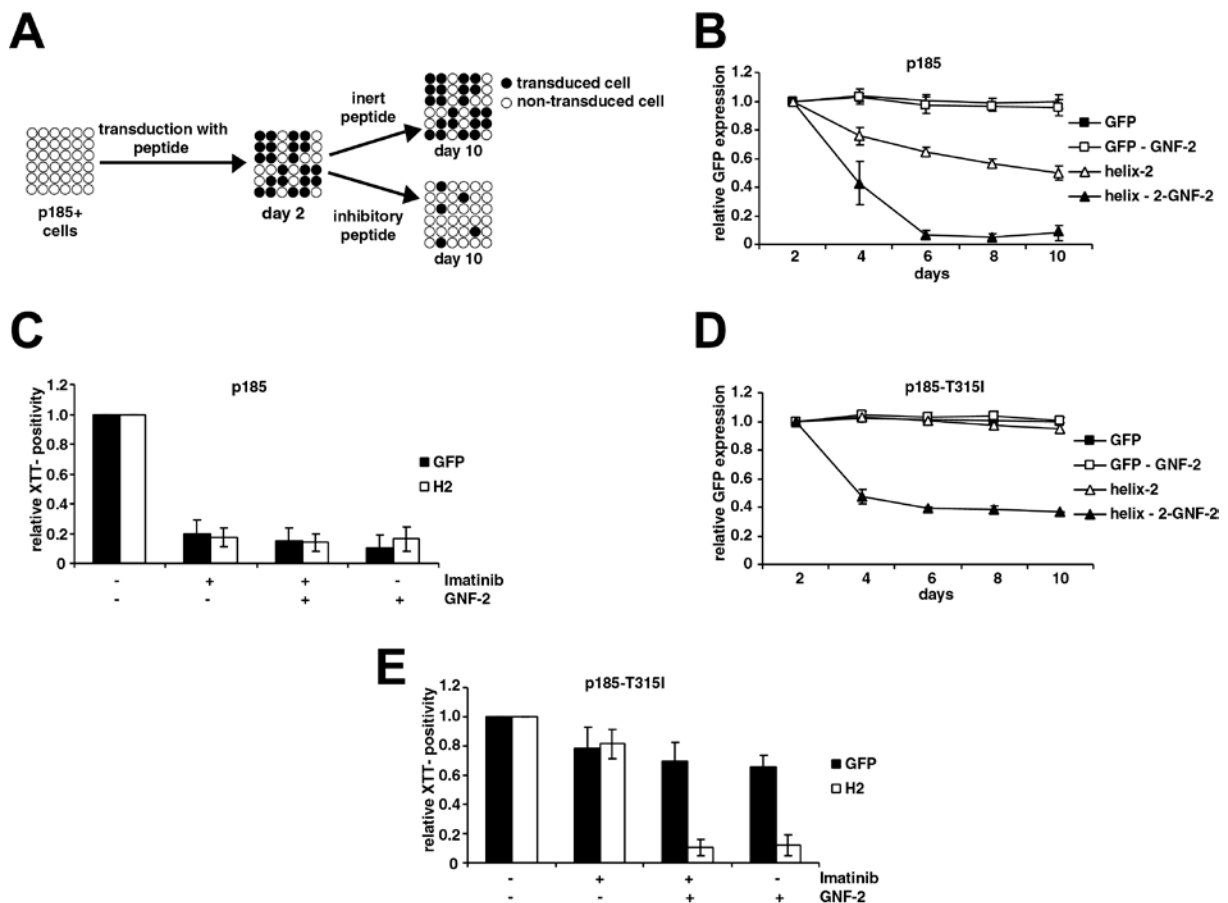


Figure 32 - Effects of the oligomerization inhibitor Helix-2 on the response of p185BCR/ABL and p185BCR/ABL T315I towards allosteric inhibition by GNF-2 (A) Schematic representation of the proliferation-competition assay. (B) Proliferation-competition assay (PCA) for BaF/3 cells expressing p185^{BCR/ABL}. Factor-independent cells (i.e. p185^{BCR/ABL} expressing Ba/F3 cells) were retrovirally infected with inert control peptides (GFP) or Helix-2-GFP. In the case of the inert GFP control, the percentage of GFP-positive cells remained constant from day 2 to day 10. In contrast, the expression of inhibitory peptides resulted in an outgrowth of peptide-expressing cells, which was revealed by progressive loss of Helix-2-GFP expression. (C) XTT assay for Ba/F3 cells expressing p185^{BCR/ABL} upon exposure to 0.5 μ M Imatininb and/or 2 μ M GNF-2 in the absence/presence of Helix-2, as indicated. Proliferation status was revealed by determination of the metabolic activity of cells given by the reduction rate of XTT to formazan. The means \pm SD of triplicates from one representative experiment out of three performed are given. (D) Proliferation-competition assay (PCA) for BaF/3 cells expressing p185^{BCR/ABL-T315I}. (E) XTT assay for Ba/F3 cells expressing p185^{BCR/ABL} upon exposure to 0.5 μ M Imatininb and/or 2 μ M GNF-2 in the absence/presence of Helix-2, as indicated. (E) Proliferation status was revealed by determination of the metabolic activity of cells given by the reduction rate of XTT to formazan. The means \pm SD of triplicates from one representative experiment out of three performed are given.

Taken together, these data suggest that the effect of GFN-2 may be enhanced by the monomerization of BCR/ABL and the combination of the two molecular approaches overcomes the resistance of BCR/ABL-T315I against the oligomerization inhibition of Helix-2 and the allosteric inhibition of GNF-2.

4.4.2 Targeting the oligomerization of BCR/ABL in combination with GNF-2 induces apoptosis in unmutated p185^{BCR/ABL} and p185^{BCR/ABL} harboring the T315I mutation

To investigate whether the observed effects on proliferation were related to the induction of apoptosis, factor-independent p185^{BCR/ABL}-expressing Ba/F3 cells in the presence/absence of Helix-2 were exposed to 2 μ M GNF-2 and stained with 7-AAD, which determines the apoptosis rate. As expected, GNF-2 increased the apoptosis rate as compared to the controls, whereas Helix-2 did not (Figure 33A). Interestingly, the combination of GNF-2 and Helix-2 induced an apoptosis rate close to 100% (Figure 33A).

Both GNF-2 and Helix-2 are known to have no effect on the induction of apoptosis in p185-T315I expressing cells (Adrian *et al.*, 2006; Beissert *et al.*, 2008). To investigate whether the combination of these two approaches are able to induce apoptosis in p185-T315I, factor-independent p185-T315I-expressing Ba/F3 cells in the presence/absence of Helix-2 were exposed to 2 μ M GNF-2. The treated cells were stained with 7-AAD after 4 days. The known resistance of these cells against GNF-2 and Helix-2 alone was confirmed in the apoptosis assays (Figure 33B). Interestingly, in combination, the two compounds were able to induce more than 60% apoptosis and nearly abolish the capacity of the p185-T315I mutant to mediate factor-independent growth (Figure 33B).

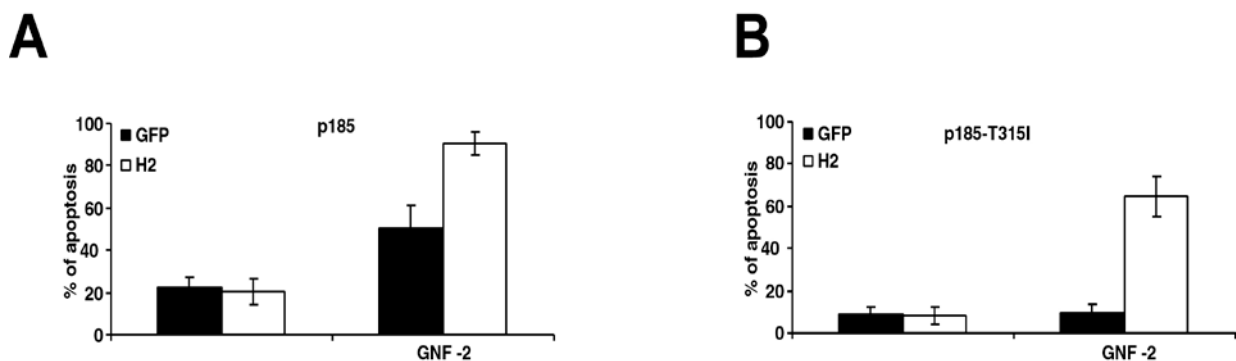


Figure 33 - Induction of apoptosis in Ba/F3 expressing p185^{BCR/ABL} and p185^{BCR/ABL}-T315I by oligomerization inhibitor Helix-2 in combination with allosteric inhibitor GNF-2 (A) Apoptosis rate of Ba/F3 cells expressing p185^{BCR/ABL} upon exposure to 2 μ M GNF-2 in the absence/presence of Helix-2, as indicated. (B) Apoptosis rate of Ba/F3 cells expressing p185^{BCR/ABL}-T315I upon exposure to 2 μ M GNF-2 in the absence/presence of Helix-2, as indicated. The apoptosis rate was determined by staining with 7-AAD. The data represent the mean and SD of three independent experiments.

Taken together, these results show that the GNF-2 induces apoptosis in p185-T315I expressing cells in combination with Helix-2 and increase sensitivity for Helix2 to overcome resistance.

4.4.3 Helix-2 in combination with GNF-2 reduce transformation potential of Fibroblast

expressing unmutated p185^{BCR/ABL} and p185-T315I

BCR/ABL-dependent signaling “substitutes” for IL-3 signaling in factor-dependent hematopoietic cell lines, such as Ba/F3. To further study the effects of GNF-2 in combination with the oligomerization inhibition, a soft agar assay was performed as a classic transformation assay in untransformed Rat-1 fibroblasts. Sorted GFP or Helix-2 positive Rat-1 cells were retrovirally transduced with p185^{BCR/ABL} and p185-T315I. The transduction efficiency was assessed by the detection of GFP and ΔLNGFR respectively. Empty-vector-transduced Rat-1 cells (mock) were used as controls. For each construct triplicates of 5,000 double infected Rat-1 cells were plated in soft agar and were then exposed to 2 μM of GNF-2. The colonies were counted after 15 days. GNF-2 alone was able to reduce the transformation potential of unmutated BCR/ABL to the same extent as Helix-2, but the combination of both nearly completely abolished the BCR/ABL-induced transformation (Figure 34A). Alone Helix-2 or GNF-2 were unable to change the transformation potential of fibroblast expressing p185-T315I but combining both the compounds significantly reduced the transformation potential of fibroblast expressing p185-T315I did not change the transformation potential of fibroblast (Figure 34B).

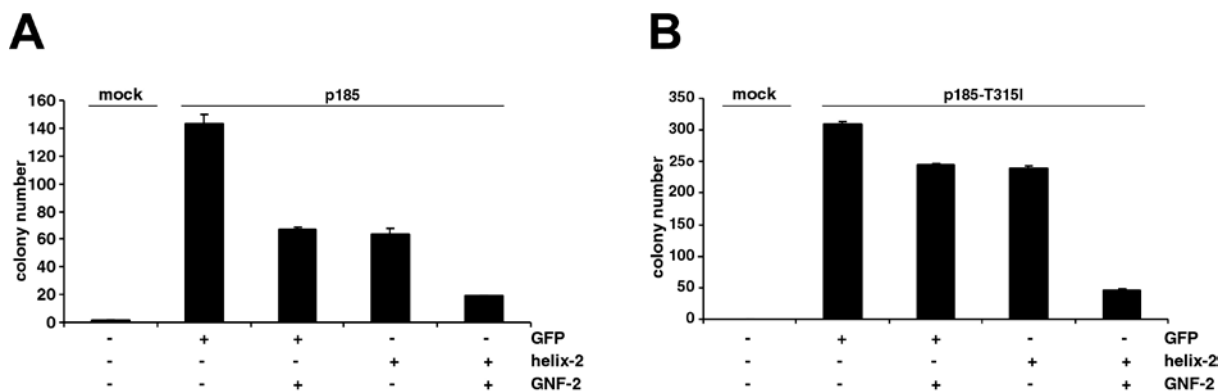


Figure 34 - Impairment of transformation potential of Fibroblast expressing unmutated p185BCR/ABL and p185BCR/ABL-T315I by GNF-2 in combination with Helix-2 (A) Transformation assay by colony formation in soft agar for Rat-1 cells expressing p185^{BCR/ABL}. (B) Transformation assay for p185^{BCR/ABL-T315I}; Rat-1 cells were retrovirally transduced with the indicated constructs, and seeded at 5×10^3 cells/well in soft-agar in 6-well-plates. After 15 days, the colonies were counted, and the means \pm SD of triplicates obtained from two representative experiments are presented.

In summary, these data strongly suggest that the combination of the two molecular approaches completely abolish the leukemogenic potential of unmutated BCR/ABL and BCR/ABL harboring T315I mutation.

4.4.4 GNF-2 completely abolishes growth of p185^{BCR/ABL} and oligomerization-deficient p185-T315I

To confirm the above data, we investigated the effects of GNF-2 on a BCR/ABL lacking the N-terminal coiled coil oligomerization (Δ CCp185 and Δ CCp185-T315I) interface in which the presence of T315I restores the transformation potential as well as the capacity to mediate factor-independent growth (Mian *et al.*, 2009c).

Therefore we retrovirally expressed the indicated constructs (Figure 35A) in Ba/F3 cells and controlled the transgene expression by Western blotting. The cells were grown without factor in the presence or absence of 2 μ M GNF-2. As reported in figure 35B, “unmutated” Δ CCp185 and p185^{BCR/ABL} in the presence of GNF-2 did not grow upon factor withdrawal, in contrast to Δ CCp185 T315I, which exhibited growth curves identical to unmutated p185^{BCR/ABL}. As expected, GNF-2 completely reverted the effect of T315I on this loss-of-function mutant (Figure 35B).

Collectively, these data confirm the effect of oligomerization and the allosteric inhibition of GNF-2 in combination, which overcomes the resistance of BCR/ABL-T315I against the oligomerization inhibition of Helix-2 and the allosteric inhibition of GNF-2 alone.

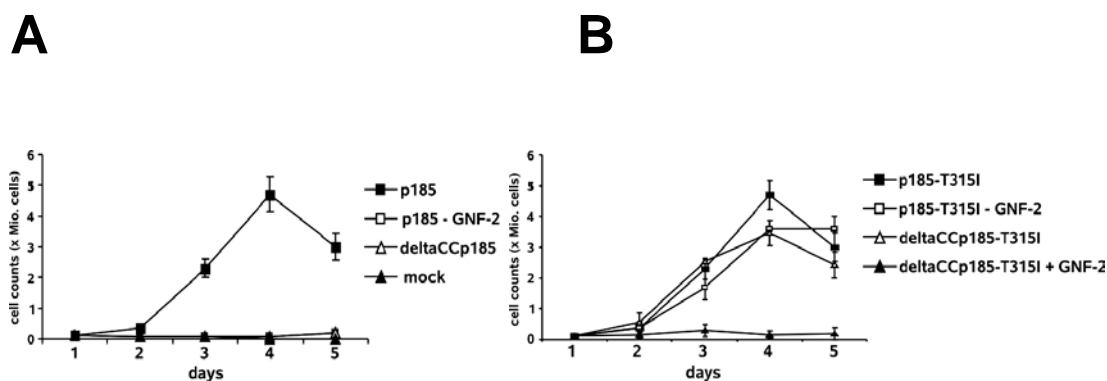


Figure 35 - Role of oligomerization in the sensitivity of unmutated p185^{BCR/ABL} and p185-T315I towards allosteric inhibition by GNF-2. To determine the factor-independent growth, Ba/F3 cells were retrovirally transduced with the indicated constructs and grown upon factor withdrawal with exposure to 2 μ M GNF-2. For factor-independent growth, the number of viable cells was determined daily by Trypan blue dye exclusion. (A) Unmutated p185^{BCR/ABL}. (B) p185^{BCR/ABL-T315I}. Data represent the mean and SD of three independent experiments.

4.4.5 Effects of the combination of GNF-2 and Helix-2 on the autophosphorylation of BCR/ABL and its downstream signaling

Our data suggest that only in combination are GNF-2 and Helix-2 able to overcome the T315I-induced stabilization of kinase activity. Therefore, we studied the effects of this

combination on the autophosphorylation and downstream signaling of p185^{BCR/ABL} and p185-T315I in Ba/F3 cells in comparison to the effects of the “single drug” approaches. We

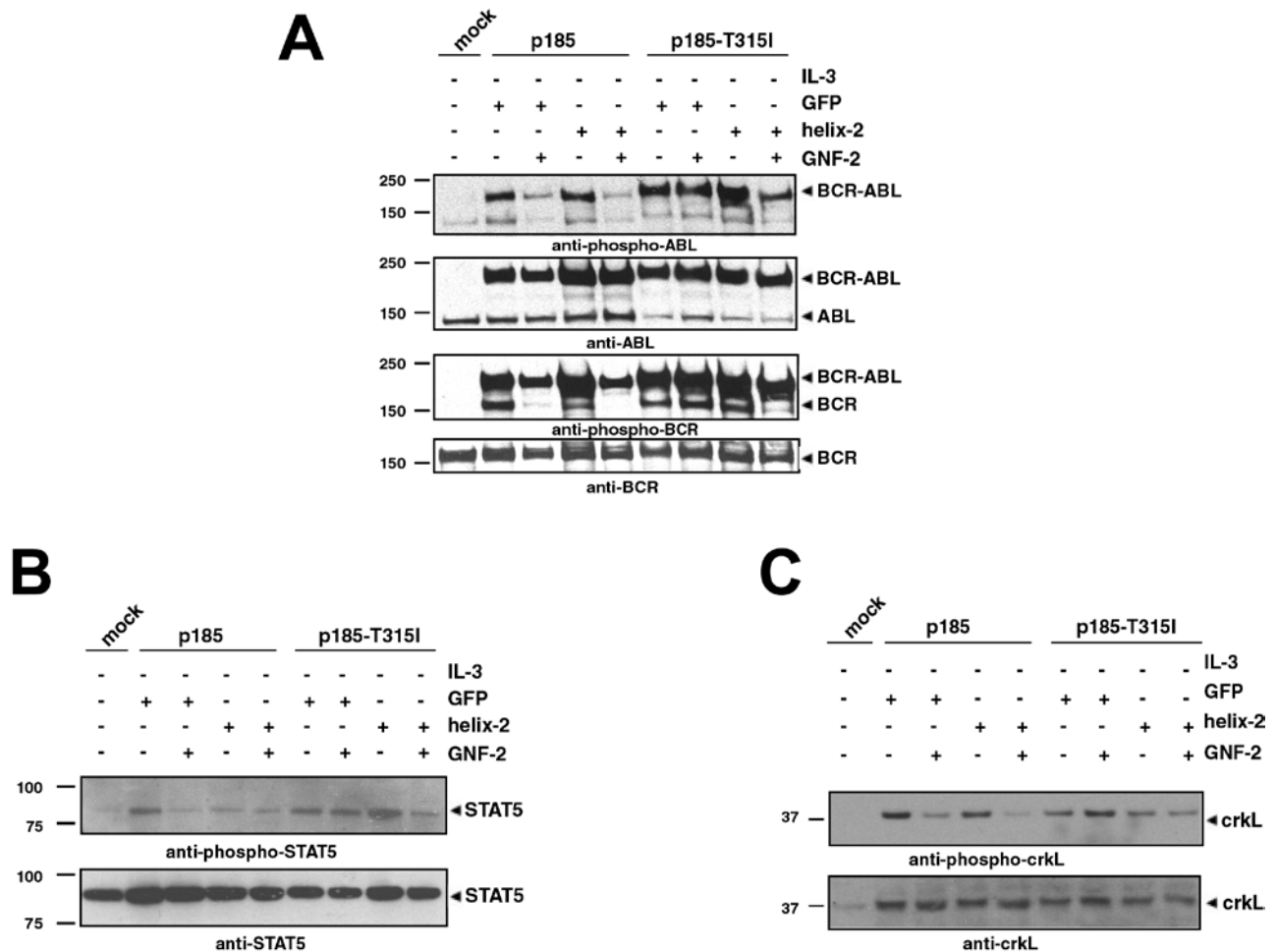


Figure 36 - The combination of Helix-2 and GNF-2 inhibits the autophosphorylation of p185-T315I and dependent signaling pathways. Western blot analysis of lysates of Ba/F3 cells expressing the indicated transgenes using antibodies directed against: (A) c-ABL, ABL Y245 (anti-phospho-ABL), BCR (anti-BCR, which did not detect BCR/ABL), BCR phosphorylated at Y177 (anti-phospho-BCR), STAT5, (B) phosphorylated STAT5 (anti-phospho-STAT5), (C) crkL and phosphorylated crkL. Molecular mass references (kDa) are presented, and c-ABL was used as a loading control.

recently demonstrated that the capacity of T315I to restore leukemogenic potential to the loss-of-function of BCR/ABL is closely related to its capacity to trans-phosphorylate endogenous BCR at position Y177 (Mian *et al.*, 2009c).

GNF-2 had a stronger effect on the autophosphorylation and substrate phosphorylation of unmutated p185^{BCR/ABL} than did Helix-2, and both interfered efficiently with the downstream signaling through, CrkL, STAT5 and inhibited the Y177 phosphorylation of endogenous BCR (Figure 37A-C). These effects were strongly increased by the combination of both, GNF-2 and Helix-2. On p185-T315I, neither GNF-2 nor Helix-2 alone was able to inhibit autophosphorylation, CrkL Phosphorylation, STAT5 activation, and trans-phosphorylation of

BCR. In contrast, the two agents in combination completely abolished the autophosphorylation, STAT5 activation, and BCR trans-phosphorylation, confirming the observations described above. The CrkL phosphorylation was slightly reduced (Figure 36A-C).

Taken together, these data show that GNF-2 in combination with Helix-2 was able to block the aberrant kinase activity of BCR/ABL harboring the T315I mutation, which is oligomerization-independent and is resistant to allosteric inhibition.

5 Discussion

The tetramerization and the formation of HMW are crucial for the leukemogenic potential of BCR/ABL, and its inhibition increases the sensitivity for the kinase inhibitor Imatinib (Beissert *et al.*, 2003; McWhirter *et al.*, 1993; Zhang *et al.*, 2001). The aim of the present study was to further develop the disruption of tetramerization as a therapeutic approach by reducing the size of the inhibiting peptide and exploring its effectiveness on p185^{BCR/ABL} mutants related to the resistance against kinase inhibitors such as Imatinib.

Here, we show that the relevant interaction interface in the N-terminal BCR coiled coil region is the 39 a.a. sequence representing the Helix-2. Helix-2 binds to p185^{BCR/ABL} to the same extent as the entire CC-domain leading to the disruption of the HMW-complexes of p185^{BCR/ABL}. This allowed us to explore the effectiveness of the inhibition of the tetramerization using a small peptide which might be utilized in future for the treatment of Ph+ leukemia, or might represent a lead structure for the development of small molecules targeting the tetramerization of BCR/ABL.

The therapeutic relevance of such an approach is given by the fact that the Helix-2 not only inhibited the function of p185^{BCR/ABL} in an artificial cell model such as the Ba/F3 and 32D cells retrovirally transduced and selected by IL-3 withdrawal, but also in the patient derived lymphatic Ph+ cell lines, SupB15 and BV173. Regarding the growth inhibition of Ba/F3 cells, the inhibitory effect of Helix-2 was similar to that of the CC-peptide, whereas in BV173 and SupB15 cells the inhibitory effect of Helix-2 was stronger than that of the CC-peptide. Regarding the decrease of p185^{BCR/ABL} autophosphorylation, Helix-2 exhibited a similar inhibitory potential than the peptide representing the entire CC-domain.

Current therapies often lack tissue specificity in the context of high variability in pharmacokinetics. This deficit has led to multiple strategies for targeted therapy, including gene therapy (Ford *et al.*, 2000). However; successful gene transduction has not always resulted in transcription to RNA or translation to functional protein. Regardless of the current progress in protein transduction technology, tools that will bypass conventional genetic routes for modulating the cells biological activity and will thus minimize the problems associated with genetic intervention, still need to be developed (Ford *et al.*, 2000). The TAT-mediated protein delivery, a tool for the efficient and transient delivery of proteins, is one such example that has certain advantages over delivery of therapeutic genes.

Here we show the evidence that membrane permeable Helix-2 (MPH-2) transduces several different cell types with high efficiency, and remains stable for several hours. Prior research also indicates that cell permeable peptides (CPP)-assisted transduction delivered exogenous

molecules to their desired sites of action, and was similarly effective as those introduced via ectopic over expression or microinjection. Overall, the transduction requires covalent attachment of cell permeable peptides (CPPs) to protein cargos; either through the generation of fusion protein product or chemical conjugation. Transduction aided by CPPs is often rapid, uniform, and synchronized. The level of cellular uptake can be controlled to a certain extent through adjusting the concentration of the fusion protein in the media (Schwarze and Dowdy, 2000).

The tetramerization and the formation of high molecular weight complexes are crucial for the leukemogenic potential of BCR/ABL, and inhibition of this process increases the sensitivity to the kinase inhibitor Imatinib (Beissert *et al.*, 2003). Our aim was to develop a therapeutic approach, by creating membrane permeable inhibitory peptides and exploring their effectiveness in treating Ph⁺ leukemia.

We previously showed that the 39 a.a. sequence of the N-terminal BCR coiled-coil region, representing the Helix-2, binds to BCR/ABL when expressed using a retroviral transduction system (Beissert *et al.*, 2008). Here, we show that MPH-2, representing the Helix-2, fused to a peptide transduction tag effectively binds to BCR/ABL, which inhibits the aberrant kinase activity of BCR/ABL, and suppresses the growth of BCR/ABL dependent leukemic cell lines. The therapeutic relevance of such an approach is given by the fact that the Helix-2 inhibited the function of BCR/ABL in the patient derived lymphatic Ph⁺ cell lines, SupB15 and BV173 transduced with membrane permeable peptides. Regarding the growth inhibition of lymphatic Ph⁺ cell lines, Tom-1 and BV173 and myeloid Ph⁺ cell line, K562, the inhibitory effect of MPH-2 in this study was similar or even stronger than that of retrovirally transduced Helix-2 as shown by (Beissert *et al.*, 2008).

We assumed that the inhibition of tetramerization by MPH-2 peptides should inhibit the kinase activity of BCR/ABL. Consistent with this hypothesis we found that MPH-2 reduces the autophosphorylation of Ph⁺ leukemic cells to extent as retrovirally transduced Helix2 peptide.

In this study, we found that the MPH-2 administrated by i.v. injection efficiently transduced the MNCs in the peripheral blood, bone marrow and spleen, and was stable for about 6 hr, which correlated with its *in vitro* stability.

The potential of the HIV-TAT as a peptide transduction tag was previously extensively explored using the model of TAT fused to β -galactosidase. These studies showed that TAT fused β -galactosidase is effectively delivered to many tissues, including the liver, kidney,

heart, muscle, lung, spleen, and brain of mice by i.p. injection, and it fully maintains its biological activity (Cai *et al.*, 2006; Schwarze *et al.*, 1999).

A complex formed by TAT and technetium in 99 minutes after administering it by i.v. bolus in mice showed a rapid distribution throughout the body, with a gamma imaging pattern consistent with organ perfusion. The complex reached peak organ levels within 5 min after injection (liver > kidney > small intestine > lung > spleen > brain), and displayed modestly rapid blood clearance. Over the subsequent 2 hr, the complex was cleared by both renal and hepatobiliary excretion, with activity appearing in the urinary bladder and bowel (Polyakov *et al.*, 2000). These findings along with our data strongly suggest that the TAT-delivered Helix-2 peptide may provide the basis for a novel therapeutic approach to treat Ph+ leukemia.

We assumed that the inhibition of tetramerization by Helix-2 peptides should inhibit the kinase activity and transforming capacity of BCR/ABL irrespective of the presence of point-mutations in the tyrosine kinase domain that confer Imatinib-resistance. Consistent with this hypothesis we found that Helix-2 reduces the autophosphorylation of unmutated and mutant BCR/ABL to the same extent. Furthermore, Helix-2 inhibits the anchorage independent growth and restores the contact inhibition of Rat-1 fibroblasts transformed by unmutated BCR/ABL and partially restores the contact inhibition of mutant BCR/ABL. However, when we analyzed the inhibitory effects of Helix-2 on the factor independent proliferation of hematopoietic cells expressing p185^{BCR/ABL} harboring these mutations we revealed unexpected differences in the response of mutant BCR/ABL. Consistent with the inhibitory effects of Helix-2 on BCR/ABL-transformed fibroblasts we found that Helix-2 inhibits unmutated p185^{BCR/ABL}, p185^{BCR/ABL-E255K} and p185^{BCR/ABL-Y253F} expressing Ba/F3 and 32D cells. In contrast, p185^{BCR/ABL-T315I} expressing hematopoietic cells did not respond to Helix-2. These data indicate that the point mutation T315I induces changes in the biological activity of BCR/ABL which alters the response towards Helix-2. This point mutation seemingly enables p185^{BCR/ABL} to mediate factor independence independently from its autophosphorylation. The observation that the unresponsiveness of T315I towards Helix-2 peptides manifest themselves in hematopoietic cells but not in fibroblasts is in accordance to our previously published data: several artificial ABL-chimeras between ABL and the isolated oligomerization domains derived from BCR, TEL, PLZF or PML lead to oligomerization of ABL and confer factor independence but are unable to satisfy classical criteria of oncogenic transformation (Beissert *et al.*, 2003). The same results were observed for CC-deletion mutants of BCR/ABL (Beissert *et al.*, 2003).

Furthermore, these data are in accordance to a recently published study showing that p210^{BCR/ABL} mutated at position T315I exhibits an increased transformation capacity of primary bone marrow cells despite a reduced kinase activity (Skaggs *et al.*, 2006).

Our HPLC studies revealed specific features of the T315I mutation which might explain the resistance towards Helix-2 peptides: p185^{BCR/ABL-T315I} exhibits a different HMW pattern as compared to unmutated p185^{BCR/ABL} and the other mutants. The HMW pattern of p185^{BCR/ABL-T315I} was characterized by two different peaks: i) one of about 1070 kDa, less pronounced in unmutated p185^{BCR/ABL} and absent in the p-loop mutants, which did not respond to the Helix-2; ii) and another peak at lower MW which is not present in unmutated p185^{BCR/ABL}, was shifted towards even lower MW in the presence of Helix-2 peptides. This p185^{BCR/ABL-T315I} specific HMW-complex pattern might be due to differences in the stability or the composition of the HMW-complexes. Although we observed HMW-complexes of 1070 kDa (fraction no. 25) in unmutated p185^{BCR/ABL}, this fraction was not a peak fraction but the upper limit of the unmutated HMW-pattern. The predominant elution of the p185^{BCR/ABL-T315I} complexes at 1070 kDa indicates that these complexes exhibit a higher stability as compared to those formed by unmutated p185^{BCR/ABL}, which are distributed over a wider MW-range. Furthermore, the p185^{BCR/ABL-T315I} complexes at 1070 kDa are not disrupted by Helix-2 which also indicates a higher stability. Another reason for the modified HMW-complex pattern of p185^{BCR/ABL-T315I} might also be an aberrant recruitment of unknown binding partners that do not interact with unmutated p185^{BCR/ABL}. In contrast the HMW-complexes of p185^{BCR/ABL-T315I} of lower MW responded at least partially to Helix-2 peptides. This is in accordance to our co-immunoprecipitation experiments which revealed that Helix-2 binds to p185^{BCR/ABL-T315I}. Therefore we can exclude a lack of interaction between Helix-2 and p185^{BCR/ABL-T315I} as a reason for resistance against the peptide. In summary our data indicate that p185^{BCR/ABL-T315I} forms a subset of complexes unresponsive towards Helix-2 that provides a sufficient survival signal.

Regarding the response of mutated BCR/ABL towards Imatinib in presence of Helix-2 we found that Helix-2 expression overcomes the Imatinib-resistance of p185^{BCR/ABL-Y253F} and p185^{BCR/ABL-E255K}, but not of p185^{BCR/ABL-T315I}. The fundamental difference between T315I and Y253F or E255K might be due to the gatekeeper function of T315. It is widely accepted that Imatinib binds to the inactive ABL-kinase conformation (Schindler *et al.*, 2000) and thus one can hypothesize that the inhibition of the BCR/ABL TK-activity caused by the interaction with Helix-2 is related to conformational changes in the ABL-kinase domain that increase the

affinity towards Imatinib of mutations that do not confer complete resistance such as the p-loop mutations.

Here we show for the first time that p185^{BCR/ABL} harboring mutations related to Imatinib-resistance are responsive to the inhibition of the tetramerization by Helix-2 in classical transformation assays. This is of particular clinical significance, because it establishes the targeting of the tetramerization interface of BCR/ABL as a new therapeutic approach, which could contribute together with clinical relevant ABL-kinase inhibitors to an improved molecular targeting of BCR/ABL.

T315I is the only mutation that confers resistance against virtually all ATP competitors and oligomerization inhibitors (Beissert *et al.*, 2008; Druker, 2008). So we wanted to determine i.) Why p185^{BCR/ABL} can be inhibited by the exposure to competitive peptides in the presence of the Y253F or the E255K mutations but not in the presence of the T315I (Beissert *et al.*, 2008) and ii.) whether the AKI-resistance mutations confer additional features to the biology of p185^{BCR/ABL} that modify its leukemogenic potential.

Through our experiments on the oligomerization-deficient p185^{BCR/ABL}, we found that Y253F and E255K are not inert regarding the response to the inhibition of oligomerization. In contrast to T315I, which induces complete resistance, Y253F and E255K confer a partial resistance that is stronger in the case of Y253F as compared to E255K. This effect against oligomerization inhibition is hardly revealed in the available models of AKI-resistant BCR/ABL, and only by deleting the CC-domain were the effects of Y253F and E255K unmasked. The fact that these mutations were able to restore not only factor-independence but also full transformation potential indicates that they probably induce conformational changes within the molecule that allow the activation of BCR/ABL as a monomer.

T315I requires the autophosphorylation at Y177 of BCR/ABL for the resistance against the inhibition of oligomerization. In fact, all mutants in which autophosphorylation at the Y177 was present exhibited resistance against the competitive Helix-2 peptide. The phosphorylated Y177 represents the GRB-2 binding site, which is at the top of the RAS-signaling pathway initiated by BCR/ABL ((Faderl *et al.*, 1999), suggesting an important role for RAS-signaling in the inhibition of the oligomerization.

Interestingly the T315I was able to restore the activity of an oligomerization deficient BCR/ABL lacking also the Y177 phosphorylation site, the Δ CCp185-Y177F. Seemingly at odds with this finding is our observation that autophosphorylation at Y177 is a prerequisite for T315I mediated resistance against the treatment with Helix-2 suggesting that a mutant in which oligomerization is inhibited by the deletion of CC would behave like the p185-Y177F-

T315I in the presence of Helix-2. A possible explanation of this discrepancy is the ability of activated BCR to substitute the autophosphorylation of BCR/ABL. In addition the activation of BCR by the T315I does not appear to require the interaction between BCR/ABL and BCR, suggesting that in the case of the p185-Y177F-T315I there are two relevant targets of the Helix-2, being one the BCR/ABL mutants itself and the other endogenous BCR. Thus the Helix-2 might inhibit not only the oligomerization of BCR/ABL, but also that of BCR as well as the hetero-oligomerization between BCR/ABL and BCR.

Until now, the grade of transformation activity of BCR/ABL was thought to be directly correlated to the degree of its kinase activity (Laurent *et al.*, 2001; Lugo *et al.*, 1990). Recently, the first evidence was raised that BCR/ABL harboring the “gatekeeper” mutation T315I mutation responsible for the resistance against kinase inhibitors such as Imatinib, Nilotinib, or Dasatinib exhibits ABL-kinase activity that may be higher or lower than that of unmutated BCR/ABL depending on the model (Griswold *et al.*, 2006).

These findings suggested that the kinase activity might be not the decisive parameter causing T315I-positive cells to overgrow in the presence of cells whose unmutated BCR/ABL kinase activity is efficiently suppressed by inhibitors. Our findings on the different mutants clearly showed that the capacity of T315I to improve the functionality of the respective mutants is closely related to functional ABL-kinase activity. Thus, we can exclude the possibility that T315I confers activities that are independent of the ABL-kinase activity of BCR/ABL. In fact, in all cases, the presence of T315I led to an increase in or an activation of the kinase activity of the respective mutant. These data confirm recent findings showing that mutations of the highly conserved “gatekeeper” threonine, which lies within the hinge region of the enzymatic cleft of many kinases, represent a crucial structural feature. The mutation of threonine promotes kinase activation sufficient to confer the capacity to mediate factor-independent growth for several native non-receptor and receptor tyrosine kinases, such as c-SRC, PDGFRA, and EGFR (Azam *et al.*, 2008). In the case of the isolated ABL-portion of BCR/ABL, either this activation was unable to reach levels high enough for biological activity or this activation, the intensity of which reached the level of other biologically active mutants, is not sufficient by itself to exert full biological activity. In fact, in cells expressing #ABL-T315I, endogenous BCR was not phosphorylated. Our results indicate a relationship between the phosphorylation of endogenous BCR and the biological activity of T315I. The BCR-phosphorylation is most likely the expression of an increased substrate phosphorylation activity of the ABL-kinase in the presence of the T315I an effect exerted by all mutants with biological activity. The phosphorylation seems to be independent of the overall kinase activity

of the respective mutants, which was variable. One can speculate on the existence of a still unknown mechanism involved in the phosphorylation of BCR by the ABL-kinase, the inhibition of which is released in the case of the deletion of the SH3 domain of ABL.

In summary, our data show that T315I not only interferes with the affinity of ATP-analogs for the ABL-kinase but also increases the kinase activity of different ABL and BCR/ABL-mutants, conferring strong biological activity that seems to be related to the phosphorylation of endogenous BCR. These findings introduce possible new approaches for the molecular therapy of patients harboring AKI-resistant BCR/ABL.

Recently, much effort has been undertaken to solve the problem of Imatinib resistance *in vitro*, but not in patients, many point mutations are inhibited by increased doses of Imatinib, as the achievable serum levels of Imatinib are below the concentrations necessary to overcome resistance (O'Hare *et al.*, 2005a; Weisberg *et al.*, 2005). Therefore research focuses mainly on the development of second generation kinase inhibitors. Nilotinib (Novartis, Basle), like Imatinib, is a selective ABL-kinase inhibitor. Nilotinib inhibits many Imatinib-resistant point mutants because of its 20-fold higher affinity for the ABL kinase domain and achievable plasma levels for Nilotinib are sufficient for inhibition (O'Hare *et al.*, 2005b). The dual SRC-ABL kinase inhibitor Dasatinib (Bristol-Myer-Squibb, New York) takes advantage of a characteristic difference between SRC- and ABL-kinase domain conformations to inhibit Imatinib-resistant mutations: the inactive conformations of SRC and ABL are different, while the active conformations are closely related (Schindler *et al.*, 2000). Dasatinib has a 325-fold higher affinity towards ABL than Imatinib (O'Hare *et al.*, 2005a). Imatinib and Nilotinib bind to the inactive ABL-kinase conformation which is the reason for their selectivity, while Dasatinib binds to active ABL and active SRC. Therefore the binding of Dasatinib is dependent on another choice of aminoacid residues as Imatinib or Nilotinib (O'Hare *et al.*, 2005b; Schindler *et al.*, 2000). Dasatinib inhibits most mutations identified in Imatinib resistant patients (O'Hare *et al.*, 2005a). Unfortunately, the mutation T315I, which clinically accounts for about 20% of Imatinib-resistant cases, is neither inhibited by Nilotinib nor Dasatinib (O'Hare *et al.*, 2005a; von Bubnoff *et al.*, 2006).

As outlined above, the possibilities to overcome resistance towards a particular kinase inhibitor by choosing a second or third inhibitor might finally fail. Therefore, a closer look to other critical functions of the BCR/ABL fusion protein itself or to the BCR/ABL activated signaling pathways is now undertaken. Strategies under investigation include: the tetramerization interface (Beissert *et al.*, 2008; Beissert *et al.*, 2003), targeting the substrate

binding site, the allosteric site and downstream pathways (for review(Quintas-Cardama *et al.*, 2007).

The major therapeutic challenge is to efficiently treat patients with BCR/ABL harboring the T315I mutation. Unfortunately, T315I not only confers resistance against AKI, but also against the inhibition of oligomerization by Helix-2 (Beissert *et al.*, 2008) and the allosteric inhibition by GNF-2 (Adrian *et al.*, 2006).

The T315I mutation is the most recalcitrant to inhibition due to a combination of several factors, including steric hindrance of drug binding, loss of a key hydrogen-bonding interaction with the T315 side-chain hydroxyl group that is exploited by Imatinib, Nilotinib, and Dasatinib, and potentially through increasing aberrant intrinsic kinase activity accompanied by aberrant substrate phosphorylation (Azam *et al.*, 2008; Mian *et al.*, 2009b).

Iacob *et al.* 2009 has detected conformational disturbances distant to the site of mutation in Abl(Myristoylated)T315I. There was an unexpected alteration to deuterium exchange in the RT-loop of the SH3 domain in T315I whereas no changes were detected in any location in the other 2 mutants. Activation by distant mutation may involve conformational changes that are communicated allosterically to the active sites like coiled coil (CC) domain or Grb-2 binding site etc. We speculate that deleting of CC domain could assist inhibition of the T315I mutant when myristoylated (Iacob *et al.*, 2009).

Our data strongly suggest that both the sensitivity of unmutated p185^{BCR/ABL} and the resistance of p185-T315I toward the allosteric inhibition by GNF-2 are oligomerization-dependent. In fact, the inhibition of oligomerization by the competitive Helix-2 peptide not only increased the response of unmutated p185^{BCR/ABL}, but also restored the response of p185-T315I to the level of unmutated p185^{BCR/ABL}. This was also confirmed by the high sensitivity of the oligomerization-deficient p185-T315I mutant towards GNF-2. The relationship between the resistance against GNF-2 and oligomerization was already anticipated by the work of Adrian and co-workers, who showed that activation of the kinase activity of ABL by the oligomerization interfaces of NPM or of TEL was not reverted by GNF-2 (Adrian *et al.*, 2006). We previously showed that the helix-loop-helix (HLH) oligomerization interface of TEL directly fused to the ABL-portion of the fusion protein HLH/ABL showed enhanced ABL-kinase activity along with a decreased response to Imatinib, as compared to unmutated p185^{BCR/ABL} or other ABL chimeras (Beissert *et al.*, 2003). Furthermore, the HLH/ABL chimera formed complexes of higher molecular weight than even the unmutated p185^{BCR/ABL} (Beissert *et al.*, 2003). This indicated that the level of resistance against GNF-2 might increase in parallel with the grade of oligomerization or HMW-formation by the ABL-fusion

proteins, which seems to parallel the sensitivity towards Imatinib, which also decreases with the oligomerization status of ABL fusion proteins (Beissert *et al.*, 2003). Thus, one can speculate that GNF-2 exhibits a reduced capacity to bind MBP when BCR/ABL is present as an oligomer as compared to a monomer. Given that the oligomerization of BCR/ABL is a dynamic process, equilibrium between monomers and oligomers must exist. It is possible to increase the sensitivity of unmutated p185^{BCR/ABL}, as well as that of p185-T315I, for allosteric inhibition through a switch of this balance in favor of monomers by competitive peptides such as Helix-2.

Taken together, our results establish a new approach for the molecular targeting of unmutated BCR/ABL, as well as BCR/ABL harboring the multi-resistance mutation T315I, which is the combination of oligomerization inhibitors and allosteric inhibitors.

To further develop competitive peptides as therapeutic approach the following aspects have to be addressed. i) Optimization of the peptides themselves. ii) peptides as lead structure for *in silico* drug designing. iii) Delivery of the peptides.

The Helix-2 peptides will be further optimized by *in Silico* design for an improved affinity to the N-terminal oligomerization interface of BCR/ABL. Improving the current peptide design which included the entire CC-domain of BCR/ABL, will be performed by restricting the sequence optimization to the Helix-2 which represents most of the protein-protein interface positions, while the shorter Helix-1 only includes about 10% of the interface residues.

Shortening that sequence to a single Helix-2 analog may increase flexibility thus requiring considering several structures. "Snapshots" from Molecular Dynamics (MD) of this peptide will be collected and the most diverse structures from MD will be used for the optimization of interface residues. Repeats of Polyethylene Glycol (PEG) will be covalently attached to the helical structure and their structural effect will be examined under similar MD conditions. The sequences of each of the unique structures will be optimized by applying our Iterative Stochastic Elimination (ISE) procedure. ISE is interface optimization software give a binary protein-protein complex, in which we denote the proteins as A and B, we redesign B and create new proteins with stronger binding affinity to A than the binding affinity of B to A. We also demand that the self affinity of the designed protein (in a B-B complex) will be less than that of B to A. The computer designed peptides for improved affinity to the target will be validated *in vitro* by biochemical experiments like interaction with BCR/ABL and inhibition of BCR/ABL autophosphorylation/kinase activity. The improved BCR/ABL inhibition effect will be controlled by biological experiments like growth curves and proliferation competition assays. Redesigned peptides will be evaluated on the basis of better interaction with

BCR/ABL, better growth inhibition and reduced self oligomerization. The peptides will be further optimized by reduction in size, reduction of self-oligomerization, increased affinity to the target and biological stability.

The structures of biomolecular targets, proteins in most cases, must be presented as models from experiments or constructed by a reliable modeling method. Docking consists of “driving” a small molecule toward its target and finding the best possible positions for their mutual interactions. Most current information on small molecule-target complexes is from X-ray crystallography (Berman *et al.*, 2000) but nuclear magnetic resonance is becoming an additional major tool for probing biomolecular-ligand complexes (Meyer and Peters, 2003). A few recent studies suggest that a small molecule may be bound to its target in more than a single conformation (Cameron *et al.*, 2005; Ekroos and Sjogren, 2006; Gales *et al.*, 2005; Hamilton and Benson, 2001). It has also been shown that conformations of bound ligands are structurally different than their predominant solution conformations and are higher in energy (Perola and Charifson, 2004; Stockwell and Thornton, 2006). Many protein targets have flexible conformations, most frequently displaying variations of side chain positions in their active sites as well as in their backbone (Teague, 2003). “How to hit a moving target” (Carlson, 2002) becomes a landmark title for the efforts to develop small molecules that bind efficiently to flexible proteins.

Keeping in mind we have planned to shorten the Helix-2 peptide to 5-15 amino acids to serve as lead structure for computer-based design of small molecule. To exclude those peptides which will not have improved efficacy in comparison to the original Helix-2 peptide, the efficacy of newly designed peptides will be investigated by expressing their cDNA by retroviral transduction into BCR/ABL transformed cells. The “read out” is represented by their effects on autophosphorylation and substrate phosphorylation of BCR/ABL and its Imatinib-resistant mutants by specific antibodies against ABL, Crkl, Stat5 and their phosphorylated forms in the Western blotting (Beissert *et al.*, 2008; Beissert *et al.*, 2003; Mian *et al.*, 2009a)

The most efficient peptides will be biochemically evaluated for i.) their capacity to disrupt the BCR/ABL oligomers in the cells by separating the cell lysates by size exclusion chromatography (Beissert *et al.*, 2008; Beissert *et al.*, 2003) ; ii.) their binding affinity to the CC-domain of BCR/ABL using recombinant peptides produced in E.coli on a Biacore platform available in the “Biocenter” of the Goethe-University in Frankfurt on service for fee base.

At the final stage, the peptides will be biologically validated using different techniques like colony formation (Puccetti *et al.*, 2000), dye exclusion using Trypan-blue, Proliferation completion assay and apoptosis assay (Beissert *et al.*, 2008; Mian *et al.*, 2009b).

One of the major problems hindering the use of peptides in therapy is their stability and their delivery to the target cells *in vivo*. There are several chemical methods to overcome this problem but none leads to the specific targeting of specific tumor cell subpopulations. Here we aim to combine efforts in order to develop suitable peptide delivery approach for the inhibition of oligomerization of BCRA/BL for the molecular therapy of Ph⁺ leukemia.

A particular therapeutic challenge is represented by the Ph⁺ ALL whose prognosis notwithstanding the recent advances of molecular therapy of Ph⁺ leukemia remains poor. This is mainly due to the fact that the actual therapy regimen are unable to eradicate a very small number of leukemic cells, which determine the long term growth of the leukemia - the so-called “leukemia-stem cell” (LSC) - the source of the relapse, when not completely eradicated. Very recent results indicate that the LSC of Ph⁺ ALL exhibit a CD34⁺, CD38^{+/-} and CD19⁺ phenotype (Kong *et al.*, 2008). These findings define CD19 as a valid therapeutic target for eradicating the Ph⁺ALL LSC as already shown for other disease entities such as the B-cell lymphomas.

Liposomes are one of the best drug delivery systems for low molecular weight drugs, imaging agents, peptides, proteins, and nucleic acids (Barenholz *et al.*, 1994, Gregoriadis, 2007, Lasic and Barenholz, 1996). Nanoliposomes ($d \leq 120$ nm), when administrated intravenously, may improve the therapeutic index of some drugs due to the enhancement of permeability and retention effect (Barenholz, 2001; Barenholz, 2003; Voinea and Simionescu, 2002), while larger liposomes ($d. 2-6 \mu\text{m}$) have a similar effect when administrated locally (Alam and Hartrick, 2005; Grant *et al.*, 2004). Thus more than 11 liposome-based drugs are in clinical use. A major achievement in liposome medical application is the ability to load a sufficient amount of drug needed to achieve therapeutic efficacy. In most cases this requires a remote loading approach (Clerc and Barenholz, 1995; Clerc and Barenholz, 1998; Haran *et al.*, 1993), where the drug is loaded into preformed liposomes.

Liposomes and especially pegylated nano-liposomes (“sterically stabilized nano liposomes” = nSSL) are potent drug delivery systems protecting the drug from degradation and delivering a high drug payload to tumors. For an efficient attachment to the nSSL the effect of binding to several optional lengths of PEG will be examined by comparing the flexibility of the isolated Helix-2 with its N-terminus bound to PEGs.

Together with other anti-leukemic drugs (Doxorubicin, Imatinib or GNF-2, respectively) these new peptides will be loaded on nano-liposomes for an improved drug delivery *in vivo*. Directing these nano-liposomes to the “right” cell in order to eradicate the leukemia will be obtained by loading them with specific scFv for the LSC-population.

The vast majority of proteins do not enter the cytoplasm of living cells. An 11 a.a. peptide sequence derived from the human immunodeficiency virus protein TAT, the HIVTAT-domain, leads to the transport of heterologous proteins or peptides into living cells when fused to them (Fawell *et al.*, 1994). This phenomenon is called peptide transduction (PT). A number of other peptide transduction domains (PTD) have been identified or developed up to now. The common feature is that they are composed of basic a.a. sequence stretches of usually 9 – 11 a.a. which are rich in arginine residues (for review(Zhao and Weissleder, 2004).

In order to proceed with the development of Helix-2 peptides towards a therapeutic peptide, we have recently established the peptide transduction technology (Mian *et al.*, 2009 submitted).

Multicellular spheroids are well defined three dimensional models that mimic the cellular environment in tissues in a much better way than monolayer cultures. These spheroids are aggregates of about 100000 cells and 250 µm in diameter that spontaneously form when stroma cell lines are plated in agarose coated microwell plates. The migration of hematopoietic cells into the stromal bone marrow microenvironment can be modeled using spheroids of stroma cell (Bug *et al.*, 2002). To this aim we co-cultivated spheroids with hematopoietic cells for 24 to 48 hours. After extensive washing in PBS and dissociation of the spheroids with trypsin the migrated cells were identified by FACS using surface markers specific for hematopoietic cells (CD19, CD45). The ability of cells to migrate into spheroids is characteristic for different cell lines e.g. after 48h of migration spheroids contain 70% Nalm-6 cells, 20% CD34+ cells and 10% K562 cells . Alternatively cryostat sections of paraffin embedded spheroids can be stained immune-histochemically to identify migrated cells (Bug *et al.*, 2002).

The efficient secretion of proteins requires an N-terminal signal peptide (SP) that targets the mRNA-ribosome complexes to the endoplasmatic reticulum (ER) (Walter *et al.*, 1984). In addition to the SP the 3' untranslated region (UTR) of the mRNA encoding the secretory protein plays an important role for the proper localization of the mRNA to the ER and subsequently for the efficiency of protein secretion: for the secretion of heterologous proteins it is important that the SP as well as the 3'UTR are derived from the same secretory protein

(Partridge *et al.*, 1999). Furthermore the group of Beate Stern (University of Bergen & Unitargeting Research AS, Bergen, Norway) that cooperates with us for this proposal has shown that the level of synthesis and secretion is dependent on the choice of the SP. The SP of *Gaussia princeps* luciferase resulted in much more efficient secretion than Interleukin-2 or albumin SP (Knappskog *et al.*, 2007). Mrs. Stern and Unitargeting, Research AS provided their optimized vector for the secretion of heterologous proteins which led to the efficient secretion of human endostatin under the control of the *Gaussia princeps* luciferase SP. This secretion system is destined for a commercial distribution by Unitargeting Research AS.

This work is planned for the development of a cell based delivery system for biological active peptides *in vivo*. The delivery will be accomplished by producer cells that secrete cell permeable peptides *in loco*. *In vitro* the intercellular transfer of HIVTAT-tagged GFP has been demonstrated before (Barka *et al.*, 2004). This paracrine peptide transduction system will avoid the systemic application of transducible peptides and reduce the risk of entrapment of the peptides in unspecific sinks in the organism. The sustained *in loco* secretion will result in a high local concentration in proximity of the target cells. Furthermore the repeated administration of the peptides to animals by injections or oral gavage which harbors a manipulation related health risk will be omitted.

Fibroblast cells secreting HIVTAT-tagged luciferase, GFP, Helix-2-GFP fusion proteins will be co-cultivated with hematopoietic cells. The transduction efficiencies and cell proliferation will be examined. We will study the inhibition BCR/ABL kinase activity and the inhibition of downstream pathways.

To mimic the *in vivo* 3D organization of the bone marrow stromal microenvironment, we will use an *in vitro* 3D stroma cell spheroid model. Spheroids of peptide secreting stroma cells will be co-cultivated with hematopoietic cells which migrate into the spheroids. The paracrine delivery of the peptides will be measured. The inhibition of BCR/ABL kinase activity and downstream pathways will be assessed.

Bone marrow hematopoietic cells and mesenchymal stem cells isolated from C57BL6/N donor mice will be used to secrete peptides *in loco*. Upon transplantation in syngeneic hosts the serum level of the secreted peptides and the peptide delivery to host cells in hematopoietic organs will be examined. Human BCR/ABL negative cell lines and primary CDC34+ cells will serve as peptide secreting cells in a similar NOD/SCID mouse model.

In order to examine the antileukemic potential of paracrine delivered peptides, the inhibition of leukemia induction will be studied by co-transplantation of BCR/ABL expressing cells together with the peptide secreting cells.

6 Summary

In Philadelphia Chromosome (Ph) positive ALL and CML the fusion between BCR and ABL leads to the BCR/ABL fusion proteins, which induces the leukemic phenotype because of the constitutive activation of multiple signaling pathways down-stream to the aberrant BCR/ABL fusion tyrosine kinase. Targeted inhibition of BCR/ABL by ABL-kinase inhibitors induces apoptosis in BCR/ABL transformed cells and leads to complete remission in Ph positive leukemia patients. However, a large portion of patients with advanced Ph⁺ leukemia relapse and acquire resistance. Kinase domain (KD) mutations interfering with inhibitor binding represent the major mechanism of acquired resistance in patients with Ph⁺ leukemia.

Tetramerization of BCR/ABL through the N-terminal coiled-coil region (CC) of BCR is essential for the ABL-kinase activation. Targeting the CC-domain forces BCR/ABL into a monomeric conformation, reduces its kinase activity and increases the sensitivity for Imatinib. Here we show that i.) targeting the tetramerization by a peptide representing the Helix-2 of the CC efficiently reduced the autophosphorylation of both WT BCR/ABL and its mutants; ii.) Helix-2 inhibited the transformation potential of BCR/ABL independently of the presence of mutations; iii.) Helix-2 efficiently cooperated with Imatinib as revealed by their effects on the transformation potential and the factor-independence related to BCR/ABL with the exception of mutant T315I. These findings suggest that BCR/ABL harboring the T315I mutation have a transformation potential which is at least partially independent from its kinase activity.

Targeted inhibition of BCR/ABL by small molecule inhibitors reverses the transformation potential of BCR/ABL. We definitively proved that targeting the tetramerization of BCR/ABL mediated by the N-terminal coiled-coil domain (CC) using competitive peptides, representing the Helix-2 of the CC, represents a valid therapeutic approach for treating Ph⁺ leukemia. To further develop competitive peptides for targeting BCR/ABL, we created a membrane permeable Helix-2 peptide (MPH-2) by fusing the Helix-2 peptide with a peptide transduction tag. In this study, we report that the MPH-2: (i) interacted with BCR/ABL *in vivo*; (ii) efficiently inhibited the autophosphorylation of BCR/ABL; (iii) suppressed the growth and viability of Ph⁺ leukemic cells; and (iv) was efficiently transduced into mononuclear cells (MNC) in an *in vivo* mouse model.

The T315I mutation confers resistance against all actually approved ABL-kinase inhibitors and competitive peptides. It seems not only to decrease affinity for kinase inhibitors but to confer additional features to the leukemogenic potential of BCR/ABL. To determine the role of T315I in resistance to the inhibition of oligomerization and in the leukemogenic potential

of BCR/ABL, we investigated its influence on loss-of-function mutants with regard to the capacity to mediate factor-independence. Thus we studied the effects of T315I on BCR/ABL mutants lacking functional domains in the BCR portion indispensable for the oncogenic activity of BCR/ABL such as the N-terminal coiled coil (CC), the tyrosine phosphorylation site Y177 and the serine/threonine kinase domain (ST), as well as on the ABL portion of BCR/ABL (#ABL-T315I) with or without the inhibitory SH3 (Δ SH3-ABL) domain. Here we report that i.) T315I restored the capacity to mediate factor independence of oligomerization_deficient p185BCR/ABL; ii.) resistance of p185-T315I against inhibition of the oligomerization depends on the phosphorylation at Y177; iii.) autophosphorylation at Y177 is not affected by the oligomerization inhibition, but phosphorylation at Y177 of endogenous BCR parallels the effects of T315I; iv.) the effects of T315I are associated with an intact ABL_kinase activity; v.) the presence of T315I is associated with an increased ABL_kinase activity also in mutants unable to induce Y177 phosphorylation of endogenous BCR; vi.) there is no direct relationship between the ABL-kinase activity and the capacity to mediate factor_independence induced by T315I as revealed by the #ABL-T315I mutant, which was unable to induce Y177 phosphorylation of BCR only in the presence of the SH3 domain.

In contrast to its physiological counterpart c-ABL, the BCR/ABL kinase is constitutively activated, inducing the leukemic phenotype. The N-terminus of c-ABL (Cap region) contributes to the regulation of its kinase function. It is myristoylated, and the myristate residue binds to a hydrophobic pocket in the kinase domain known as the myristoyl binding pocket in a process called “capping”, which results in an auto-inhibited conformation. Because the cap region is replaced by the N-terminus of BCR, BCR/ABL “escapes” this auto-inhibition. Allosteric inhibition by myristate “mimics”, such as GNF-2, is able to inhibit unmutated BCR/ABL, but not the BCR/ABL that harbors the “gatekeeper” mutation T315I. Here we investigated the possibility of increasing the efficacy of allosteric inhibition by blocking BCR/ABL oligomerization. We demonstrate that inhibition of oligomerization was able not only to increase the efficacy of GNF-2 on unmutated BCR/ABL, but also to overcome the resistance of BCR/ABL-T315I to allosteric inhibition. These results strongly suggest that the response to allosteric inhibition by GNF-2 is inversely related to the degree of oligomerization of BCR/ABL.

Taken together these data suggest that the inhibition of tetramerization inhibits BCR/ABL-mediated transformation and can contribute to overcome Imatinib-resistance. The study pro-

vides the first evidence that an efficient peptide transduction system facilitates the employment of competitive peptides to target the oligomerization interface of BCR/ABL *in vivo*.

Further the data show that T315I confers additional leukemogenic activity to BCR/ABL, which might explain the clinical behavior of patients with BCR/ABL -T315I-positive blasts.

In summary, our observations establish a new approach for the molecular targeting of BCR/ABL and its resistant mutants represented by the combination of oligomerization and allosteric inhibitors.

7 Zusammenfassung

In der Philadelphia Chromosome (Ph) positiven ALL und CML hat die Fusion von BCR und ABL die Bildung eines BCR/ABL Fusionsprotein zur Folge. Dieses Fusionsprotein ist für den leukämischen Phänotypen aufgrund der konstitutiven Aktivierung vieler Signalwege unterhalb/Downstream der veränderten BCR/ABL fusionierten Tyrosinkinase. Eine zielgerichtete Inhibierung von BCR/ABL mittels ABL-Kinase-Inhibitoren induziert Apoptose in BCR/ABL transformierten Zellen und hat eine komplette Remission in Ph⁺ Leukämie Patienten zur Folge. Eine große Anzahl an Patienten mit fortgeschrittener Ph⁺ Leukämie erleiden einen Rückfall und entwickeln Resistenzen. Die Mutation der Kinasedomäne verhindert die Bindung von Inhibitoren und stellt somit den häufigsten Mechanismus von erworbenen Resistenzen in Patienten mit Ph⁺ Leukämie.

Die Tetramerisierung von BCR/ABL mittels der N-Terminalen coiled-coil region (CC) von BCR ist notwendig für die Aktivierung der ABL-Kinase. Das Targeting der CC-Domäne zwingt BCR/ABL in eine monomere Konformation, was zu einer Reduzierung der Kinasaktivität und einer erhöhten Imatinib-Sensitivität führt. Wir können zeigen, daß i) das Angreifen der Tetramerisierung mittels einem Peptide, welches die Helix2 der CC-Domäne repräsentiert, reduziert die Autophosphorylierung sowohl von WT BCR/ABL, als auch seinen Mutanten. ii) Die Helix-2 inhibiert unabhängig von vorkommenden Mutationen das transformierende Potential von BCR/ABL. iii) Aufgrund der Effekte auf das transformierende Potential und dem Faktor unabhängigen Wachstum von BCR/ABL, mit Ausnahme der T315I-Mutation, konnte eine effektive Kooperation zwischen Helix-2 und Imatinib gezeigt werden.

Die gezielte Hemmung von BCR/ABL durch Inhibitoren in Form kleiner Moleküle macht das Potential zur Transformation von BCR/ABL rückgängig. Wir haben eindeutig bewiesen, dass das Zielen auf die, durch die N-terminale coiled-coil Domäne (CC) vermittelte, Tetramerisierung von BCR/ABL mithilfe kompetitiver Peptide, welche die Helix-2 von CC repräsentieren, ein wirkungsvoller therapeutischer Ansatz zur Behandlung der Ph⁺Leukämie ist. Um die kompetitiven Peptide zum Angriff auf BCR/ABL weiter zu entwickeln, erzeugten wir eine Membran permeables Helix-2 Peptid (MPH-2), indem wir die Helix-2 Peptide mit einem Peptid-Transduktions-Tag fusionierten. In dieser Studie berichten wir, dass MPH-2: (i) mit BCR/ABL *in vivo* interagiert; (ii) effizient die Autophosphorylierung von BCR/ABL hemmt; (iii) Wachstum und Viabilität von Ph⁺ leukämischen Zellen unterdrückt; und (iv) in einem *in vivo* Maus-Modell effizient in mononukleäre Zellen (MNC) transduziert wurde.

Die T315I Mutation von BCR/ABL weist eine Resistenz gegen alle momentan sich in medizinischen Studien befindlichen ABL-kinase Inhibitoren und kompetitiven Peptiden auf.

Es scheint nicht nur die Bindungsaffinität der Kinase Inhibitoren zu vermindern sondern erzeugt zusätzliche Eigenschaften, die das leukämogene Potential von BCR/ABL verstärken. Um die Rolle der T315I Mutation auf dessen fehlender Inhibition der für das leukämogene Potential wichtigen Oligomerisierung von BCR/ABL näher zu bestimmen, untersuchten wir seinen Einfluß auf zusätzliche "loss-of-function" Mutanten von BCR/ABL in bezug auf deren Fähigkeit eine Faktor-Unabhängigkeit zu erzeugen. Entsprechend erzeugten wir BCR/ABL Mutanten, denen notwendige funktionale Domänen bezüglich des onkogenen Potenzials fehlen. Im BCR-Anteil deletierten wir die N-terminale coiled coil (CC) Domäne, die Tyrosine Phosphorylierungs Stelle Y177 und die Serine/Threonine Kinase Domäne (ST) sowie im ABL-Anteil die inhibitorische SH3 (Δ SH3-ABL) Domäne.

Aus den vorliegenden Arbeiten ergaben sich folgende Ergebnisse i.) T315I stellt die fehlende Faktor Unabhängigkeit von hämatopoetischen Zellen mit Oligomerisations defizienten p185BCR/ABL Mutanten wieder her; ii.) Die Resistenz von p185-T315I gegen die Inhibition der Oligomerisation ist abhängig von der Phosphorylierung am Y177; iii.) Die Autophosphorylierung am Y177 wird durch die Inhibition der Oligomerisierung nicht beeinträchtigt, jedoch die Phosphorylierung am Y177 von endogenem BCR wird durch die T315I Mutation verstärkt; iv.) Die Effekte von T315I sind mit einer intakten ABL_Kinase Aktivität assoziiert; v.) Das Vorhandensein der T315I Mutation ist assoziiert mit einer verstärkten ABL_kinase Aktivität, welches sich auch in Mutanten zeigt, die die Y177 Phosphorylierung von endogenem BCR nicht induzieren; vi.) Es gibt keinen direkten Zusammenhang zwischen der ABL-Kinase Aktivität und der durch T315I induzierten Faktorunabhängigkeit. Im Gegensatz zu der ABL-T315I Mutante, die nur in der Anwesenheit der SH3 Domäne nicht in der Lage war eine Phosphorylierung am Y177 von endogenem BCR zu induzieren.

Im Gegensatz zu seinem physiologischen Pendant c-Abl, ist die BCR/ABL Kinase, die den leukämischen Phänotyp induziert, konstitutiv aktiviert. Der N-Terminus von c-ABL (Cap region) wirkt an der Regulation seiner Kinasefunktion mit. Er ist myristoyliert und in einem Prozess, genannt „capping“ bindet der Myristinsäurerest an eine hydrophobe Tasche in der Kinasedomäne, bekannt als Myristinsäurebindungstasche. Daraus resultiert eine autoinhibitorische Konformation. Da die Cap-region durch den N-terminus von BCR/ABL ersetzt wurde, entgeht BCR/ABL dieser Autoinhibition. Allosterische Inhibition durch Myristeinimitatoren, wie GNF-2, sind in der Lage nicht mutiertes BCR/ABL zu inhibieren, nicht jedoch BCR/ABL, das die „Gatekeeper“-Mutation T315I beherbergt.

Wir untersuchen hier die Möglichkeit die Effizienz der allosterischen Inhibition durch Blockierung der BCR/ABL-Oligomerisierung zu erhöhen. Wir demonstrieren, dass die Inhibition der Oligomerisierung nicht nur in der Lage war die Effizienz von GNF-2 auf das nicht mutierte BCR/ABL zu erhöhen, sondern auch die Resistenz von BCR/ABL-T315I zu überwinden hin zur allosterischen Hemmung. Diese Ergebnisse lassen stark annehmen, dass das Ansprechen der allosterischen Hemmung durch GNF-2 in umgekehrtem Verhältnis zum Grad der Oligomerisierung von BCR/ABL steht.

Zusammengenommen deuten diese Daten auf eine Inhibierung der Tetramerisierung hin, welche die BCR/ABL vermittelte Transformation hemmt. Diese führt zu einer Überwindung der Imatinib Resistenz. Diese Studie bietet erste Evidenz, dass ein effizientes Peptid-Transduktions-System die Anwendung von kompetitiven Peptiden, um auf die Oligomerisierungs-Schnittstelle von BCR/ABL zu zielen, *in vivo* unterstützt. Des weitern zeigen die Daten, daß T315I zusätzliche leukämische Aktivität von BCR/ABL induziert, welches eine mögliche Erklärung für klinische Prognose von Patienten mit BCR/ABL-T315I positiven Blasten darstellt. Zusammenfassend lässt sich sagen, dass unsere Beobachtungen einen neuen Ansatz für molekulare Angriffspunkte für BCR/ABL und seine resistenten Mutanten etablieren, bestehend aus der Kombination von Oligomerisierungs- und allosterischen Inhibitoren.

8 References

Adrian FJ, Ding Q, Sim T, Velentza A, Sloan C, Liu Y *et al* (2006). Allosteric inhibitors of Bcr-abl-dependent cell proliferation. *Nat Chem Biol* **2**: 95-102.

Alam M, Hartrick CT (2005). Extended-release epidural morphine (DepoDur): an old drug with a new profile. *Pain Pract* **5**: 349-53.

Annino L, Goekbuget N, Delannoy A (2002). Acute lymphoblastic leukemia in the elderly. *Hematol J* **3**: 219-23.

Asoh S, Ohsawa I, Mori T, Katsura K, Hiraide T, Katayama Y *et al* (2002). Protection against ischemic brain injury by protein therapeutics. *Proc Natl Acad Sci U S A* **99**: 17107-12.

Azam M, Seeliger MA, Gray NS, Kuriyan J, Daley GQ (2008). Activation of tyrosine kinases by mutation of the gatekeeper threonine. *Nat Struct Mol Biol* **15**: 1109-18.

Barenholz Y (2001). Liposome application: problems and prospects. *Current Opinion in Colloid & Interface Science* **6**: 66-77.

Barenholz Y (2003). Relevancy of drug loading to liposomal formulation therapeutic efficacy. *Journal of Liposome Research* **13**: 1-8.

Barila D, Superti-Furga G (1998). An intramolecular SH3-domain interaction regulates c-Abl activity. *Nat Genet* **18**: 280-2.

Barka T, Gresik ES, Henderson SC (2004). Production of cell lines secreting TAT fusion proteins. *J Histochem Cytochem* **52**: 469-77.

Begemann M, Kashimawo SA, Heitjan DF, Schiff PB, Bruce JN, Weinstein IB (1998a). Treatment of human glioblastoma cells with the staurosporine derivative CGP 41251 inhibits CDC2 and CDK2 kinase activity and increases radiation sensitivity. *Anticancer Res* **18**: 2275-82.

Begemann M, Kashimawo SA, Lunn RM, Delohery T, Choi YJ, Kim S *et al* (1998b). Growth inhibition induced by Ro 31-8220 and calphostin C in human glioblastoma cell lines is associated with apoptosis and inhibition of CDC2 kinase. *Anticancer Res* **18**: 3139-52.

Beissert T, Hundertmark A, Kaburova V, Travaglini L, Mian AA, Nervi C *et al* (2008). Targeting of the N-terminal coiled coil oligomerization interface by a helix-2 peptide inhibits unmutated and imatinib-resistant BCR/ABL. *Int J Cancer* **122**: 2744-52.

Beissert T, Puccetti E, Bianchini A, Guller S, Boehrer S, Hoelzer D *et al* (2003). Targeting of the N-terminal coiled coil oligomerization interface of BCR interferes with the transformation potential of BCR-ABL and increases sensitivity to STI571. *Blood* **102**: 2985-93.

Bennett JM, Catovsky D, Daniel MT, Flandrin G, Galton DA, Gralnick HR *et al* (1985). Proposed revised criteria for the classification of acute myeloid leukemia. A report of the French-American-British Cooperative Group. *Ann Intern Med* **103**: 620-5.

- Berman HM, Westbrook J, Feng Z, Gilliland G, Bhat TN, Weissig H *et al* (2000). The Protein Data Bank. *Nucleic Acids Res* **28**: 235-42.
- Bug G, Rossmannith T, Henschler R, Kunz-Schughart LA, Schroder B, Kampfmann M *et al* (2002). Rho family small GTPases control migration of hematopoietic progenitor cells into multicellular spheroids of bone marrow stroma cells. *J Leukoc Biol* **72**: 837-45.
- Cai SR, Xu G, Becker-Hapak M, Ma M, Dowdy SF, McLeod HL (2006). The kinetics and tissue distribution of protein transduction in mice. *Eur J Pharm Sci* **27**: 311-9.
- Calabretta B, Perrotti D (2004). The biology of CML blast crisis. *Blood* **103**: 4010-22.
- Cameron MD, Wen B, Allen KE, Roberts AG, Schuman JT, Campbell AP *et al* (2005). Cooperative binding of midazolam with testosterone and alpha-naphthoflavone within the CYP3A4 active site: a NMR T1 paramagnetic relaxation study. *Biochemistry* **44**: 14143-51.
- Cao G, Pei W, Ge H, Liang Q, Luo Y, Sharp FR *et al* (2002). In Vivo Delivery of a Bcl-xL Fusion Protein Containing the TAT Protein Transduction Domain Protects against Ischemic Brain Injury and Neuronal Apoptosis. *J Neurosci* **22**: 5423-31.
- Carlson HA (2002). Protein flexibility and drug design: how to hit a moving target. *Curr Opin Chem Biol* **6**: 447-52.
- Clerc S, Barenholz Y (1995). Loading of amphipathic weak acids into liposomes in response to transmembrane calcium acetate gradients. *Biochim Biophys Acta* **1240**: 257-65.
- Clerc S, Barenholz Y (1998). A quantitative model for using acridine orange as a transmembrane pH gradient probe. *Anal Biochem* **259**: 104-11.
- Cohen GB, Ren R, Baltimore D (1995). Modular binding domains in signal transduction proteins. *Cell* **80**: 237-48.
- Cowan-Jacob SW, Guez V, Fendrich G, Griffin JD, Fabbro D, Furet P *et al* (2004). Imatinib (STI571) resistance in chronic myelogenous leukemia: molecular basis of the underlying mechanisms and potential strategies for treatment. *Mini Rev Med Chem* **4**: 285-99.
- Dai Z, Quackenbush RC, Courtney KD, Grove M, Cortez D, Reuther GW *et al* (1998). Oncogenic Abl and Src tyrosine kinases elicit the ubiquitin-dependent degradation of target proteins through a Ras-independent pathway. *Genes Dev* **12**: 1415-24.
- Darnell JE, Jr. (1997). STATs and gene regulation. *Science* **277**: 1630-5.
- Deininger M (2005). Resistance to imatinib: mechanisms and management. *J Natl Compr Canc Netw* **3**: 757-68.
- Deininger M, Buchdunger E, Druker BJ (2005). The development of imatinib as a therapeutic agent for chronic myeloid leukemia. *Blood* **105**: 2640-53.
- Deininger MW, Goldman JM, Lydon N, Melo JV (1997). The tyrosine kinase inhibitor CGP57148B selectively inhibits the growth of BCR-ABL-positive cells. *Blood* **90**: 3691-8.
- Deininger MW, Goldman JM, Melo JV (2000). The molecular biology of chronic myeloid leukemia. *Blood* **96**: 3343-56.

- Delannoy A, Ferrant A, Bosly A, Chatelain C, Doyen C, Martiat P *et al* (1990). Acute lymphoblastic leukemia in the elderly. *Eur J Haematol* **45**: 90-3.
- Denicourt C, Dowdy SF (2003). Protein transduction technology offers novel therapeutic approach for brain ischemia. *Trends Pharmacol Sci* **24**: 216-8.
- Diekmann D, Brill S, Garrett MD, Totty N, Hsuan J, Monfries C *et al* (1991). Bcr encodes a GTPase-activating protein for p21rac. *Nature* **351**: 400-2.
- Druker BJ (2008). Translation of the Philadelphia chromosome into therapy for CML. *Blood* **112**: 4808-17.
- Druker BJ, Lydon NB (2000). Lessons learned from the development of an abl tyrosine kinase inhibitor for chronic myelogenous leukemia. *J Clin Invest* **105**: 3-7.
- Druker BJ, Talpaz M, Resta DJ, Peng B, Buchdunger E, Ford JM *et al* (2001). Efficacy and safety of a specific inhibitor of the BCR-ABL tyrosine kinase in chronic myeloid leukemia. *N Engl J Med* **344**: 1031-7.
- Druker BJ, Tamura S, Buchdunger E, Ohno S, Segal GM, Fanning S *et al* (1996). Effects of a selective inhibitor of the Abl tyrosine kinase on the growth of Bcr-Abl positive cells. *Nat Med* **2**: 561-6.
- Ekroos M, Sjogren T (2006). Structural basis for ligand promiscuity in cytochrome P450 3A4. *Proc Natl Acad Sci U S A* **103**: 13682-7.
- Faderl S, Talpaz M, Estrov Z, O'Brien S, Kurzrock R, Kantarjian HM (1999). The biology of chronic myeloid leukemia. *N Engl J Med* **341**: 164-72.
- Fawell S, Seery J, Daikh Y, Moore C, Chen LL, Pepinsky B *et al* (1994). Tat-mediated delivery of heterologous proteins into cells. *Proc Natl Acad Sci U S A* **91**: 664-8.
- Feller SM, Knudsen B, Hanafusa H (1994). c-Abl kinase regulates the protein binding activity of c-Crk. *EMBO J* **13**: 2341-51.
- Ferti A, Panani A, Dervenoulas J, Raptis SA (1996). Cytogenetic findings in a Fanconi anemia patient with AML. *Cancer Genet Cytogenet* **90**: 182-3.
- Ford AM, Ridge SA, Cabrera ME, Mahmoud H, Steel CM, Chan LC *et al* (1993). In utero rearrangements in the trithorax-related oncogene in infant leukaemias. *Nature* **363**: 358-60.
- Ford KG, Darling D, Souberbielle B, Farzaneh F (2000). Protein transduction: a new tool for the study of cellular ageing and senescence. *Mech Ageing Dev* **121**: 113-21.
- Franz WM, Berger P, Wang JY (1989). Deletion of an N-terminal regulatory domain of the c-abl tyrosine kinase activates its oncogenic potential. *EMBO J* **8**: 137-47.
- Gales L, Macedo-Ribeiro S, Arsequell G, Valencia G, Saraiva MJ, Damas AM (2005). Human transthyretin in complex with iododiflunisal: structural features associated with a potent amyloid inhibitor. *Biochem J* **388**: 615-21.

- Gambacorti-Passerini C, Barni R, le Coutre P, Zucchetti M, Cabrita G, Cleris L *et al* (2000). Role of alpha1 acid glycoprotein in the in vivo resistance of human BCR-ABL(+) leukemic cells to the abl inhibitor STI571. *J Natl Cancer Inst* **92**: 1641-50.
- Gambacorti-Passerini C, le Coutre P, Mologni L, Fanelli M, Bertazzoli C, Marchesi E *et al* (1997). Inhibition of the ABL kinase activity blocks the proliferation of BCR/ABL+ leukemic cells and induces apoptosis. *Blood Cells Mol Dis* **23**: 380-94.
- Gleissner B, Gokbuget N, Bartram CR, Janssen B, Rieder H, Janssen JW *et al* (2002). Leading prognostic relevance of the BCR-ABL translocation in adult acute B-lineage lymphoblastic leukemia: a prospective study of the German Multicenter Trial Group and confirmed polymerase chain reaction analysis. *Blood* **99**: 1536-43.
- Goga A, McLaughlin J, Pendergast AM, Parmar K, Muller A, Rosenberg N *et al* (1993). Oncogenic activation of c-ABL by mutation within its last exon. *Mol Cell Biol* **13**: 4967-75.
- Gokbuget N, Hoelzer D, Arnold R, Bohme A, Bartram CR, Freund M *et al* (2000). Treatment of Adult ALL according to protocols of the German Multicenter Study Group for Adult ALL (GMALL). *Hematol Oncol Clin North Am* **14**: 1307-25, ix.
- Gorre ME, Mohammed M, Ellwood K, Hsu N, Paquette R, Rao PN *et al* (2001). Clinical resistance to STI-571 cancer therapy caused by BCR-ABL gene mutation or amplification. *Science* **293**: 876-80.
- Grant GJ, Barenholz Y, Bolotin EM, Bansinath M, Turndorf H, Piskoun B *et al* (2004). A novel liposomal bupivacaine formulation to produce ultralong-acting analgesia. *Anesthesiology* **101**: 133-7.
- Grignani F, Kinsella T, Mencarelli A, Valtieri M, Riganelli D, Lanfrancone L *et al* (1998). High-efficiency gene transfer and selection of human hematopoietic progenitor cells with a hybrid EBV/retroviral vector expressing the green fluorescence protein. *Cancer Res* **58**: 14-9.
- Griswold IJ, MacPartlin M, Bumm T, Goss VL, O'Hare T, Lee KA *et al* (2006). Kinase domain mutants of Bcr-Abl exhibit altered transformation potency, kinase activity, and substrate utilization, irrespective of sensitivity to imatinib. *Mol Cell Biol* **26**: 6082-93.
- Guo XY, Cuillerot JM, Wang T, Wu Y, Arlinghaus R, Claxton D *et al* (1998). Peptide containing the BCR oligomerization domain (AA 1-160) reverses the transformed phenotype of p210bcr-abl positive 32D myeloid leukemia cells. *Oncogene* **17**: 825-33.
- Hamilton JA, Benson MD (2001). Transthyretin: a review from a structural perspective. *Cell Mol Life Sci* **58**: 1491-521.
- Hantschel O, Nagar B, Guettler S, Kretzschmar J, Dorey K, Kuriyan J *et al* (2003). A myristoyl/phosphotyrosine switch regulates c-Abl. *Cell* **112**: 845-57.
- Hantschel O, Superti-Furga G (2004). Regulation of the c-Abl and Bcr-Abl tyrosine kinases. *Nat Rev Mol Cell Biol* **5**: 33-44.
- Haran G, Cohen R, Bar LK, Barenholz Y (1993). Transmembrane ammonium sulfate gradients in liposomes produce efficient and stable entrapment of amphipathic weak bases. *Biochim Biophys Acta* **1151**: 201-15.
- Huettner CS, Zhang P, Van Etten RA, Tenen DG (2000). Reversibility of acute B-cell leukaemia induced by BCR-ABL1. *Nat Genet* **24**: 57-60.

- Iacob RE, Pene-Dumitrescu T, Zhang J, Gray NS, Smithgall TE, Engen JR (2009). Conformational disturbance in Abl kinase upon mutation and deregulation. *Proc Natl Acad Sci U S A* **106**: 1386-91.
- Ilaria RL, Jr., Van Etten RA (1996). P210 and P190(BCR/ABL) induce the tyrosine phosphorylation and DNA binding activity of multiple specific STAT family members. *J Biol Chem* **271**: 31704-10.
- Kelliher MA, McLaughlin J, Witte ON, Rosenberg N (1990). Induction of a chronic myelogenous leukemia-like syndrome in mice with v-abl and BCR/ABL. *Proc Natl Acad Sci U S A* **87**: 6649-53.
- Klejman A, Schreiner SJ, Nieborowska-Skorska M, Slupianek A, Wilson M, Smithgall TE *et al* (2002). The Src family kinase Hck couples BCR/ABL to STAT5 activation in myeloid leukemia cells. *EMBO J* **21**: 5766-74.
- Knappskog S, Ravneberg H, Gjerdrum C, Trosse C, Stern B, Pryme IF (2007). The level of synthesis and secretion of Gaussia princeps luciferase in transfected CHO cells is heavily dependent on the choice of signal peptide. *J Biotechnol* **128**: 705-15.
- Kolyvanos U, Kaser L, Vetter W (2003). [Hypercalcemia]. *Praxis (Bern 1994)* **92**: 1567-71.
- Komatsu N, Watanabe T, Uchida M, Mori M, Kirito K, Kikuchi S *et al* (2003). A member of Forkhead transcription factor FKHRL1 is a downstream effector of STI571-induced cell cycle arrest in BCR-ABL-expressing cells. *J Biol Chem* **278**: 6411-9.
- Kong Y, Yoshida S, Saito Y, Doi T, Nagatoshi Y, Fukata M *et al* (2008). CD34+CD38+CD19+ as well as CD34+CD38-CD19+ cells are leukemia-initiating cells with self-renewal capacity in human B-precursor ALL. *Leukemia* **22**: 1207-13.
- Laneuville P (1995). Abl tyrosine protein kinase. *Semin Immunol* **7**: 255-66.
- Laurent E, Talpaz M, Kantarjian H, Kurzrock R (2001). The BCR gene and philadelphia chromosome-positive leukemogenesis. *Cancer Res* **61**: 2343-55.
- Lemez P (1989). [Acute leukemias in humans. I. Definition, etiology, and pathogenesis of acute leukemias. Classification of acute myeloid leukemia]. *Sb Lek* **91**: 368-84.
- Lewis JM, Baskaran R, Taagepera S, Schwartz MA, Wang JY (1996). Integrin regulation of c-Abl tyrosine kinase activity and cytoplasmic-nuclear transport. *Proc Natl Acad Sci U S A* **93**: 15174-9.
- Lin F, Monaco G, Sun T, Liu J, Lin H, Stephens C *et al* (2001). BCR gene expression blocks Bcr-Abl induced pathogenicity in a mouse model. *Oncogene* **20**: 1873-81.
- Ling X, Ma G, Sun T, Liu J, Arlinghaus RB (2003). Bcr and Abl interaction: oncogenic activation of c-Abl by sequestering Bcr. *Cancer Res* **63**: 298-303.
- Litzow MR (2006). Imatinib resistance: obstacles and opportunities. *Arch Pathol Lab Med* **130**: 669-79.
- Lugo TG, Pendergast AM, Muller AJ, Witte ON (1990). Tyrosine kinase activity and transformation potency of bcr-abl oncogene products. *Science* **247**: 1079-82.
- Ma G, Lu D, Wu Y, Liu J, Arlinghaus RB (1997). Bcr phosphorylated on tyrosine 177 binds Grb2. *Oncogene* **14**: 2367-72.

- Maru Y, Witte ON (1991). The BCR gene encodes a novel serine/threonine kinase activity within a single exon. *Cell* **67**: 459-68.
- Mauro MJ, Druker BJ (2001). STI571: a gene product-targeted therapy for leukemia. *Curr Oncol Rep* **3**: 223-7.
- Mayer BJ, Baltimore D (1994). Mutagenic analysis of the roles of SH2 and SH3 domains in regulation of the Abl tyrosine kinase. *Mol Cell Biol* **14**: 2883-94.
- McWhirter JR, Galasso DL, Wang JY (1993). A coiled-coil oligomerization domain of Bcr is essential for the transforming function of Bcr-Abl oncoproteins. *Mol Cell Biol* **13**: 7587-95.
- Melo JV (1996). The diversity of BCR-ABL fusion proteins and their relationship to leukemia phenotype. *Blood* **88**: 2375-84.
- Meyer B, Peters T (2003). NMR spectroscopy techniques for screening and identifying ligand binding to protein receptors. *Angew Chem Int Ed Engl* **42**: 864-90.
- Mian AA, Oancea C, Zhao Z, Ottmann OG, Ruthardt M (2009a). Oligomerization inhibition, combined with allosteric inhibition, abrogates the transformation potential of T315I-positive BCR/ABL. *Leukemia*.
- Mian AA, Schull M, Zhao Z, Oancea C, Hundertmark A, Beissert T *et al* (2009b). The gatekeeper mutation T315I confers resistance against small molecules by increasing or restoring the ABL-kinase activity accompanied by aberrant transphosphorylation of endogenous BCR, even in loss-of-function mutants of BCR/ABL. *Leukemia* **23**: 1614-21.
- Minucci S, Maccarana M, Cioce M, De Luca P, Gelmetti V, Segalla S *et al* (2000). Oligomerization of RAR and AML1 transcription factors as a novel mechanism of oncogenic activation. *Mol Cell* **5**: 811-20.
- Nagar B, Bornmann WG, Pellicena P, Schindler T, Veach DR, Miller WT *et al* (2002). Crystal structures of the kinase domain of c-Abl in complex with the small molecule inhibitors PD173955 and imatinib (STI-571). *Cancer Res* **62**: 4236-43.
- Nardi V, Azam M, Daley GQ (2004). Mechanisms and implications of imatinib resistance mutations in BCR-ABL. *Curr Opin Hematol* **11**: 35-43.
- Nieborowska-Skorska M, Wasik MA, Slupianek A, Salomoni P, Kitamura T, Calabretta B *et al* (1999). Signal transducer and activator of transcription (STAT)5 activation by BCR/ABL is dependent on intact Src homology (SH)3 and SH2 domains of BCR/ABL and is required for leukemogenesis. *J Exp Med* **189**: 1229-42.
- Nimmanapalli R, Bhalla K (2002). Mechanisms of resistance to imatinib mesylate in Bcr-Abl-positive leukemias. *Curr Opin Oncol* **14**: 616-20.
- O'Dwyer ME, Mauro MJ, Druker BJ (2003). STI571 as a targeted therapy for CML. *Cancer Invest* **21**: 429-38.
- O'Hare T, Walters DK, Stoffregen EP, Jia T, Manley PW, Mestan J *et al* (2005a). In vitro activity of Bcr-Abl inhibitors AMN107 and BMS-354825 against clinically relevant imatinib-resistant Abl kinase domain mutants. *Cancer Res* **65**: 4500-5.

- O'Hare T, Walters DK, Stoffregen EP, Sherbenou DW, Heinrich MC, Deininger MW *et al* (2005b). Combined Abl inhibitor therapy for minimizing drug resistance in chronic myeloid leukemia: Src/Abl inhibitors are compatible with imatinib. *Clin Cancer Res* **11**: 6987-93.
- Ottmann OG, Hoelzer D (2002). The ABL tyrosine kinase inhibitor STI571 (Glivec) in Philadelphia positive acute lymphoblastic leukemia - promises, pitfalls and possibilities. *Hematol J* **3**: 2-6.
- Pane F, Frigeri F, Sindona M, Luciano L, Ferrara F, Cimino R *et al* (1996). Neutrophilic-chronic myeloid leukemia: a distinct disease with a specific molecular marker (BCR/ABL with C3/A2 junction). *Blood* **88**: 2410-4.
- Partridge KA, Johannessen A, Tauler A, Pryme IF, Hesketh JE (1999). Competition between the signal sequence and a 3'UTR localisation signal during redirection of beta-globin mRNA to the endoplasmic reticulum: implications for biotechnology. *Cytotechnology* **30**: 37-47.
- Passegue E, Jamieson CH, Ailles LE, Weissman IL (2003). Normal and leukemic hematopoiesis: are leukemias a stem cell disorder or a reacquisition of stem cell characteristics? *Proc Natl Acad Sci U S A* **100 Suppl 1**: 11842-9.
- Pendergast AM, Quilliam LA, Cripe LD, Bassing CH, Dai Z, Li N *et al* (1993). BCR-ABL-induced oncogenesis is mediated by direct interaction with the SH2 domain of the GRB-2 adaptor protein. *Cell* **75**: 175-85.
- Perola E, Charifson PS (2004). Conformational analysis of drug-like molecules bound to proteins: an extensive study of ligand reorganization upon binding. *J Med Chem* **47**: 2499-510.
- Polyakov V, Sharma V, Dahlheimer JL, Pica CM, Luker GD, Piwnica-Worms D (2000). Novel Tat-peptide chelates for direct transduction of technetium-99m and rhenium into human cells for imaging and radiotherapy. *Bioconjug Chem* **11**: 762-71.
- Puccetti E, Guller S, Orleth A, Bruggenolte N, Hoelzer D, Ottmann OG *et al* (2000). BCR-ABL mediates arsenic trioxide-induced apoptosis independently of its aberrant kinase activity. *Cancer Res* **60**: 3409-13.
- Quintas-Cardama A, Kantarjian H, Cortes J (2007). Flying under the radar: the new wave of BCR-ABL inhibitors. *Nat Rev Drug Discov* **6**: 834-48.
- Radich JP (2001). Philadelphia chromosome-positive acute lymphocytic leukemia. *Hematol Oncol Clin North Am* **15**: 21-36.
- Ramirez P, DiPersio JF (2008). Therapy options in imatinib failures. *Oncologist* **13**: 424-34.
- Ravandi F, Cortes J, Albitar M, Arlinghaus R, Qiang Guo J, Talpaz M *et al* (1999). Chronic myelogenous leukaemia with p185(BCR/ABL) expression: characteristics and clinical significance. *Br J Haematol* **107**: 581-6.
- Ren R (2005). Mechanisms of BCR-ABL in the pathogenesis of chronic myelogenous leukaemia. *Nat Rev Cancer* **5**: 172-83.
- Sattler M, Salgia R, Okuda K, Uemura N, Durstin MA, Pisick E *et al* (1996). The proto-oncogene product p120CBL and the adaptor proteins CRKL and c-CRK link c-ABL, p190BCR/ABL and p210BCR/ABL to the phosphatidylinositol-3' kinase pathway. *Oncogene* **12**: 839-46.

- Savage DG, Antman KH (2002). Imatinib mesylate--a new oral targeted therapy. *N Engl J Med* **346**: 683-93.
- Schiffer CA, Hehlmann R, Larson R (2003). Perspectives on the treatment of chronic phase and advanced phase CML and Philadelphia chromosome positive ALL(1). *Leukemia* **17**: 691-9.
- Schindler T, Bornmann W, Pellicena P, Miller WT, Clarkson B, Kuriyan J (2000). Structural mechanism for STI-571 inhibition of abelson tyrosine kinase. *Science* **289**: 1938-42.
- Schmid I, Uittenbogaart CH, Keld B, Giorgi JV (1994). A rapid method for measuring apoptosis and dual-color immunofluorescence by single laser flow cytometry. *J Immunol Methods* **170**: 145-57.
- Schwarze SR, Dowdy SF (2000). In vivo protein transduction: intracellular delivery of biologically active proteins, compounds and DNA. *Trends Pharmacol Sci* **21**: 45-8.
- Schwarze SR, Ho A, Vocero-Akbani A, Dowdy SF (1999). In vivo protein transduction: delivery of a biologically active protein into the mouse. *Science* **285**: 1569-72.
- Seipelt G, Hofmann WK, Martin H, Wassmann B, Boehme A, Ottmann OG *et al* (1998). Comparison of toxicity and outcome in patients with acute myeloid leukemia treated with high-dose cytosine arabinoside consolidation after induction with a regimen containing idarubicin or daunorubicin. *Ann Hematol* **76**: 145-51.
- Selivanova G, Iotsova V, Okan I, Fritsche M, Strom M, Groner B *et al* (1997). Restoration of the growth suppression function of mutant p53 by a synthetic peptide derived from the p53 C-terminal domain. *Nat Med* **3**: 632-8.
- Shah NP, Nicoll JM, Nagar B, Gorre ME, Paquette RL, Kuriyan J *et al* (2002). Multiple BCR-ABL kinase domain mutations confer polyclonal resistance to the tyrosine kinase inhibitor imatinib (STI571) in chronic phase and blast crisis chronic myeloid leukemia. *Cancer Cell* **2**: 117-25.
- Silverman N, Maniatis T (2001). NF-kappaB signaling pathways in mammalian and insect innate immunity. *Genes Dev* **15**: 2321-42.
- Skaggs BJ, Gorre ME, Ryvkin A, Burgess MR, Xie Y, Han Y *et al* (2006). Phosphorylation of the ATP-binding loop directs oncogenicity of drug-resistant BCR-ABL mutants. *Proc Natl Acad Sci U S A* **103**: 19466-71.
- Smith KM, Yacobi R, Van Etten RA (2003). Autoinhibition of Bcr-Abl through its SH3 domain. *Mol Cell* **12**: 27-37.
- Stockwell GR, Thornton JM (2006). Conformational diversity of ligands bound to proteins. *J Mol Biol* **356**: 928-44.
- Sugioka R, Shimizu S, Funatsu T, Tamagawa H, Sawa Y, Kawakami T *et al* (2003). BH4-domain peptide from Bcl-xL exerts anti-apoptotic activity in vivo. *Oncogene* **22**: 8432-40.
- Talpaz M, McCredie KB, Mavligit GM, Gutterman JU (1983). Leukocyte interferon-induced myeloid cyto-reduction in chronic myelogenous leukemia. *Blood* **62**: 689-92.

- Tauchi T, Miyazawa K, Feng GS, Broxmeyer HE, Toyama K (1997). A coiled-coil tetramerization domain of BCR-ABL is essential for the interactions of SH2-containing signal transduction molecules. *J Biol Chem* **272**: 1389-94.
- Teague SJ (2003). Implications of protein flexibility for drug discovery. *Nat Rev Drug Discov* **2**: 527-41.
- Vivanco I, Sawyers CL (2002). The phosphatidylinositol 3-Kinase AKT pathway in human cancer. *Nat Rev Cancer* **2**: 489-501.
- Voinea M, Simionescu M (2002). Designing of 'intelligent' liposomes for efficient delivery of drugs. *J Cell Mol Med* **6**: 465-74.
- von Bubnoff N, Manley PW, Mestan J, Sanger J, Peschel C, Duyster J (2006). Bcr-Abl resistance screening predicts a limited spectrum of point mutations to be associated with clinical resistance to the Abl kinase inhibitor nilotinib (AMN107). *Blood* **108**: 1328-33.
- von Bubnoff N, Veach DR, van der Kuip H, Aulitzky WE, Sanger J, Seipel P *et al* (2005). A cell-based screen for resistance of Bcr-Abl-positive leukemia identifies the mutation pattern for PD166326, an alternative Abl kinase inhibitor. *Blood* **105**: 1652-9.
- Voncken JW, Kaartinen V, Groffen J, Heisterkamp N (1998). Bcr/Abl associated leukemogenesis in bcr null mutant mice. *Oncogene* **16**: 2029-32.
- Walter P, Gilmore R, Blobel G (1984). Protein translocation across the endoplasmic reticulum. *Cell* **38**: 5-8.
- Walz C, Sattler M (2006). Novel targeted therapies to overcome imatinib mesylate resistance in chronic myeloid leukemia (CML). *Crit Rev Oncol Hematol* **57**: 145-64.
- Wassmann B, Scheuring U, Pfeifer H, Binckebanck A, Kabisch A, Lubbert M *et al* (2003). Efficacy and safety of imatinib mesylate (Glivec) in combination with interferon-alpha (IFN-alpha) in Philadelphia chromosome-positive acute lymphoblastic leukemia (Ph+ALL). *Leukemia* **17**: 1919-24.
- Weisberg E, Griffin JD (2000). Mechanism of resistance to the ABL tyrosine kinase inhibitor STI571 in BCR/ABL-transformed hematopoietic cell lines. *Blood* **95**: 3498-505.
- Weisberg E, Manley P, Mestan J, Cowan-Jacob S, Ray A, Griffin JD (2006). AMN107 (nilotinib): a novel and selective inhibitor of BCR-ABL. *Br J Cancer* **94**: 1765-9.
- Weisberg E, Manley PW, Breitenstein W, Bruggen J, Cowan-Jacob SW, Ray A *et al* (2005). Characterization of AMN107, a selective inhibitor of native and mutant Bcr-Abl. *Cancer Cell* **7**: 129-41.
- Wilson MB, Schreiner SJ, Choi HJ, Kamens J, Smithgall TE (2002). Selective pyrrolo-pyrimidine inhibitors reveal a necessary role for Src family kinases in Bcr-Abl signal transduction and oncogenesis. *Oncogene* **21**: 8075-88.
- Zhang X, Subrahmanyam R, Wong R, Gross AW, Ren R (2001). The NH(2)-terminal coiled-coil domain and tyrosine 177 play important roles in induction of a myeloproliferative disease in mice by Bcr-Abl. *Mol Cell Biol* **21**: 840-53.
- Zhao M, Weissleder R (2004). Intracellular cargo delivery using tat peptide and derivatives. *Med Res Rev* **24**: 1-12.

Zhao X, Ghaffari S, Lodish H, Malashkevich VN, Kim PS (2002). Structure of the Bcr-Abl oncoprotein oligomerization domain. *Nat Struct Biol* **9**: 117-20.

Zheng X, Beissert T, Kukoc-Zivojnov N, Puccetti E, Altschmied J, Stolz C *et al* (2004). Gamma-catenin contributes to leukemogenesis induced by AML-associated translocation products by increasing the self-renewal of very primitive progenitor cells. *Blood* **103**: 3535-43.

Zheng X, Oancea C, Henschler R, Ruthardt M (2009). Cooperation between constitutively activated c-Kit signaling and leukemogenic transcription factors in the determination of the leukemic phenotype in murine hematopoietic stem cells. *Int J Oncol* **34**: 1521-31.

Abbreviations

+	Positive
-	Negetive
%	Percent
a.a	Amino acid
7-AAD	7-Aminoactinomycin
ABL	Abelson murine leukaemia virus homology gene
ALL	Acute lymphatic leukemia
AML	Acute myeloid leukemia
AMP	Ampicillin
Arg	Argenin
ATP	Adenosin-5'-triphosphate
attP site	<i>Attachement site</i>
BCR	Breakpoint cluster region
BCR/ABL	Breakpoint cluster region/ Abelson murine leukaemia virus
BM	Bone marrow
BrdU	5-bromo-2-deoxyuridine
BSA	Bovine serum albumin
°C	Celsius
Ca ²⁺	Calcium
CC	coiled-coil
ΔCC	Deleted coiled-coil
CD	Cluster of differentiation
cDNA	Complementary DNA
cm	Centimeter
CSF	Colony stimulating factor
CFU	Colony-forming unit
CFU-GEMM	CFU-granulocyte erythroid megacaryocyte macrophage
CFU-GM	Colony-forming unit granulocyte, macrophage
CIP	Calf intestinal phosphatase
CLL	Chronic lymphatic leukaemia
CLP	Common lymphoid progenitors

CML	Chronic myeloid leukaemia
CMP	Common myeloid progenitors
CMV	<i>Cytomegalovirus</i>
CR	Complete remission
CTP	Cytoplasmic transduction peptide
dATP	desoxy Adenintriphosphat
dCTP	desoxy Cytosintriphosphat
ddH ₂ O	Double distilled water
DEPC	Diethylpyrocarbonate
dGTP	desoxy Guanosintriphosphat
DMEM	Dulbecco's Modified Eagle Medium
DMSO	Dimethyl sulfoxide
DSMZ	German Collection of Microorganisms and Cell Cultures
DNA	Desoxyribonucleic acid
DNTPs	deoxyribonucleotide triphosphate
DTT	Dithiothreitol (Threo-1,4-Dimercapto-2,3-Butandiol)
dTTP	desoxy Thymintriphosphat
<i>E. coli</i>	<i>Escherichia coli</i>
EBV	Epstein Barr virus
ECL	Enhanced chemiluminescence
EDTA	Ethylenediaminetetraacetate
EGFR	<i>epidermal growth factor receptor</i>
eGFP	Enhanced green fluorescent protein
ERK	<i>extracellular signal regulated kinase</i>
FAB classification	French American British classification
FACS	Fluorescence activated cell sorting
Fak	Focal adhesion kinase
FCS	Fetal calf serum
FITC	Fluorescein Isothiocyanate
g	Gram
Gal	Galactose

GFP	Green fluorescent protein
Grb-2	Growth factor receptor-bound protein 2
GST	Glutathione <i>S</i> -transferase
GTP	Guanosintriphosphate
Gy	Gray
HEPES	4-2-hydroxyethyl-1-piperazineethanesulfonic acid
HIV	Human immunodeficiency virus
HMW	High molecular weight
HPLC	High performance liquid chromatography
HRP	Horse radish peroxidase
HSCs	Hematopoietic stem cells
IFN- α	Interferon alpha
IgG	Immunglobulin G
IMDM	Iscove's Modified Dulbecco's Medium
IL-3	Interleukin 3
IPTG	Isopropyl-1-thio-Beta-D-galactopyranoside
ISE	Iterative Stochastic Elimination
i.v	Intravenous
Jak-Stat	Janus kinase-signal transducers and activators of transcription
JNK	<i>c-Jun-N-terminal kinase</i>
Kb	Kilo base pairs
kDa	Kilodalton(s)
LB-Medium	Luria-Bertani-Medium
Δ LNGFR	Low affinity nerve growth factor receptor
LSC	Leukemic-stem cell
LT-HSC	Long-term hematopoietic stem cells
M	Molar
MACS	Magnetic activated cell sorting
MAPK	Mitogen activated protein kinase

M-BCR	Major Breakpoint cluster region
m-BCR	Minor Breakpoint cluster region
μ -BCR	Third Breakpoint in the BCR gene, downstream of the M-BCR
MBP	Myristoyl binding pocket
mg	Milligram
Min	Minutes
ml	Milliliter
μ g	Microgram
ml	Milli Liter
μ l	Microliter
μ M	Micro molar
mM	Milli Molar
MNCs	Mononuclear
MPD	Myeloproliferative diseases
MPH-2	Membrane permeable helix-2
MPP	Multipotent progenitor cells
mSCF	Murine stem cell factor
N	Amino
Ng	nano gram
NK	Natural killer
NLSs	Nuclear localization signal sequences
nSSL	Sterically stabilized nano liposomes
OD	Optical density
ORF	Open reading frame
p185 ^{BCR-ABL}	185 kDa fusion protein of t(9;22)
p210 ^{BCR-ABL}	210 kDa fusion protein of t(9;22)
PAGE	Polyacrylamide gel electrophoresis
PBS	Phosphate-buffered saline
PCR	Polymerase chain reaction
PE	Phycoerythrin

pH	Reverse logarithmic representation of hydrogen ion concentration
Ph+	Philadelphia chromosom positive
Ph-	Philadelphia chromosom negativ
PI	Propidium iodide
PI3K	Phosphatidylinositol-3-kinase
PLZF	Promyelocytic leukemia zinc finger
PML	Promyelocytic leukemia protein
Pmol	Pico Molar
PT	Peptide transduction
PTD	Peptide transduction domains
RAR	<i>retinoic acid receptor</i>
RNA	Ribonucleic acid
rmIL-3	Recombinant murine interleukin-3
rmIL-6	Recombinant murine interleukin-3
RNA	Ribonucleic acid
Rnase	Ribonuclease
rpm	Revolution per minute
RPMI-Medium	Roswell Park Memorial Institute-Medium
RT	Reverse Transcriptase
Sca-1	Stem cell antigene 1
SCF	Stem cell factor
SDS	sodium dodecyl sulfate
SDS-PAGE	SDS-Polyacrylamide gel electrophoresis
Ser	Serin
S/T	Serine/threonine
STAT	Signal transducers and activators of transcription
ST-HSC	Short-term hematopoietic stem cells
STI	Signaltransductions inhibitor
SOS	son of sevenless
T	Translocation

t(9;22)	Translocation of Chromosom 9 and 22
TAE	Tris-acetate-EDTA
TAT	Trans-Activator of Transcription
TBS	Tris-buffered saline
TBST	Tris-buffered saline plus Tween 20
TE	Tris-EDTA
TEMED	Tetramethylethylenediamine
Thr	Threonin
TK	Tyrosine kinase
Tris	Tris(hydroxymethyl)aminomethane
TSA	Trichostatin A
Tyr	Tyrosin
U	Enzyme unit
UTR	Untranslated region
UV	Ultraviolet
V	Volt
v/v	volume per volume
w/v	weight per volume
WBC	White blood cell count
WT	Wildtype
XTT	Tetrazolium salt
Y177	Tyrosine at a.a. position 177
Y177F	Tyrosine mutated to phenylalanine at a.a. position 177

9 Ehrenwörtliche Erklärung

EHRENWÖRTLICHE ERKLÄRUNG

Ich erkläre hiermit ehrenwörtlich, daß ich die dem Fachbereich Biochemie, Chemie und Pharmazie zur Promotionsprüfung eingereichte Arbeit mit dem Titel

**„Neue Ansätze des Molekularen Targetings bei der Philadelphia-Chromosom positiven
Leukämie“**

im Zentrum der Inneren Medizin, Medizinische Klinik III, Abteilung Hämatologie des Universitätsklinikums Frankfurt bei Prof. Dr. Hubert Serve und unter Leitung von Prof. Dr. Rolf Marschalek mit Unterstützung von PD. Dr. Martin Ruthardt ohne sonstige Hilfe selbst durchgeführt und bei der Abfassung der Arbeit keine anderen als die in der Dissertation angeführten Hilfsmittel benutzt habe.

Ich habe bisher an keiner in- oder ausländischen Biologischen Fakultät ein Gesuch um Zulassung zur Promotion eingereicht noch die vorliegende Arbeit als Dissertation vorgelegt.

Inhalte der vorliegenden Arbeit wurden in Leukemia 2009 Sep; 23(9):1614-21 und Leukemia 2009 Oct 1[Epub ahead of print] publiziert. Ein weiteres Manuskript befindet sich bei IJH unter Revision.

Frankfurt, den 07.11.2009

M.Phil. Biol. Afsar A. Mian

10 Curriculum Vitae

Afsar A. Mian, M.Phil.

Date of Birth 27.04.1976

Marital status Married

Nationality Pakistani

Address: Labor für Tumorstammzellbiologie (PD. Dr. Martin Ruthardt)
 Medizinische Klinik II/Abt. Hämatologie
 Klinikum der Johann Wolfgang Goethe-Universität
 Theodor-Stern Kai 7
 60590 Frankfurt
 Germany
 Phone : 069-6301-6358/6129
 Fax : 069-6301-6131
 E-mail: mian@med.uni-frankfurt.de

Private: Sandhoefer Allee 8, 60528 Frankfurt am Main Germany
 Phone : 069-17517436
 Mobile : 0176 21706839

Education and Institutions

1991-1992 SSC Government High school Shalpin Swat (Pakistan)
1993-95 F.Sc Government Degree College Matta Swat (Pakistan)
1996-2000 B.Sc (Honors) Breeding and Genetics (Natural Science) University of Agriculture, Faisalabad (Pakistan)
2001-2003 M.Phil. Molecular Biology National Centre of Excellence in Molecular Biology, University of the Punjab, Lahore, (Pakistan)
Master Thesis: “Regeneration potential of stem cells in damaged organ”
2004-2005 Involvement of MAP-kinases in up regulation of Invertase enzyme due to different stresses.
 Pharmazeutische Biologie (Prof. Dr.Thomas Roitsch) Julius-Von- Sachs, Institute für Biowissenschaften Würzburg Germany

Ph.D 2005 to date “Philadelphia Chromosome positive Leukemia: “Pathology of the Disease and Molecular Targeting”.
Laboratory for Tumor Stem Cell Biology, Department of Hematology, Medical School of Goethe University, Frankfurt, Germany.

Honours and Awards

1996 Scholarship under President Talent Farming Scheme (Higher Education Commission, Islamabad, Pakistan).

2002 Promotion of Education in Pakistan (PEP) fellowship (New York, USA)

2004-2005 DAAD fellowship: Involvement of MAP-kinases in up regulation of Invertase enzyme due to different stresses

Publications

Original papers

Beissert, T., Hundertmark, A., Kaburova, V., Travaglini, L., **Mian, AA.**, Nervi, C., and Ruthardt, M. (2008) Targeting of the N-terminal Coiled Coil Oligomerization Interface by a Helix-2 Peptide Inhibits Unmutated and Imatinib Resistant Mutant BCR/ABL. *Int. J. Cancer* 122(12):2744-2752

Mian, A.A., Schüll, M., Zhao, Z., Oancea, C., Hundertmark, A., Beissert, T., Ottmann, O.G. and Ruthardt, M. (2009) The gatekeeper mutation T315I confers resistance against small molecules by increasing or restoring the ABL-kinase activity accompanied by aberrant transphosphorylation of endogenous BCR, even in loss-of-function mutants of BCR/ABL. *Leukemia* 2009 Sep;23(9):1614-21

Mian, A.A., Oancea, C., Zhao, Z., Ottmann OG., and Ruthardt, M. (2009) Oligomerization inhibition combined with allosteric inhibition abrogates the transformation potential of BCR/ABL harboring the “gatekeeper” mutation T315I. *Leukemia* 2009 Oc 1. [Epub ahead of print]

Mian, A.A., Schüll, M., Oancea, C., Beissert, T., and Ruthardt, M. (2009) Targeting the oligomerization of BCR/ABL by membrane permeable competitive peptides inhibits the proliferation of Philadelphia chromosome positive leukemic cells. *Int. J. Hematology, under revision*

Abstracts

Mian, A. A., Fatima, T., Husnain, T., Ronald, P. C. and Riazuddin, S. (2003). 7th PSBMB conference. Abstract #106. Lahore, Pakistan

Mian, A. A., Kayani, M. A., and Riazuddin, S. (2003). Studies on Regeneration Potential of Stem Cells in Damaged Organ. CPC-International Conference & training workshop on Stem Cells 2003. Abstract # 04 . Lahore, Pakistan

Mian, A.A., Fatima, T., Husnain, T., and Riazuddin, S. (2004). Second National Conference of Biology. Lahore, Pakistan

Beissert, T., Kaburova, V., **Mian, A.A.**, Ottmann, O.G. Hoelzer, D., and Ruthardt, M. (2006). 11th congress EHA, June 15-18, 2006, Abstract # 1606. Amsterdam, Holland

Beissert, T., **Mian, A. A.**, Hoelzer, D., Ottmann, O. G. and Ruthardt, M. (2006). DGHO, November, 4-8, 2006., Abstract # V137. Leipzig, Germany

Beissert, T., Hundertmark, A., Kaburova, V., **Mian, A.A.**, Travaglini, L., Ottmann, O.G. Hoelzer, D., Nervi, C., and Ruthardt, M. (2006), Blood vol. 108 No.11, Abstract #2186. Orlando, Florida, USA

Mian, A.A., Kaburova, V., Hundertmark, A., Travaglini, L., Hoelzer, D., Nervi, C., Ruthardt, M. and Beissert, T. (2007). Disruption of Complexes Formed by the Leukemic Fusion Protein BCR/ABL with Interfering Peptides to overcome Imatinib Resistance. Oral presentation, SIBC-PSM 2007. Oral presentation, Abstract #15. Islamabad, Pakistan

Mian, A. A., Ruthardt, M. and Beissert, T. (2008) HIV-TAT Mediated Transduction of Competitive Peptide 13th congress EHA, June 12-15, 2008, Abstract # 0285. Copenhagen Denmark

Mian, A.A., Beissert, T. and Ruthardt, M. (2008). Targeting the Oligomerization of BCR/ABL by Membrane Permeable Competitive Peptides Inhibits the Proliferation of Philadelphia Chromosome Positive Leukemic Cells. DGHO, October, 10-14, 2008. oral presentation, Abstract # V250. Vienna Austria

Mian, A. A., Beissert, T. and Ruthardt, M. (2009) Targeting the Oligomerization of BCR/ABL by Membrane Permeable Competitive Peptides Inhibits the Proliferation of Philadelphia Chromosome Positive Leukemic Cells. 8th Shaikat Khanum Memorial Cancer Symposium , February, 26-28, 2009. Oral presentation page #54. Lahore, Pakistan

Mian, A. A., Kaburova, V., Hundertmark, A., Travaglini, L., Hoelzer, D., Nervi, C., Ruthardt, M. and Beissert, T. (2009) Targeting of the N-terminal Coiled Coil Oligomerization Interface by a Helix-2 Peptide Inhibits Unmutated and Imatinib Resistant Mutant BCR/ABL. 8th Shaikat Khanum Memorial Cancer Symposium, February, 26-28, 2009. Oral presentation, Abstract #76. Lahore, Pakistan

Oancea, C., **Mian, A. A.**, Rüster, B., Henschler, R. and Ruthardt, M. (2009) The t(6;9) associated DEK/CAN fusion protein: Its effects on primitive hematopoietic stem cells and its leukemogenic potential. AACR, April, 18-22, 2009. Abstract #4242. Denver, CO USA.

Mian, A.A., Schüll, M., Zhao, Z., Oancea, C., Hundertmark, A., Beissert, T., Ottmann, O.G. and Ruthardt, M. (2009) The gatekeeper mutation T315I confers resistance against small molecules by increasing or restoring the ABL-kinase activity accompanied by aberrant transphosphorylation of endogenous BCR, even in loss-of-function mutants of BCR/ABL. 14th congress EHA, June 4-7, 2009, Abstract # 0331. Berlin Germany

Mian, A.A., Oancea, C., Zhao, Z., Serve, H., Ottmann OG and Ruthardt, M. (2009) Oligomerization inhibition combined with allosteric inhibition abrogates the transformation potential of BCR/ABL harboring the “gatekeeper” mutation T315I. 51st ASH annual meeting, Dec 5-8, 2009, New Orleans USA. Accepted